Development and Characterization of an Osteochondral Tissue Engineering Strategy Utilizing Biochemical and Biomechanical Cues to Guide hMSC Differentiation in PEG-based Hydrogels

by

Neven Jolene Steinmetz

B.S., Texas Tech University, 2000

M.S., University of Colorado, 2002

A thesis submitted to the

Faculty of the Graduate School of the

University of Colorado in partial fulfillment

of the requirement for the degree of

Doctor of Philosophy

Department of Chemical and Biological Engineering

2011

This thesis entitled:

Development and Characterization of an Osteochondral Tissue Engineering Strategy Utilizing Biochemical and Biomechanical Cues to Guide hMSC Differentiation in PEG-based Hydrogels

written by Neven Jolene Steinmetz

has been approved for the Department of Chemical and Biological Engineering

_____

Stephanie J. Bryant

_____

Virginia L. Ferguson

Date_____

The final copy of this thesis has been examined by
the signatories, and we find that both the content and the form
meet acceptable presentation standards of scholarly work
in the above mentioned discipline.

Abstract

Steinmetz, Neven Jolene (Ph.D., Chemical Engineering)
Department of Chemical and Biological Engineering, University of Colorado

Development and Characterization of an Osteochondral Tissue Engineering Strategy Utilizing Biochemical and Biomechanical Cues to Guide hMSC Differentiation in PEG-based Hydrogels

Thesis directed by Associate Professor Stephanie J. Bryant

Osteoarthritis (OA) is a debilitating joint disease that affects millions of Americans, young and old. This disease primarily involves the protective cartilage found on the ends of articulating bone surfaces in joints. Inherently, cartilage does not heal well, and the current clinical therapies available to treat cartilage injuries and OA patients often lead to healing with mechanically inferior fibrocartilage. Tissue engineering (TE) strategies could offer a viable alternative to the current therapies available. It important for tissue engineered cartilage to successfully integrate with the underlying subchondral bone, and attention must be given to the unique and complex interface that connects the bone and cartilage: the osteochondral interface. This research works towards developing an osteochondral tissue engineering strategy that utilizes a scaffold engineered to guide the concomitant differentiation of a single undifferentiated cell source down both chondrogenic and osteogenic lineages with the ultimate goal of synthesizing spatially organized bone, cartilage, and osteochondral interface extracellular matrix (ECM) molecules. Progress has been made towards this goal by investigating the response of human mesenchymal stromal cells (hMSCs) to external biochemical and biomechanical cues. The scaffolds selected for this research were poly(ethylene glycol) (PEG) based hydrogels modified with either a generic cell binding peptide (RGD), a cartilage ECM moiety (chondroitin sulfate), or a type I collagen analog peptide (P-15) as a bone ECM moiety. hMSCs encapsulated

in these hydrogels were subjected to dynamic loading to impart biomechanical cues on the cells in combination with the biochemical cues from the modified scaffolds. Results indicated that RGD modified and ChS modified PEG scaffolds supported chondrogenic differentiation and the production of cartilage ECM matrix molecules including aggrecan, collagen II and collagen X. However, the application of a 15% intermittent dynamic compressive strain, whether applied immediately (RGD modified) or after an initial differentiation induction period (ChS) inhibited the production of the articular cartilage specific collagen II protein, suggesting that the 15% strain may be too large for guiding the hMSCs down an articular cartilage lineage. Further results indicated that hMSCs encapsulated in RGD modified scaffolds, in the absence of dynamic strain but in the presence of soluble osteogenic differentiation cues, produced significant collagen I, the primary collagen found in bone. Additional results suggested that P-15 modified hydrogels supported hMSC attachment, but did not offer enhanced production of bone biomarker molecules by encapsulated hMSCs. While optimal biochemical and biomechanical cues that guide hMSC differentiation remain to be elucidated, strategies to design multi-layer PEG based hydrogels were investigated and characterized. To mimic the variations in ECM and mechanical properties between bone and cartilage spanning the osteochondral interface, scaffolds were fabricated, characterized, and subjected to dynamic loading. When hMSCs were encapsulated in these scaffolds and cultured under free swelling or subjected to dynamic loading in osteochondral differentiation medium, the spatial presentation of biochemical and mechanical cues gave rise to characteristically different cartilage and bone protein expressions by hMSCs in each layer. These results indicate that it is possible to use the combination of biochemical and biomechanical cues to affect the spatial production of bone and cartilage specific ECM molecules in a scaffold with a single encapsulated cell source. As a better understanding of the

cues that drive differentiation of adult human MSC differentiation become elucidated, findings from this research will aid in the development of complex 3D scaffolds for osteochondral tissue engineering strategies that are capable of delivering local cues to concomitantly guide a single cell source down bone, articular cartilage, and hypertrophic lineages within a single scaffold.

Dedicated to the pursuit of always following your dream...

even if the path it takes you down is a completely foreign one.

Acknowledgements

First, I would like to thank my research advisor, Stephanie Bryant. Thank you for allowing me to join your lab, facilitating my return to the CU Chemical and Biological Engineering Department after a couple year hiatus. Although this research project has not taken quite the path that either of us probably envisioned for it 5 years ago, I know that I have learned a great deal about science, research, and problem solving, and definitely have a new appreciation for perseverance and overcoming adversity in research. From this experience, I know that I am well prepared to begin my postdoctoral research.

Thank you to each of my thesis committee members: John Kisiday, Kristi Anseth, Ginger Ferguson, and Jeff Stansbury. I really appreciate your guidance, helpful suggestions, and most importantly, the time you have taken to help me grow and develop as a PhD student during my time in this program. I have learned a great deal from each of you along the way.

Since my project was new to the group, and nobody else in our group worked on a similar project, I had to seek the help and advice of experts outside of our lab for a lot of my questions. Many very talented people have helped me along the way. Specifically, several people in Kristi Anseth's group have spent a considerable amount of time teaching me about human mesenchymal stem cells, PCR, and bone as well as letting me use their equipment and providing some not always obvious insights. Charlie Nuttelman, Chelsea Salinas, Pete Mariner, April Kloxin, and Victoria Bingham: thank you all for all of your help along the way.

I would also like to thank my friends Chris Baddick and Melissa Buhl. Although Chris is not a tissue engineer, he has helped me immensely with some of my histology hurdles as well as entertaining engaging discussions about research in general. Melissa has shown me better than anyone else that is it possible to pursue

higher education goals whilst concurrently pursing a successful professional mountain bike racing career.

I would especially like to thank Timothy Jackson for all of his encouragement, as well as healthy distractions, during the last 6 months of writing my thesis. Sometimes a rabbit needs a carrot to chase to really start running.

Thank you to all of the current and former Bryant and Mahoney group members for all of your help, suggestions, and insights in this challenging game of "The Pursuit of a PhD." Specifically, I would like to thank Garret Nicodemus, who spent countless hours teaching me about qRTPCR, our custom bioreactors, and histology as well as providing the encouragement to keep asking the hard questions.

Lastly, I would like to thank my family. Most importantly, I would like to thank my Grandparents who always placed a high regard on the value of education and made my entire engineering education possible for me. My Mom and Dad both provided constant support and encouragement through the last 22 (!!) years of education. My sister, Tori, set a shining example for me about how it might seem completely impossible to actually finish an advanced degree, but if you don't let anything stand in the way of your dreams, in the end the reward is so worth it! Finally, I would like to thank my nephew, Marshall. For even though he probably never realized what an inspiration to me he has been, watching his insatiable desire to learn and continue trying new things in the past couple of years has been a constant reminder to me that above all else, it is about the pursuit of knowledge, which can only come about if you keep learning and asking questions.

TABLE OF CONTENTS

CHAPTER 7

CHAPTER 8

List of Tables

List of Figures

Chapter 1: Introduction and Background

1.1 Clinical Problem: Osteoarthritis

Osteoarthritis (OA), a joint disease that primarily affects cartilage, is the leading cause of disability among aging adults [2]. As of 2010, over 20 million Americans suffer from some form of the disease and the numbers are expected to rise to 40 million (more than 10% of the population) by 2020 [3]. Clinically, there are two types of OA: primary and secondary. Primary OA affects people who have no known cause for the disease whereas secondary OA typically has an identifiable cause, such as a previous injury. The majority of people who suffer from secondary OA suffer post-traumatic OA, which is largely attributed to joint injuries suffered previously in their life. Many elderly people suffer from primary OA, but a large portion of the younger population suffer secondary OA and require a much longer term solution for their disease [4]. Many of the short-term solutions currently available are insufficient for life-long or even long-term fixes for these patients.

There are many injurious causes that can ultimately lead to OA in a patient including focal defects due to injuries or trauma, which increase a patient's chance of developing OA later in life. Many people who suffer secondary OA have incurred a joint injury due to repetitive loading or overuse, a torsional injury resulting in tearing, misaligned joints, or foreign bodies such as bone fragments or bone matrix crystals in the joint cavity [4]. Due to the avascular nature and low cell density in articular cartilage, cartilage injuries typically do not heal well, and when the body is able to "heal" the cartilage, it is often with fibrocartilage, which is mechanically inferior to native cartilage and does not provide a long-term solution for the patient [4].

When people experience cartilage injuries, they fall into one of three categories: cartilage microfractures, chondral defects, or osteochondral defects [4]. Osteochondral defects have the highest likelihood of healing given that they span the region down to the subchondral bone, which is vascular and can supply the injury with critical components for healing: nutrients and new mesenchymal stromal cells. However, even with the higher likelihood of healing, these injuries often heal with mechanically inferior fibrocartilage as well.

Given the large percentage of the population that this disease affects, there is a substantial economic driving force to develop successful tissue engineering strategies to replace the current therapies available to patients suffering from the various forms of this disease. The costs of OA, in the U.S. alone exceed $65 billion per year in lost wages and medical costs [4]. Currently there are no consistently successful cartilage or osteochondral solutions available to either young or old patients who suffer from this disease.

1.2 Joint Biology

Joints are complex structures comprised of several types of tissues and fluids such as bone, cartilage, tendon, ligament, and synovial fluid. When these tissues and lubricating fluids are healthy, they work in a near frictionless manner to allow many types of fluid and painless movements in the body. Articular cartilage is the cartilage that lines the ends of articulating bones in the joints [4]. Breakdown of this tissue, either due to injury, or an unidentifiable cause, leads to pain and loss of mobility [4]. Bone is the primary component of the human skeletal system, which serves the important role of providing the structural support of the body and protecting vital organs [5]. Within joints, the articulating ends of bones form a continuum of tissue through the osteochondral interface, integrating seamlessly with the protective articular

cartilage on the bone surface through several different zones: subchondral bone, tidemark, calcified cartilage, and then the deep, middle, and superficial zones of the protective articular cartilage [1] (Fig. 1).

1.2.1 Cartilage

Cartilage tissue serves an important role in the body and has very unique properties that allow this soft tissue to perform its rigorous role for many decades. Articular cartilage provides a very low friction surface on the ends of articular bones in the joints (Fig. 1), which combined with lubricating synovial fluid provide a near frictionless environment for healthy joints to articulate for the lifetime of a person. Although cartilage is considered a soft tissue, it has a remarkable capacity to bear very large loads. This is due to the unique properties of the integrated network of constituent components that make up cartilage: water, collagen, and proteoglycans. Cartilage is comprised of 70-80% water. Of the remaining 20-30% of the components, collagen makes up 50-70%, proteoglycans comprise 15-30%, and the remainder is made up of cells (chondrocytes) and other small molecules [4].

The combination of the molecules (collagen and proteoglycans) that make up the interconnected network in cartilage work together with the joint synovial fluid to provide resistance to the daily compressive rigors experienced in joints. There are several types of collagen found in connective tissues in the body. The primary collagen found in articular cartilage is type II collagen, which provides tensile strength to the cartilage [1]. Type X collagen is also present, but is primarily located in hypertrophic cartilage in the osteochondral interface region, which will be discussed in more detail later. Type II collagen plays a critical role in proper skeletal development as well as in the proper functioning of cartilage [6].

Proteoglycans are large macromolecules comprised of a protein core with glycosaminoglycans (GAG) (polysaccharide chains) attached to the core [4]. The primary proteoglycan in articular cartilage is aggrecan, which contains the GAGs chondroitin sulfate (ChS) and keratin sulfate (KS). These negatively charged molecules are interdispersed throughout the organized type II collagen network, forming the extracellular matrix (ECM) of cartilage. The negative charge on the proteoglycans allows the ECM to imbibe fluid, which contributes significantly to the unique mechanical properties of cartilage which allow joints to withstand routine daily forces of 2.5-3.5 times a person's bodyweight [4].

The normal aging process imparts several changes to the constituents of cartilage that ultimately lead to degradation, which can, in turn, lead to OA. Cartilage is a metabolically active

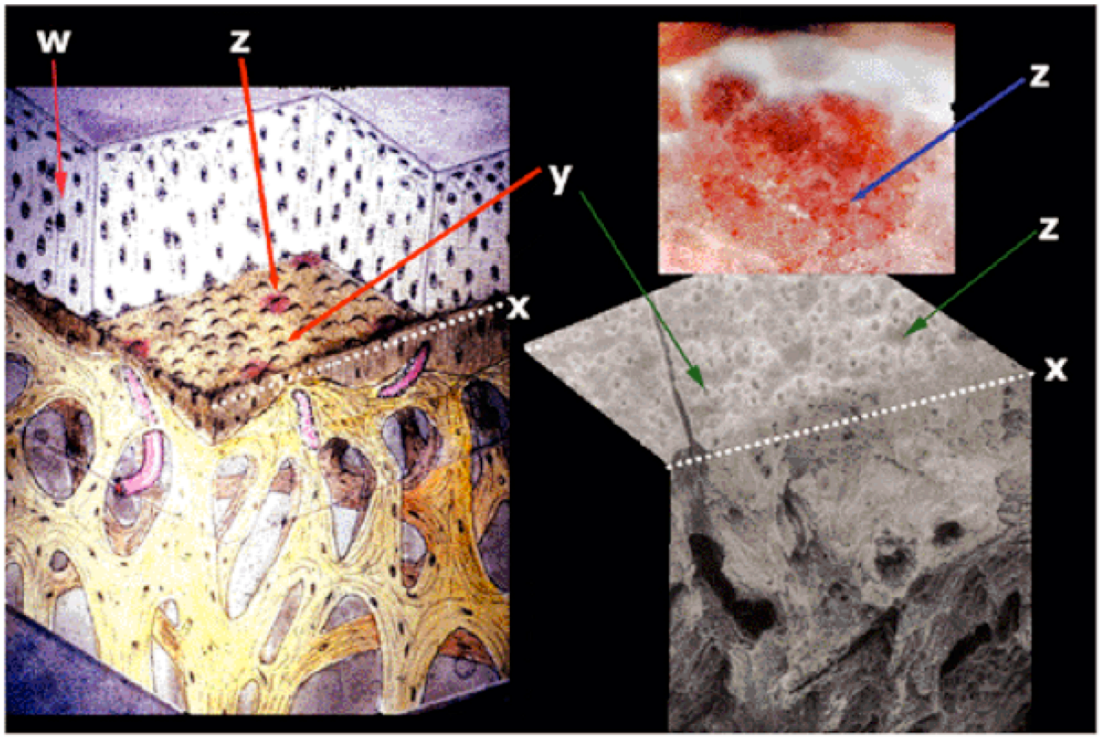

Figure 1.1: This diagram depicts the articular surface of the osteochondral (bone/cartilage) interface in a joint. The variation of the organization of cells in the protective articular cartilage can be seen at arrow **w**. The surface of the tidemark is visible in the cutout, **x**. **y** depicts the hypertrophic, calcification front. The vascularization that begins to penetrate the hypertrophic cartilage region is shown at **z** in the upper right. The bottom right is a scanning electron micrograph image of the corresponding diagram at **x**.
Image reprinted with permission [1]

tissue, although, it is only active in the region directly surrounding chondrocytes, and given the low cell density of cartilage, the turnover of aggrecan is slow (8-300 days) and collagen is very slow (>100 years) [4], making cartilage a tissue that does not have the capacity to repair itself. As a person ages, the limited repair capacity of cartilage is hindered even further. The cellularity of the tissue decreases as well as the availability of chondrogenic progenitor cells. Additionally, the composition of the ECM begins to change with a decrease in aggrecan content as well as undesired cross-linking and a reduction of the molecular weight of the collagen fibrils causing the collagen to become more stiff and ultimately more brittle [4].

Cartilage has a very limited capacity to heal itself. As mentioned previously, there are generally three categories of cartilage injuries: cartilage microfractures, chondral defects, or osteochondral defects. Cartilage microfractures and chondral defects do not heal well because there are very few articular chondrocytes and few healing components can diffuse through the dense ECM. The healing process continues on for ~2 weeks, but it rarely fills the defect and typically fills it with mechanically inferior fibrocartilage [4]. If the injury is osteochondral in nature, progenitor cells are recruited to the injury site and dominate the healing process. A fibrin clot is formed, mesenchymal stromal cells are recruited and differentiate, and synthesize both types I and II collagen. Both hyaline and fibrocartilage are typically formed, but due to the formation of fibrocartilage, ultimately the "healed" cartilage breaks down and can be a precursor to OA.

1.2.2 Osteochondral Interface

In addition to forming mature articular chondrocytes, chondrocytes also have the potential of becoming hypertrophic chondrocytes, depending on their spatial location within the

cartilage, which participate in endochondral ossification [7]. Osteogenesis to form bone can occur through two different methods, directly through the conversion of mesenchymal tissue into bone, known as intramembranous ossification, or through the calcification of cartilage tissue, known as endochondral ossification [4]. Since there is a transition region between articular cartilage and the underlying subchondral bone (osteochondral interface), the chondrocytes in this region become hypertrophic (Fig. 1). Hypertrophic chondrocytes increase their cell volume, begin producing type X collagen, initiate the calcification process, and upregulate VEGF which ultimately leads to the vascularization that is present in bone [4].

The osteochondral interface serves to provide the important attachment for articular cartilage to the underlying subchondral bone. This interface also serves to provide a transition region for the dissimilar mechanical properties of articular cartilage and bone. Through this mechanical property transition, this tissue interface allows for a transmission of the mechanical forces present in the joint [8]. This interfacial region contains a zone of calcified cartilage bordered by a wavy tidemark region. This tidemark provides the boundary between the junction of the mineralized and non-mineralized cartilage zones [9]. The surface of the underlying subchondral bone is highly irregular [9]. It is thought that the subchondral bone and the overlying calcified cartilage region are held together through interdigitation of the irregular boney surface "into" the cartilage region rather than through collagenous fibers that might span the two regions [9]. Therefore, the osteochondral interface serves an invaluable role in healthy and normal joint function.

1.2.3 Bone

There are two types of bone structure found in the body: cortical and trabecular bone. Cortical bone is the primary type of bone in the body (80% of the total mass of the skeleton [5]). It is the type of bone found on the articulating surfaces in the joints, whereas trabecular bone fills the inner portion of the proximal and distal ends of the long bones. Cortical bone is a very dense tissue comprised primarily of type I collagen, mineralized matrix, and water [5].

Type I collagen, the most abundant collagen in bone provides tensile strength and flexibility in bones. In addition to type I collagen, there are several other non-collagenous proteins which have a variety of functions within bone, including, but not limited to: alkaline phosphatase (ALP) (a cell surface glycoprotein that hydrolyzes mineral deposition inhibitors and serves as a an indicator of bone metabolism [10]), osteocalcin (may regulate the activity of osteoblasts and their precursors), osteonectin (selectively binds to both hydroxyapatite and type I collagen ECM phases serving to initiate active mineralization [11]), and osteopontin (may regulate cell attachment) [5]. The mineralized matrix in bone, known as hydroxyapatite (HA), provides bone with stiffness and strength [5]. Additionally, water plays an important role in the mechanical integrity of bone, contributing significantly to the viscoelastic component of bone through hydrogen bonding interactions with collagen [5].

Although osteoarthritis often begins with injury or degradation of the cartilage, it also affects the underlying bone. When the protective cartilage is damaged or eroded, the underlying bone begins to experience overloading potentially resulting in microfractures and/or the formation of bone or bone/cartilage fragments [1]. Although bone itself has a high capacity for self renewal and repair, articulating bone requires the “protective coating” that the articular

cartilage provides. As such, the role of bone in OA, and subsequently, the need to include subchondral bone in cartilage and osteochondral repair strategies is crucial.

1.3 Current Clinical and Tissue Engineering Therapies

1.3.1 *Current Clinical Therapies*

Currently there are a variety of nonsurgical and surgical therapy options available to treat both primary and secondary OA conditions. Nonsurgical treatments include injections of corticosteroids or visco-supplementation, i.e. SYNVISC® of Hyalgan® and pain management using NSAIDS or COX-2 inhibitors. Although these treatments are noninvasive, they only serve to provide a temporary fix and certainly do not provide a solution to fix the underlying cause of the OA.

There are also several surgical techniques available that have shown limited success in reducing pain and restoring joint mobility in severe OA cases. These therapies include, but are not limited to partial knee resurfacing (PKR) (~70,000 in the U.S. every year) [12], mosaicplasty, autologous chondrocyte implantation (ACI) [4, 13], microfracture [14], or total knee replacement (~130,000 in the U.S. every year) [15].

Although many of these therapies provide short-term solutions and increased pain management, there remains a need for a therapy capable of regenerating functional articular cartilage with appropriate mechanical properties capable of integrating with both the underlying bone through the osteochondral interface as well as with the surrounding cartilage tissue. As such, there is an obvious need to develop an *in vitro* osteochondral tissue engineering model to investigate the necessary components towards the future development of a successful *in vivo* osteochondral tissue engineering therapy.

1.3.2 Current Tissue Engineering Therapies

Current clinical tissue engineering (TE) strategies for OA conditions are limited to treatment of secondary OA cases and have logistical implementation difficulties. Currently, the available treatments are limited to focal adhesions and injurious models, typically involving repair spanning the subchondral bone. Two current osteochondral TE strategies that have been used for well over a decade are bone morphogenetic protein (BMP) laden collagen sponges [16, 17] and exogenous fibrin clots [18]. While both therapies provide improved healing response, they are limited by problems with lack of integration of the engineered tissue with the surrounding tissue and with difficulties concerning sterilization methods while maintaining the efficacy of the utilized cytokines (BMPs).

1.4 Tissue Engineering Strategies

Since the adult human body has minimal capacity to functionally regenerate articular cartilage, cartilage has been a primary target for tissue engineering strategies for several decades [4]. Tissue engineering strategies aim to create a new, functional tissue with similar biochemical and biomechanical properties to the native tissue that is also able to integrate with the surrounding healthy tissue. To accomplish this successful integration, it is also important for musculoskeletal tissue engineering strategies to consider the interfacial transitions between distinct tissues such as tendon/ligament to bone (enthesis), muscle to tendon (myotendinous), and cartilage to bone (osteochondral). As such, developing an osteochondral tissue engineering strategy involving cartilage, bone, and the interfacial region between the two distinct tissues will ultimately be required to implement successful cartilage tissue engineering strategies. To this end, the current tissue engineering paradigm involves selecting a suitable cell source, developing

an appropriate 3D scaffold for the application, and delivering appropriate biochemical and biomechanical cues [19].

1.4.1 Cell Source

Adult mesenchymal stem cells or more appropriately referred to as marrow stromal cells (MSCs) provide an attractive cell source due to their ability to differentiate down several lineages including cartilage and bone [7, 20-24] as well as the ease with which they are obtained and can be expanded in culture whilst maintaining their ability to differentiation down several useful lineages [25, 26]. As scientists begin to better understand the internal and external cues that direct stem cell differentiation, we are able to utilize the unrealized potential of these cells for many tissue engineering applications [24, 27].

Specifically, investigating the use of human MSCs (hMSCs) is important for potential clinical applications of tissue engineering therapies in the future, as the use of an autologous cell source would mitigate the problem of the requirement of a lifetime of immunosuppressant drugs necessary for allogeneic treatments. Additionally, although there are many sources of MSCs such as equine, porcine and bovine that many investigators elect to investigate (both adolescent and adult), each species of cells behave differently under similar experimental conditions [28-32]. As such, human MSCs are a logical choice to use to investigate the biochemical and biomechanical cues that are important when designing an appropriate scaffold for osteochondral tissue engineering applications.

1.4.2 Scaffold

There are many natural and synthetic biomaterial choices available to design scaffolds for orthopedic tissue engineering applications. There are many examples of hydroxyapatite based scaffolds for bone applications [33-35] and natural polymers such as agarose [36] and alginate [37] for cartilage applications. Additionally, several synthetic polymers such as poly(ethylene glycol) based [38], poly(aldehyde guluronate) based [39], and poly(vinyl alcohol) based hydrogels [40] have been used for both chondrogenic and osteogenic applications [41].

Synthetic hydrogels are a popular platform to study the behavior of encapsulated cells with the goal of developing tissue engineering strategies [41, 42l]. Specifically, photopolymerizable poly(ethylene glycol) (PEG) hydrogels have several attractive properties for tissue engineering applications and have been widely studied and characterized, previously [43, 44]. They have mild reaction chemistries suitable for viable cell encapsulations, easily tunable macroscopic properties such as hydrogel stiffness, and are highly water swollen [45] as well as being *in situ* forming [46] for potential clinical applications. While PEG itself is bioinert, it is easy to covalently incorporate biologically active moieties [47, 48] into these hydrogels.

1.4.2.1 Incorporation of ECM Moieties

Several groups are investigating the presentation of biochemical cues in scaffolds fabricated with ECM components and ECM component analogs found in both bone and cartilage [49-52]. Tampieri *et al*. [52] have reported success using biomimetic scaffolds with Mg-doped hydroxyapatite crystals seeded onto type I collagen fibers. Noth *et al*. [53] have demonstrated successful chondrogenic differentiation of MSCs embedded in type I collagen scaffolds in the presence of TGF-β. P-15 adsorbed onto anorganic bone matrix particles has been shown to

enhance mineralized matrix formation by periodontal ligament fibroblasts [54]. Many approaches to biomimetic ECM presentation in 3D have been explored using both cellular and acellular scaffolds for applications to bone, cartilage, and osteochondral tissue engineering strategies.

1.4.3 Biomechanical Cues

It is well known that biomechanical forces present in joints are necessary to maintain tissue homeostasis and healthy joint function; subsequently these forces also contribute to the normal healing process of bone and cartilage [55-58]. To date, many studies have focused on the exogenous delivery of biochemical cues to direct MSCs down chondrogenic and osteogenic lineages when cultured in several different types of 3D scaffolds [49, 59-61], however there is mounting evidence that mechanical forces also play an important role in stem cell differentiation. A seminal paper by Engler *et al*. [62] demonstrated that matrix stiffness was sufficient to direct stem cell differentiation in 2D down different lineages in the absence of any specific soluble biochemical cues, where the more stiff substrates promoted osteogenesis. A number of studies have demonstrated that applied mechanical forces can influence stem cell fate. Recently, dynamic loading of goat MSCs in unmodified PEG hydrogels was shown to have a positive effect on chondrogenic differentiation [30].

Several investigators have found that dynamic compressive loading applied in a variety of forms to MSCs in combination with chondrogenic biochemical factors enhance chondrogenic gene expression and cartilage matrix deposition [28, 29] while others have reported that dynamic loading inhibits chondrogenesis [63]. A few studies have reported that in the absence of TGF-β, a known chondrogenic differentiation factor, the application of dynamic compressive loading

alone may be sufficient to induce chondrogenic differentiation [28, 29, 32]. Dynamic loading has led to variable responses for chondrogenic differentiation of MSCs suggesting that the 3D scaffold environment may play an important role in the differentiation behavior of encapsulated MSCs with the application of dynamic loading.

Additionally, a number of studies have shown that cyclic tensile strain applied to MSCs promotes osteogenesis in 2D and 3D [64-67]. However, the effect of dynamic compressive strains in the osteogenesis of MSCs is not well known even though osteoblasts have been shown to respond favorably to cyclic compressive strains [68, 69]. Even fewer groups have looked at the application of loading to composite scaffolds for osteochondral applications, with the majority of the work to date being theoretical simulations [70, 71].

1.5 Current osteochondral tissue engineering strategies

Given that a successful osteochondral tissue engineering strategy will require engineering three distinctly different tissues, current strategies have taken several widely varied approaches to this challenging problem [72]. One approach is to combine a form of inorganic mineralized matrix such as tricalcium phosphate or decellularized trabecular bone, which would mimic the stiff boney region, with soft hydrogel polymers such as poly(lactic-co-glycolic acid), poly(lactic acid), or agarose to represent the cartilage region [73-77]. Alternatively, hydrogel only approaches, with the advantage of being *in situ* forming, have been taken [78, 79]. For example, individual layers of poly(ethylene glycol)-based hydrogels have been formed from the same structure, but with different cell types and growth factors to guide the formation of both bone and cartilage within a single scaffold [79].

1.6 Approach of this thesis

Towards developing osteochondral tissue engineering strategies, it is evident that there still remains a need to better understand the external cues that can concomitantly differentiate MSCs down both chondrogenic and osteogenic lineages within a single scaffold. To this end, given that mechanical and biochemical cues are present and inextricably linked *in vivo*, this research aims to investigate biochemical (through scaffold design) and biomechanical (through controlled external mechanical stimuli) cues towards developing a successful scaffold for guiding osteochondral tissue engineering applications.

Two key areas of focus that this thesis specifically addresses that are currently lacking in the field are: 1.) the fabrication and characterization of an appropriate scaffold specifically designed for the osteochondral tissue interface, and 2.) the investigation of the combined effect of biochemical and physiological biomechanical cues on encapsulated, undifferentiated hMSCs in these osteochondral scaffolds. The work presented in this thesis advances our understanding of how hMSCS behave in biomimetically modified PEG based hydrogels. Two biomimetic moieties of specific interest to this research are chondroitin sulfate (ChS) and P-15. ChS is a sulfated glycosaminoglycan (GAG) that is found natively in cartilage, which has previously been shown to support chondrogenic MSC differentiation in 3D scaffolds modified with ChS [80] but has not been investigated with human MSCs, and P-15 which is a 15 amino acid binding peptide analog of type I collagen and has shown great promise in enhancing cell attachment and osteoblastic activity [54, 81-83] but has yet to be investigated with MSCs in 3D PEG hydrogels.

This work describes the investigation of the behavior of hMSCs in several modified PEG based hydrogels as well as the behavior of these cells in an osteochondral composite, biomimetic PEG based scaffold combined with mechanical stimulation.

1.7 References

[1] Bullough PG. Histology for Pathologists, 3rd Edition In: Mills SE, editor. Philladelphia, PA: Lippincott Williams & Wilkins 2007.

[2] Hunter DJ. Osteoarthritis Preface. Clinics in Geriatric Medicine 2010;26:Xi.

[3] Losina E, Walensky RP, Reichmann WM, Holt HL, Gerlovin H, Solomon DH, Jordan JM, Hunter DJ, Suter LG, Weinstein AM, Paltiel AD, Katz JN. Impact of Obesity and Knee Osteoarthritis on Morbidity and Mortality in Older Americans. Ann. Intern. Med. 2011;154:217.

[4] Kyriacos A. Athanasiou EMD, Jerry C. Hu. Articular Cartilage Tissue Engineering. Kyriacos A. Athanasiou, editor. Synthesis Lectures on Tissue Engineering. electronic: Morgan & Claypool, 2010. p.182.

[5] X. Wang JSN, X. Dong, H. Leng, M. Reyes. Fundamental Biomechanics in Bone Tissue Engineering. In: Kyriacos A. Athanasiou JKL, editor. Synthesis Lectures on Tissue Engineering: Morgan & Claypool Publishers, 2010.

[6] Aszodi A, Hunziker EB, Olsen BR, Fassler R. The role of collagen II and cartilage fibril-associated molecules in skeletal development. Osteoarthritis Cartilage 2001;9:S150.

[7] Johnstone B, Hering TM, Caplan AI, Goldberg VM, Yoo JU. In vitro chondrogenesis of bone marrow-derived mesenchymal progenitor cells. Exp. Cell Res. 1998;238:265.

[8] Burr DB. Anatomy and physiology of the mineralized tissues: roles in the pathogenesis of osteoarthritis. Osteoarthritis Cartilage 2004;12:S20.

[9] Oegema TR, Carpenter RJ, Hofmeister F, Thompson RC. The interaction of the zone of calcified cartilage and subchondral bone in osteoarthritis. Microscopy Research and Technique 1997;37:324.

[10] Kress BC. Bone alkaline phosphatase: Methods of quantitation and clinical utility. Journal of Clinical Ligand Assay 1998;21:139.

[11] Termine JD, Kleinman HK, Whitson SW, Conn KM, McGarvey ML, Martin GR. Osteonectin, a bone-specific protein linking mineral to collagen. Cell 1981;26:99.

[12] Partial Knee Resurfacing. 2011.

[13] Mirzayan R. Cartilage Injury in the Athlete. New York, NY: Thieme Medical Publishers, 2006.

[14] Mithoefer K, Williams RJ, Warren RF, Wickiewicz TL, Marx RG. High-impact athletics after knee articular cartilage repair: a prospective evaluation of the microfracture technique. The American journal of sports medicine 2006;34:1413.

[15] Simon H Palmer MMJC, MBBS, FRACS. Total Knee Arthroplasty. WebMD, Sep 21, 2010.

[16] Friess W, Uludag H, Foskett S, Biron R. Bone regeneration with recombinant human bone morphogenetic protein-2 (rhBMP-2) using absorbable collagen sponges (ACS): Influence of processing on ACS characteristics and formulation. Pharmaceutical Development and Technology 1999;4:387.

[17] Geiger M, Li RH, Friess W. Collagen sponges for bone regeneration with rhBMP-2. Advanced Drug Delivery Reviews 2003;55:1613.

[18] Paletta GA, Arnoczky SP, Warren RF. The Repair of Osteochondral Defects Using an Exogenous Fibrin Clot - an Experimental-Study in Dogs. American Journal of Sports Medicine 1992;20:725.

[19] Lenas P, Luyten FP. An Emerging Paradigm in Tissue Engineering: From Chemical Engineering to Developmental Engineering for Bioartificial Tissue Formation through a Series of Unit Operations that Simulate the In Vivo Successive Developmental Stages. Industrial & Engineering Chemistry Research 2011;50:482.

[20] Caplan AI. Mesenchymal stem cells. J. Orthop. Res. 1991;9:641.

[21] Pittenger MF, Mackay AM, Beck SC, Jaiswal RK, Douglas R, Mosca JD, Moorman MA, Simonetti DW, Craig S, Marshak DR. Multilineage potential of adult human mesenchymal stem cells. Science 1999;284:143.

[22] Yoo JU, Barthel TS, Nishimura K, Solchaga L, Caplan AI, Goldberg VM, Johnstone B. The chondrogenic potential of human bone-marrow-derived mesenchymal progenitor cells. J Bone Joint Surg Am 1998;80A:1745.

[23] Richardson SM, Hoyland JA, Mobasheri R, Csaki C, Shakibaei M, Mobasheri A. Mesenchymal Stem Cells in Regenerative Medicine: Opportunities and Challenges for Articular Cartilage and Intervertebral Disc Tissue Engineering. J. Cell. Physiol. 2010;222:23.

[24] Bruder SP, Fink DJ, Caplan AI. Mesenchymal stem cells in bone development, bone repair, and skeletal regeneration therapy. Journal of Cellular Biochemistry 1994;56:283.

[25] Otto WR, Rao J. Tomorrow's skeleton staff: mesenchymal stem cells and the repair of bone and cartilage. Cell Proliferation 2004;37:97.

[26] Gimble JM, Guilak F, Nuttall ME, Sathishkumar S, Vidal M, Bunnell BA. In vitro differentiation potential of mesenchymal stem cells. Transfusion Medicine and Hemotherapy 2008;35:228.

[27] Bruder SP, Jaiswal N, Ricalton NS, Mosca JD, Kraus KH, Kadiyala S. Mesenchymal stem cells in osteobiology and applied bone regeneration. Clinical Orthopaedics and Related Research 1998:S247.

[28] Huang CYC, Hagar KL, Frost LE, Sun YB, Cheung HS. Effects of cyclic compressive loading on chondrogenesis of rabbit bone-marrow derived mesenchymal stem cells. Stem Cells 2004;22:313.

[29] Campbell JJ, Lee DA, Bader DL. Dynamic compressive strain influences chondrogenic gene expression in human mesenchymal stem cells. Biorheology 2006;43:455.

[30] Terraciano V, Hwang N, Moroni L, Park HB, Zhang Z, Mizrahi J, Seliktar D, Elisseeff J. Differential response of adult and embryonic mesenchymal progenitor cells to mechanical compression in hydrogels. Stem Cells 2007;25:2730.

[31] Bosnakovski D, Mizuno M, Kim G, Ishiguro T, Okumura M, Iwanaga T, Kadosawa T, Fujinaga T. Chondrogenic differentiation of bovine bone marrow mesenchymal stem cells in pellet cultural system. Experimental Hematology 2004;32:502.

[32] Kisiday JD, Frisbie DD, McIlwraith CW, Grodzinsky AJ. Dynamic Compression Stimulates Proteoglycan Synthesis by Mesenchymal Stem Cells in the Absence of Chondrogenic Cytokines. Tissue Engineering Part A 2009;15:2817.

[33] Oliveira JM, Rodrigues MT, Silva SS, Malafaya PB, Gomes ME, Viegas CA, Dias IR, Azevedo JT, Mano JF, Reis RL. Novel hydroxyapatite/chitosan bilayered scaffold for osteochondral tissue-engineering applications: Scaffold design and its performance when seeded with goat bone marrow stromal cells. Biomaterials 2006;27:6123.

[34] Venugopal J, Prabhakaran MP, Zhang YZ, Low S, Choon AT, Ramakrishna S. Biomimetic hydroxyapatite-containing composite nanofibrous substrates for bone tissue engineering. Philos. Trans. R. Soc. A-Math. Phys. Eng. Sci. 2010;368:2065.

[35] Yoshikawa H, Tamai N, Murase T, Myoui A. Interconnected porous hydroxyapatite ceramics for bone tissue engineering. J. R. Soc. Interface 2009;6:S341.

[36] Mauck RL, Soltz MA, Wang CCB, Wong DD, Chao PHG, Valhmu WB, Hung CT, Ateshian GA. Functional tissue engineering of articular cartilage through dynamic loading of chondrocyte-seeded agarose gels. J Biomech Eng-T Asme 2000;122:252.

[37] Connelly JT, Garcia AJ, Levenston ME. Inhibition of in vitro chondrogenesis in RGD-modified three-dimensional alginate gels. Biomaterials 2007;28:1071.

[38] Bryant SJ, Anseth KS. Controlling the spatial distribution of ECM components in degradable PEG hydrogels for tissue engineering cartilage. Journal of Biomedical Materials Research Part A 2003;64A:70.

[39] Bouhadir KH, Hausman DS, Mooney DJ. Synthesis of cross-linked poly(aldehyde guluronate) hydrogels. Polymer 1999;40:3575.

[40] Martens P, Anseth KS. Characterization of hydrogels formed from acrylate modified poly(vinyl alcohol) macromers. Polymer 2000;41:7715.

[41] Drury JL, Mooney DJ. Hydrogels for tissue engineering: scaffold design variables and applications. Biomaterials 2003;24:4337.

[42] Liu SQ, Tay R, Khan M, Ee PLR, Hedrick JL, Yang YY. Synthetic hydrogels for controlled stem cell differentiation. Soft Matter 2010;6:67.

[43] Bryant SJ, Anseth KS, Lee DA, Bader DL. Crosslinking density influences the morphology of chondrocytes photoencapsulated in PEG hydrogels during the application of compressive strain. J. Orthop. Res. 2004;22:1143.

[44] Bryant SJ, Anseth, K. S. . Photopolymerization of Hydogel Scaffolds.69.

[45] Bryant SJ, Anseth KS. Hydrogel properties influence ECM production by chondrocytes photoencapsulated in poly(ethylene glycol) hydrogels. Journal of Biomedical Materials Research 2002;59:63.

[46] Anseth KS, Metters AT, Bryant SJ, Martens PJ, Elisseeff JH, Bowman CN. In situ forming degradable networks and their application in tissue engineering and drug delivery. J Control Release 2002;78:199.

[47] Hern DL, Hubbell JA. Incorporation of adhesion peptides into nonadhesive hydrogels useful for tissue resurfacing. Journal of Biomedical Materials Research 1998;39:266.

[48] Zhu JM. Bioactive modification of poly(ethylene glycol) hydrogels for tissue engineering. Biomaterials 2010;31:4639.

[49] Ho STB, Cool SM, Hui JH, Hutmacher DW. The influence of fibrin based hydrogels on the chondrogenic differentiation of human bone marrow stromal cells. Biomaterials 2010;31:38.

[50] Zhou XZ, Leung VY, Dong QR, Cheung KM, Chan D, Lu WW. Mesenchymal stem cell-based repair of articular cartilage with polyglycolic acid-hydroxyapatite biphasic scaffold. International Journal of Artificial Organs 2008;31:480.

[51] Wang W, Li B, Yang JZ, Xin L, Li YL, Yin HP, Qi YY, Jiang YZ, Ouyang HW, Gao CY. The restoration of full-thickness cartilage defects with BMSCs and TGF-beta 1 loaded PLGA/fibrin gel constructs. Biomaterials 2010;31:8964.

[52] Tampieri A, Sandri M, Landi E, Pressato D, Francioli S, Quarto R, Martin I. Design of graded biomimetic osteochondral composite scaffolds. Biomaterials 2008;29:3539.

[53] Noth U, Rackwitz L, Heymer A, Weber M, Baumann B, Steinert A, Schutze N, Jakob F, Eulert J. Chondrogenic differentiation of human mesenchymal stem cells in collagen type I hydrogels. Journal of Biomedical Materials Research Part A 2007;83A:626.

[54] Bhatnagar RS, Qian JJ, Wedrychowska A, Sadeghi M, Wu YM, Smith N. Design of biomimetic habitats for tissue engineering with P-15, a synthetic peptide analogue of collagen. Tissue Eng 1999;5:53.

[55] Bikle DD, Halloran BP. The response of bone to unloading. Journal of Bone and Mineral Metabolism 1999;17:233.

[56] Skerry TM. The response of bone to mechanical loading and disuse: Fundamental principles and influences on osteoblast/osteocyte homeostasis. Archives of Biochemistry and Biophysics 2008;473:117.

[57] Mullender M, El Haj AJ, Yang Y, van Duin MA, Burger EH, Klein-Nulend J. Mechanotransduction of bone cells in vitro: mechanobiology of bone tissue. Medical & Biological Engineering & Computing 2004;42:14.

[58] Sandell LJ, Aigner T. Articular cartilage and changes in arthritis - An introduction: Cell biology of osteoarthritis. Arthritis Research 2001;3:107.

[59] Temenoff JS, Park H, Jabbari E, Conway DE, Sheffield TL, Ambrose CG, Mikos AG. Thermally cross-linked oligo(poly(ethylene glycol) fumarate) hydrogels support osteogenic differentiation of encapsulated marrow stromal cells in vitro. Biomacromolecules 2004;5:5.

[60] Nuttelman CR, Tripodi MC, Anseth KS. In vitro osteogenic differentiation of human mesenchymal stem cells photoencapsulated in PEG hydrogels. Journal of Biomedical Materials Research Part A 2004;68A:773.

[61] Mauck RL, Yuan X, Tuan RS. Chondrogenic differentiation and functional maturation of bovine mesenchymal stem cells in long-term agarose culture. Osteoarthritis Cartilage 2006;14:179.

[62] Engler AJ, Sen S, Sweeney HL, Discher DE. Matrix elasticity directs stem cell lineage specification. Cell 2006;126:677.

[63] Thorpe SD, Buckley CT, Vinardell T, O'Brien FJ, Campbell VA, Kelly DJ. Dynamic compression can inhibit chondrogenesis of mesenchymal stem cells. Biochemical and Biophysical Research Communications 2008;377:458.

[64] Qi MC, Hu J, Zou SJ, Chen HQ, Zhou HX, Han LC. Mechanical strain induces osteogenic differentiation: Cbfa1 and Ets-1 expression in stretched rat mesenchymal stem cells. International Journal of Oral and Maxillofacial Surgery 2008;37:453.

[65] Zhao HB, Lu TD, Ma J, Ma H, Zhang XZ. Mechanotransduction in differentiation of osteogenic from mesenchymal stem cells. Progress In Biochemistry And Biophysics 2007;34:718.

[66] Sumanasinghe RD, Bernacki SH, Loboa EG. Osteogenic differentiation of human mesenchymal stem cells in collagen matrices: Effect of uniaxial cyclic tensile strain on bone morphogenetic protein (BMP-2) mRNA expression. Tissue Eng 2006;12:3459.

[67] Byrne EM, Farrell E, McMahon LA, Haugh MG, O'Brien FJ, Campbell VA, Prendergast PJ, O'Connell BC. Gene expression by marrow stromal cells in a porous collagen-glycosaminoglycan scaffold is affected by pore size and mechanical stimulation. J. Mater. Sci.-Mater. Med. 2008;19:3455.

[68] Yanagisawa M, Suzuki N, Mitsui N, Koyama Y, Otsuka K, Shimizu N. Compressive force stimulates the expression of osteogenesis-related transcription factors in ROS 17/2.8 cells. Archives Of Oral Biology 2008;53:214.

[69] Rath B, Nam J, Knobloch TJ, Lannutti JJ, Agarwal S. Compressive forces induce osteogenic gene expression in calvarial osteoblasts. J Biomech 2008;41:1095.

[70] Kelly DJ, Prendergast PJ. Mechano-regulation of stem cell differentiation and tissue regeneration in osteochondral defects. J Biomech 2005;38:1413.

[71] McMahon LA, Reid AJ, Campbell VA, Prendergast PJ. Regulatory effects of mechanical strain on the chondrogenic differentiation of MSCs in a collagen-GAG scaffold: Experimental and computational analysis. Ann Biomed Eng 2008;36:185.

[72] Schaefer D, Martin I, Shastri P, Padera RF, Langer R, Freed LE, Vunjak-Novakovic G. In vitro generation of osteochondral composites. Biomaterials 2000;21:2599.

[73] Sherwood JK, Riley SL, Palazzolo R, Brown SC, Monkhouse DC, Coates M, Griffith LG, Landeen LK, Ratcliffe A. A three-dimensional osteochondral composite scaffold for articular cartilage repair. Biomaterials 2002;23:4739.

[74] Jiang CC, Chiang H, Liao CJ, Lin YJ, Kuo TF, Shieh CS, Huang YY, Tuan RS. Repair of porcine articular cartilage defect with a biphasic osteochondral composite. J. Orthop. Res. 2007;25:1277.

[75] Lima EG, Mauck RL, Han SH, Park S, Ng KW, Ateshian GA, Hung CT. Functional tissue engineering of chondral and osteochondral constructs. Biorheology 2004;41:577.

[76] Hung CT, Lima EG, Mauck RL, Taki E, LeRoux MA, Lu HH, Stark RG, Guo XE, Ateshian GA. Anatomically shaped osteochondral constructs for articular cartilage repair. J Biomech 2003;36:1853.

[77] Lima EG, Chao PHG, Ateshian GA, Bal BS, Cook JL, Vunjak-Novakovic G, Hung CT. The effect of devitalized trabecular bone on the formation of osteochondral tissue-engineered constructs. Biomaterials 2008;29:4292.

[78] Holland TA, Bodde EWH, Baggett LS, Tabata Y, Mikos AG, Jansen JA. Osteochondral repair in the rabbit model utilizing bilayered, degradable oligo(poly(ethylene glycol) fumarate) hydrogel scaffolds. Journal of Biomedical Materials Research Part A 2005;75A:156.

[79] Liu C, Xia Z, Czernuszka JT. Design and development of three-dimensional scaffolds for tissue engineering. Chem. Eng. Res. Des. 2007;85:1051.

[80] Varghese S, Hwang NS, Canver AC, Theprungsirikul P, Lin DW, Elisseeff J. Chondroitin sulfate based niches for chondrogenic differentiation of mesenchymal stem cells. Matrix Biology 2008;27:12.

[81] Hole BB, Schwarz JA, Gilbert JL, Atkinson BL. A study of biologically active peptide sequences (P-15) on the surface of an ABM scaffold (PepGen P-15 (TM)) using AFM and FTIR. Journal of Biomedical Materials Research Part A 2005;74A:712.

[82] Nguyen H, Qian JJ, Bhatnagar RS, Li S. Enhanced cell attachment and osteoblastic activity by P-15 peptide-coated matrix in hydrogels. Biochemical and Biophysical Research Communications 2003;311:179.

[83] Lindley EM, Guerra FA, Krauser JT, Matos SM, Burger EL, Patel VV. Small peptide (P-15) bone substitute efficacy in a rabbit cancellous bone model. Journal of Biomedical Materials Research Part B-Applied Biomaterials 2010;94B:463.

Chapter 2: Objectives

To date, there have been many advances made in the field of osteochondral tissue engineering, including advances in both bone and cartilage tissue engineering. However, there still remain many challenges to overcome towards the goal of developing a successful osteochondral tissue interface engineering strategy. A functional osteochondral tissue engineering strategy not only must incorporate successful bone and cartilage tissue engineering strategies, but it must also focus on developing the critical osteochondral interface that provides for successful integration of engineered cartilage with the underlying bone, a crucial requirement for clinical success, and a requirement that is still a major challenge in the cartilage tissue engineering field, which is the driving force behind osteochondral tissue engineering strategies.

Several challenges exist in developing a strategy that involves combining two drastically different tissues such as bone and cartilage. These tissues have very different mechanical and biochemical properties that are joined together through the abrupt transition of the osteochondral interface. Although these two tissues have very different properties and functions in the body, they work synergistically, and have a common progenitor cell source, mesenchymal stromal cells (MSC). As such, this single cell source, combined with an appropriately designed 3D scaffold provides a suitable combination for developing a strategy for concomitant bone, cartilage and osteochondral interface tissue production within a single tissue engineered scaffold.

The overarching hypothesis for this research is that spatially controlling biomechanical and biochemical cues through a multi-layered hydrogel containing undifferentiated human MSCs leads to a layer of cartilage-like tissue, a layer of bone-like tissue and a region in between that has biochemical characteristics of the osteochondral region. As a first step towards testing this

overarching hypothesis, this thesis has four main objectives that are 1) to investigate the differentiation response of hMSCs to mechanical loading in PEG hydrogels during differentiation, 2) to investigate the differentiation response of hMSCs to PEG hydrogels biochemically modified with a cartilage extracellular matrix moiety, 3) to investigate the effect of PEG hydrogels biochemically modified with a bone-like extracellular matrix moiety on hMSC cell attachment and osteogenic biomarker molecule synthesis, and 4) to develop and fabricate a proof of concept three-dimensional (3D) multi-layered hydrogels with distinct biochemical and biomechanical cues in each layer.

Objective 1:

Investigate the response of hMSCs to mechanical loading in PEG hydrogels during differentiation.

Hypothesis: The application of intermittent dynamic loading enhances chondrogenic and osteogenic differentiation of hMSCs encapsulated in RGD modified PEG hydrogels.

In vivo, MSCs receive both biochemical and biomechanical differentiation cues. These cues are inextricably linked and always present in the body. As such, the development of a successful osteochondral tissue engineering strategy will need to be designed in such a way as to facilitate the local presentation of both types of cues. In this first thesis objective, we investigated how MSCs differentiate in response to the combination of external biochemical and mechanical cues through soluble differentiation factors combined with mechanical loading.

This objective investigated the effects of intermittent dynamic compressive loading on hMSCs when encapsulated in RGD modified PEG based hydrogels, in the presence and absence of chondrogenic and osteogenic soluble differentiation cues. It was hypothesized that the

application of intermittent dynamic compressive loading would enhance chondrogenic and osteogenic differentiation of hMSCs encapsulated in these hydrogels. Cell-laden hydrogels were subjected to intermittent dynamic compressive loading and hMSC response was evaluated by gene expression using real time RT-PCR for chondrogenic and osteogenic markers and histologically for matrix molecule deposition.

Objective 2

Investigate the differentiation response of hMSCs 1) to PEG hydrogels biochemically modified with a cartilage extracellular matrix moiety and 2) to the effect of mechanical loading in the biochemically modified hydrogels.

Hypothesis: The incorporation of chondroitin sulfate into PEG based scaffolds combined with intermittent dynamic loading enhances the chondrogenic differentiation of encapsulated hMSCs and the subsequent production of cartilage specific ECM molecules.

Although the generic RGD/PEG hydrogel system utilized in Objective 1 supported chondrogenic ECM molecule deposition by differentiating hMSCs in the absence of loading, we hypothesize that the hMSCs may need a more specific cartilage-like environment to provide external biochemical cues which, in combination with biomechanical cues, will further enhance cartilage ECM molecule deposition. Chondroitin sulfate (ChS) was chosen as the biomimetic moiety because it is a key ECM component in cartilage and is easily incorporated into the bioinert PEG scaffolds to provide a more "native" environment for the encapsulated hMSCs.

The goals of this study were two-fold: 1) to investigate the response of hMSCs encapsulated in ChS modified PEG based hydrogels, specifically whether the addition of the glycosaminoglycan (GAG) motif to the bioinert PEG scaffolds would promote chondrogenic

hMSC differentiation and whether the incorporation of ChS into the scaffolds would enhance chondrogenic ECM molecule production, and 2) to determine the impact of intermittent dynamic loading on hMSCs encapsulated in ChS modified PEG scaffolds. Based on the findings from the loading regime employed in Objective 1 that showed that the immediate application of dynamic compressive loading was inhibitory for the production of chondrogenic ECM matrix molecules, in addition, as part of this aim, we chose to employ an initial culture period to allow the cells time to begin chondrogenically differentiating before the application of the dynamic loading. hMSC response was evaluated via gene expression for chondrogenic differentiation markers and histologically for matrix molecule deposition.

Objective 3

Investigate the effect of PEG hydrogels biochemically modified with a bone-like extracellular matrix moiety on hMSC cell attachment and osteogenic biomarker molecule synthesis.

Hypothesis: The incorporation of the P-15 peptide motif into PEG based scaffolds promotes hMSC attachment and adhesion to PEG hydrogels and enhances the production of osteogenic biomarker molecules and the deposition of osteogenic ECM molecules.

In Objective 1, we utilized the ubiquitous peptide, RGD, to provide a cell-matrix interaction within our PEG based scaffolds. Although the RGD sequence provides a generic cell-binding domain, it is not bone ECM specific. P-15, however is a binding peptide that is an analog of type I collagen, the primary collagen found in bone. The goals of this study were to investigate the interaction and response of hMSCs with P-15 modified PEG based hydrogels. Specifically, initial studies were conducted in 2D to characterize the potential of hMSCs to

adhere to the P-15 modified PEG scaffolds, while 3D studies were conducted to address whether the addition of the biomimetic peptide motif to the bioinert PEG scaffolds would enhance cell survivability and osteogenic biomarker molecule matrix production within the cell laden hydrogel scaffolds.

To test our hypothesis that P-15 would enhance hMSC attachment to PEG hydrogels, 2D P-15 modified scaffolds were fabricated and seeded with undifferentiated hMSCs. Cells were assessed for attachment potential and analyzed for the production of an osteogenic ECM molecule via immunohistochemistry. Cell laden 3D P-15 modified scaffolds were fabricated, and we tested our hypothesis by assessing cell viability/survivability and the presence of bone biomarkers, specifically alkaline phosphatase production and calcium deposition in the P-15 modified PEG systems.

Objective 4

Develop, fabricate, and characterize a proof of concept, three-dimensional (3D) multi-layered hydrogel scaffold with distinct biochemical and biomechanical cues in each layer and to investigate the response of hMSCs to mechanical loading in the multi-layered scaffold.

Goal: To utilize the tailorability of PEG based hydrogels to develop a single multi-layered hydrogel scaffold containing layers with distinct biochemical and biomechanical cues that will support hMSCs towards the goal of spatially organized, concomitant production of both chondrogenic and osteogenic ECM molecules.

Hypothesis: The application of intermittent dynamic loading affects spatially organized production of chondrogenic and osteogenic ECM molecules by hMSCs encapsulated in multi-layered PEG hydrogels.

For this objective, we aim to show proof of concept of the development, fabrication and characterization of a single multi-layered scaffold that has three different layers (bone, cartilage, and osteochondral interface) with individually controlled mechanical and biochemical properties with the goal of guiding the development of a scaffold for osteochondral tissue engineering applications. Key findings from the first three thesis objectives critically guided the selection of material properties for the fabrication of our multi-layered hydrogel scaffold.

In vivo, cartilage cells experience much higher compressive strains than bone cells do. In light of this, our first goal was to design a scaffold with layers of varying degrees of stiffness such that under applied gross strains hMSCs encapsulated in one layer could be dynamically compressed while hMSCs in a separate layer would concurrently experience very little strain. Compressive properties of the individual layers as well as the multi-layered scaffold were measured, and Finite Element (FE) modeling was employed to help guide the appropriate selection of mechanical properties for the multi-layered hydrogel. Additionally, the local strains realized by the cells within each layer were measured and compared to the local strains predicted with the Finite Element model.

In addition to varying the mechanical properties within the scaffold, our second aim was to incorporate different biomimetic moieties into the different layers. We have covalently incorporated chondroitin sulfate (ChS) into the chondrogenic layer and the ubiquitous cell-binding domain, RGD, into the osteogenic layer, obtaining a combination of the two moieties in the osteochondral interface layer. Although RGD is a generic ECM binding domain, its

incorporation into the PEG based scaffold showed promise, in Objective 1, for the production of osteogenic matrix molecules by encapsulated hMSCs.

hMSCs were encapsulated in these scaffolds with distinct biomechanical and biochemical layers and were subjected to delayed intermittent dynamic loading as a proof of concept that a single multi-layered scaffold could be designed such that, under dynamic loading conditions, encapsulated hMSCs could concomitantly produce both chondrogenic and osteogenic ECM molecules in a spatially organized manner. This was tested through immunohistochemical analysis of several chondrogenic and osteogenic matrix molecules.

This research provides new insights into how hMSCs respond to both external biomechanical and biochemical cues. The fundamental understanding of how these cues affect hMSC differentiation and ECM production is critical for guiding the development of a successful osteochondral tissue engineering strategy.

Chapter 3

The Effects of Intermittent Dynamic Loading on Chondrogenic and Osteogenic Differentiation of Human Marrow Stromal Cells Encapsulated in RGD Modified PEG Hydrogels

(As appears in Acta Biomaterialia 7(11):3829-40 (2011))

Biochemical and biomechanical cues are known to influence the differentiation of stem cells. Biomechanical cues arise from cellular interactions with their surrounding matrix and from applied forces. This study investigates the role of biomechanical cues in chondrogenic and osteogenic differentiation of human marrow stromal cells (hMSCs) when encapsulated in synthetic hydrogels. Poly(ethylene glycol) hydrogels were fabricated with tethered cell adhesion moieties, RGD. Cell-laden hydrogels were subjected to four hour daily intermittent dynamic compressive loading (0.3 Hz, 15% amplitude strain) for up to 14 days and cell response evaluated by gene expression and matrix deposition for chondrogenic and osteogenic markers. The 3-D hydrogel supported chondrogenesis and osteogenesis under free swelling conditions as evidenced by upregulation of cartilage-related markers (SOX9, collagen II, X, and aggrecan) and staining for type II collagen and aggrecan and osteogenically by upregulation of ALP and staining for type I collagen and for mineralization. However, under dynamic loading, the expression of cartilage-related markers SOX9, collagens II, X, and aggrecan were downregulated along with reduced aggrecan staining and no positive staining for type II collagen. Additionally, bone-related markers RUNX2, Col I, and ALP were down regulated and positive staining for type I collagen and mineralization was reduced. In conclusion, the selected loading regime

appears to have an inhibitory effect on chondrogenesis and osteogenesis of hMSCs encapsulated in PEG/RGD hydrogels after 14 days in culture potentially due to overloading of the differentiating hMSCs before sufficient pericellular matrix is produced and/or due to large strains, particularly for osteogenically differentiating hMSCs.

3.1 Introduction

Biochemical and biomechanical cues are important in the overall maintenance of tissues as well as in promoting normal tissue growth during regenerative processes [1-3]. For example in the joint, biomechanical cues arise during physiological loading of joint tissues, where applied forces produce deformation and induce fluid movement within tissues. These events can lead to deformations in the cell membrane, fluid induced shear stresses at the cell surface, and a whole host of other events that will be dependent on the local physiological environment and the extracellular matrix (ECM) [1, 2, 4]. These events are sensed by the cells through processes termed mechanotransduction, which in turn regulate many cellular functions including proliferation, differentiation, and matrix synthesis [5]. From a tissue engineering perspective, mechanical forces most certainly play an important role in regenerating functional joint tissues.

It is well known that the physiological mechanical forces present in the joint are necessary to maintain tissue homeostasis in cartilage and bone while the lack of forces can lead to tissue degradation and diseases such as osteoarthritis and osteoporosis [4, 6-8]. However, mechanical signals perceived by cartilage and bone cells during normal physiological activity are complex and inextricably linked [1, 7, 9]. In cartilage, physiological loading in the form of dynamic compressive loading has led to enhanced tissue deposition by chondrocytes evidenced by increased production of proteoglycans and type II collagen, the two main components of cartilage ECM, and improved mechanical properties [2, 10-12]. For example, dynamic compressive loading at 0.1 Hz and 5% amplitude strains led to a 79% increase in glycosaminoglycan content compared to statically compressed explants [11]. In bone, interstitial fluid flow around bone cells is hypothesized to be a primary means by which mechanical information is transmitted to cells [13] with physiological strains being small in the range of 0.2-

0.3% [4, 7]. Nonetheless, several studies have shown that bone cells respond favorably to relatively large compressive strains when applied cyclically [14, 15]. For example, osteogenic genes were upregulated in osteoblasts when cultured under a 10% dynamic compressive strain [15].

In designing strategies for cartilage, bone, and/or osteochondral tissue engineering, adult human mesenchymal stem cells, or marrow stromal cells (MSCs), provide a promising cell source due to their ability to differentiate into either chondrocytes or osteoblasts [16] as well as their direct relevance in clinical applications. While many studies deliver soluble cues to direct MSCs down chondrogenic and osteogenic lineages when cultured in 3-D scaffolds [17-21], mechanical forces will be important as well [22]. Indeed, several studies have demonstrated that applied mechanical forces can influence chondrogenesis and osteogenesis of MSCs. For example, dynamic compressive loading applied in a variety of forms to MSCs from different species and in several different scaffold systems has been shown to enhance chondrogenic gene expression and/or cartilage matrix deposition either in combination with chondrogenic biochemical factors [23, 24] or alone [23-26]. However, others have reported that dynamic compressive loading inhibits chondrogenesis [27], suggesting that the biomechanical cues sensed by the cells are complex and dependent on numerous factors, e.g. scaffold type and cell source. A number of studies have shown that cyclic tensile strain applied to MSCs promotes osteogenesis in 2-D and 3-D [28-31]. The effects of dynamic compressive strains in the osteogenesis of MSCs, however, is less studied and not well known even though bone is subjected to compressive forces. Nonetheless, these studies among many others support the important role for mechanical forces in enhancing MSC differentiation, specifically for cartilage and bone tissue engineering strategies.

One promising platform for in situ delivery of MSCs for cartilage, bone and/or osteochondral tissue engineering with minimal invasiveness is hydrogels. Synthetic hydrogels are particularly attractive because they imbibe high amounts of water, their macroscopic properties, such as hydrogel stiffness, are tunable [32], and biological moieties are typically readily incorporated into the hydrogel [33]. In particular, poly(ethylene glycol) (PEG) hydrogels are one of the most common synthetic hydrogels used for cell encapsulation and have been shown to be suitable cell carries for human MSCs supporting chondrogenesis and osteogenesis [19, 20, 26, 34-36]. More recently, dynamic loading of goat MSCs in unmodified PEG hydrogels was shown to have a positive effect on chondrogenic differentiation [26]; however, the impact on human MSCs in PEG hydrogels have not been investigated to the best of our knowledge.

With the long-term goal of developing a clinically relevant in situ tissue engineering therapy for treating osteochondral defects in humans, the present study takes a first step by investigating the impact that dynamic compressive strains has on chondrogenic and osteogenic differentiation of human marrow stromal cells (hMSCs) when encapsulated in photopolymerizable PEG-based hydrogels. Based on evidence in the literature showing improved chondrogenesis [37] and osteogenesis [15] of differentiated cells under dynamic compressive loading, we hypothesized that the application of intermittent dynamic compressive loading enhances chondrogenic and osteogenic differentiation of hMSCs encapsulated in PEG-based hydrogels. A PEG hydrogel was chosen for its many benefits described above. In particular, we chose a formulation that resulted in a sufficiently loosely crosslinked network to support nutrient transport [38], cell survival [39], and macroscopic matrix evolution [32], but which exhibited mechanically integrity [40]. Furthermore, the RGD oligopeptide was chosen to incorporate into the PEG hydrogels because it represents a ubiquitous cell adhesion peptide that

is present within matrix molecules that make up both cartilage and bone [41]. It provides hMSCs, which are considered attachment dependent cells [42], a mechanism by which they can physically sense their surrounding substrate and hence enhance their survival [39], and it has been shown to support chondrogenesis [20] and osteogenesis [39] in human MSCs. As such, a RGD modified PEG hydrogel may serve as a ubiquitous 3D environment for osteochondral tissue engineering. Given the widely varied response of MSCs to different loading regimes, employed in a variety of scaffolds, reported by Babalola et al. [43], we selected an intermittent loading regime similar to one that has been shown to upregulate Col II by primary bovine chondrocytes encapsulated in PEG hydrogels [37]. Specifically, we examined hMSC differentiation in the absence and presence of intermittent dynamic loading when applied at the onset of differentiation and in the presence of chondrogenic or osteogenic differentiation medium. Differentiation was assed by gene expression and matrix deposition for chondrogenic and osteogenic markers over the course of 14 days.

3.2 Materials and Methods

3.2.1 hMSC isolation and cell culture

36 year old adult male Poietics™ Human Bone Marrow was obtained from Cambrex Bio Science (Walkersville, MD) and plated at 10 mL marrow/cm^2 in T-75 tissue culture polystyrene flasks. Marrow was supplemented with basal stem cell medium (10% fetal bovine serum (FBS, VWR; Bridgeport, NJ), 1mg/mL amphotericin B, 50 U/mL penicillin, 50 mg/mL streptomycin, and 20 mg/mL gentamicin in low glucose Dulbecco's modified Eagle medium (DMEM, Invitrogen; Carlsbad, CA) containing 1g/L glucose). The marrow/medium mixture was left untouched for one week to allow hMSC attachment. Medium was exchanged twice weekly until

confluency. hMSCs were re-plated at approximately 8000 cells/cm^2 and cultured for ~10 days. At passage two (P2), hMSCs were frozen and stored in liquid N_2 until further use. Cells were grown under standard cell culture conditions in a regulated incubator at 37ºC with 5% CO_2 conditions.

P2 cells were thawed and plated at approximately 5,000 to 6,000 cells/cm^2 in T-75 tissue culture polystyrene flasks. Cells were cultured in basal stem cell media supplemented with 1 ng/ml of recombinant human FGF-basic growth factor (b-FGF, Peprotech; Rocky Hill, NJ). Medium was changed twice weekly, and cells were split 1:3 from P2-P3 and 1:4 from P3-P4. Cells were used at P4.

3.2.2 Macromolecular Monomer Synthesis

Poly(ethylene glycol) diacrylate (PEGDA) macromolecular monomers were synthesized by reacting 3000 g/mol poly(ethylene glycol) (PEG) (Fluka, Sigma-Aldrich; St. Loius, MO) in dichloromethane with acryloyl chroride in the presence of triethylamine. The reaction was allowed to proceed for 24 hours at 4ºC. The reaction mixture was purified by precipitations with ethyl ether, filtered, and allowed to dry under vacuum.

Acryloyl-PEG-N-hydroxysuccinimide (acryloyl-PEG-SCM, 3400Da; Laysan Bio, Inc.; Arab, AL) was reacted with YRGDS (Genscript; Piscataway, NJ) in a 1:1.1 molar ratio (excess acryloly-PEG-SCM) in 50 mM sodium bicarboate buffer (pH 8.4) for 2 hrs at room temperature. The product, acryloyl-PEG-RGD was dialysed for 24 hrs, lyophilized, and stored at 4ºC.

3.2.3 hMSC Photoencapsulation

hMSCs were combined at a cell concentration of $5x10^6$ cells/mL with a sterile 10% (g/g) PEGDA solution containing 2.8 mM acryloyl-PEG-RGD and 0.05% (g/g) photoinitiator Irgacure 2959 (Ciba Specialty Chemicals; Tarrytown, NY) dissolved in one of three culture medium, basal (described above), chondrogenic differentiation medium (CDM), or osteogenic differentiation medium (ODM). CDM included 1ml/100 ml media ITS+ Premix (BD; Franklin Lakes, NJ), 100 nM dexamethasone, 5 ng/mL $TGFb_1$ (Peprotech), 50 mg/ml l-ascorbic acid 2-phosphate trisodium salt, 100 mg/ml sodium pyruvate, 1mg/mL amphotericin B, 50 U/mL penicillin, 50 mg/mL streptomycin, and 20 mg/mL gentamicin in high glucose Dulbecco's modified Eagle medium (DMEM, Invitrogen) containing 4.5g/L glucose. ODM included 100 nM dexamethasone, 50 mg/ml l-Ascorbic acid, 7 mM b-glycerophosphate, 10% fetal bovine serum (FBS, VWR), 1mg/mL amphotericin B, 50 U/mL penicillin, 50 mg/mL streptomycin, and 20 mg/mL gentamicin in low glucose Dulbecco's modified Eagle medium (DMEM, Invitrogen) containing 1g/L glucose. The cell/macromer solution was polymerized under 365 nm light with an intensity of ~5 mW/cm^2 for 10 minutes (Black Ray XX-20BLB UV Bench Lamp, Upland, CA). Cylindrical hMSC-laden hydrogel constructs (~5mm in height and 5 mm in diameter) were allowed to free swell in their respective culture medium for 24 hours at 37° and 5% CO_2 before loading.

3.2.4 Mechanical stimulation

A custom-built bioreactor system, as described elsewhere, was utilized to apply intermittent dynamic compressive strains to hMSC-laden hydrogel constructs (Fig. 3.1A) [44, 45]. The constructs were subjected to a loading regime applied at 0 to 15% strains in a sinusoidal

waveform at a frequency of 0.3 Hz (0.5hr on, 1.5hr off, repeated for 16 hours, 4 hours total loading, followed by 8hr off) for 2 weeks (Fig. 3.1B). Individual constructs were cultured in 2 ml per well of basal medium, CDM, or ODM, which was changed 2x/week, for the duration of the study. Loaded constructs (n=3) and free swelling controls (n=3) were removed at 7 days and 14 days immediately following a complete 16-hour intermittent loading cycle.

3.2.5 Live/dead analysis

Cell viability throughout the duration of the experiment was assessed using the LIVE/DEAD Viability/Cytotoxicity Kit (Invitrogen). Cell seeded constructs were imaged with a Zeiss LSM 510 confocal microscope. At each time point (days 0, 7, and 14) loaded constructs were removed, rinsed with PBS and allowed to incubate for 30 minutes in a solution of 2mM calcein and 2mM ethidium homodimer. After incubation, the constructs were removed and rinsed before imaging. Two to four images were taken for each construct (n=2) and 75-100 cells were counted for each image using Cell Counter with Image J software.

3.2.6 Gene expression

Total RNA was extracted and purified following the manufacturer's protocol using a Total RNA Mini Kit (Omega Biotek; Norcross, GA). Isolated RNA was quantified using a Nanodrop 1000 Spectrophotometer (Thermo Scientific; Portsmouth, NH). RNA ranging from 5.6 to 14.7 ng/ml was transcribed to cDNA following the manufacturer's protocol using the High Capacity cDNA Reverse Transription Kit (Applied Biosystems; Foster City, CA). Primers were designed using Primer Express 3.0 (Applied Biosystems) and purchased from Applied Biosystems or Integrated DNA Technologies (Table 3.1). Real-time polymerase chain reactions

(RT-PCR) was performed (n=3) on 1 μl cDNA with Fast SYBR® Green Master Mix (Applied Biosystems) in a total reaction volume of 20 mL (7500 Fast Real-Time PCR Machine, Applied Biosystems). All genes of interest were normalized to the housekeeping gene, L30, and relative expression levels were calculated using a modified ΔΔCt method that incorporated actual primer efficiencies (Table 3.1), as described elsewhere [46]. Relative expression data for constructs cultured under free swelling conditions in CDM or ODM were normalized to the relative expression data for the free swelling basal constructs at day 0. Relative expression data for constructs cultured under intermittent dynamic loading conditions in CDM or ODM were normalized to the relative expression data for their respective free swelling constructs at the same time point. Normalized expression data for intermittent dynamic loading are represented as $\log_2$ fold change, to determine the effect of loading on the encapsulated hMSCs. A negative value for the $\log_2$ fold change data indicates downregulation of a gene while a positive value indicates upregulation of a gene when compared to the normalizing factor and a value of 0 indicates no change.

3.2.7 Immunohistochemistry

Hydrogel constructs were fixed overnight in 4% paraformaldehyde and transferred to a 15% sucrose solution for storage (n=2). Constructs were dehydrated following standard histological protocols and embedded in paraffin. Sections (10mm) were stained for the presence of aggrecan and types I, II, and X collagen by immunohistochemistry. All samples were pretreated with Chondroitanase-ABC (500 mU/mL) (Sigma) for 60 minutes. Collagen samples were treated with protease (Sigma, 1mg/ml) for 30 minutes and type X collagen samples were treated with pepsin (1mg/ml) for 30 minutes. After permeabilization and blocking, samples were

treated overnight with anti-aggrecan (US Biologicals; Swampscott, MA, 1:5), anti-type I collagen (Abcam; Cambridge, MA, 1:400), anti-type II collagen (Abcam, 1:100), and anti-type X collagen (Developmental Studies Hybridoma Bank, Iowa City, IA, 1:2) in blocking solution at 4ºC, rinsed with PBS, and treated for 2 hr with goat anti-mouse IgG labeled with Alexa Fluor 546 or 488 (Invitrogen, 1:200) and counterstained with DAPI. Additionally, sections were stained with von Kossa and counter stained with neutral red for phosphate salts to assess mineralization and with Safranin O/Fast Green for negatively charged GAGs to assess cartilage ECM deposition.

3.2.8 Statistical analysis

Statistical analysis was performed using One Way ANOVA with a Tukey HSD Post Hoc assessment to determine differences between experimental variables (basal/differentiation media conditions and free swelling/intermittent dynamic loading conditions). Specific p values up to 0.25 are reported in the text to indicate the relative significance of the results. Data are reported as the mean ± standard deviation of the mean unless stated otherwise.

3.3 Results

An intermittent dynamic loading regime was utilized to load compressively hMSC-laden PEG-RGD constructs (Fig. 3.1C) while control constructs were allowed to free swell for the duration of the study. MSC differentiation was assessed by gene expression and matrix deposition for cartilage and bone markers. To assess chondrogenesis, gene expression for SOX9, an early transcriptional factor involved in chondrogenesis, and for cartilage matrix molecules, aggrecan (ACAN) and type II collagen (Col II), were assessed. To assess osteogenesis, gene

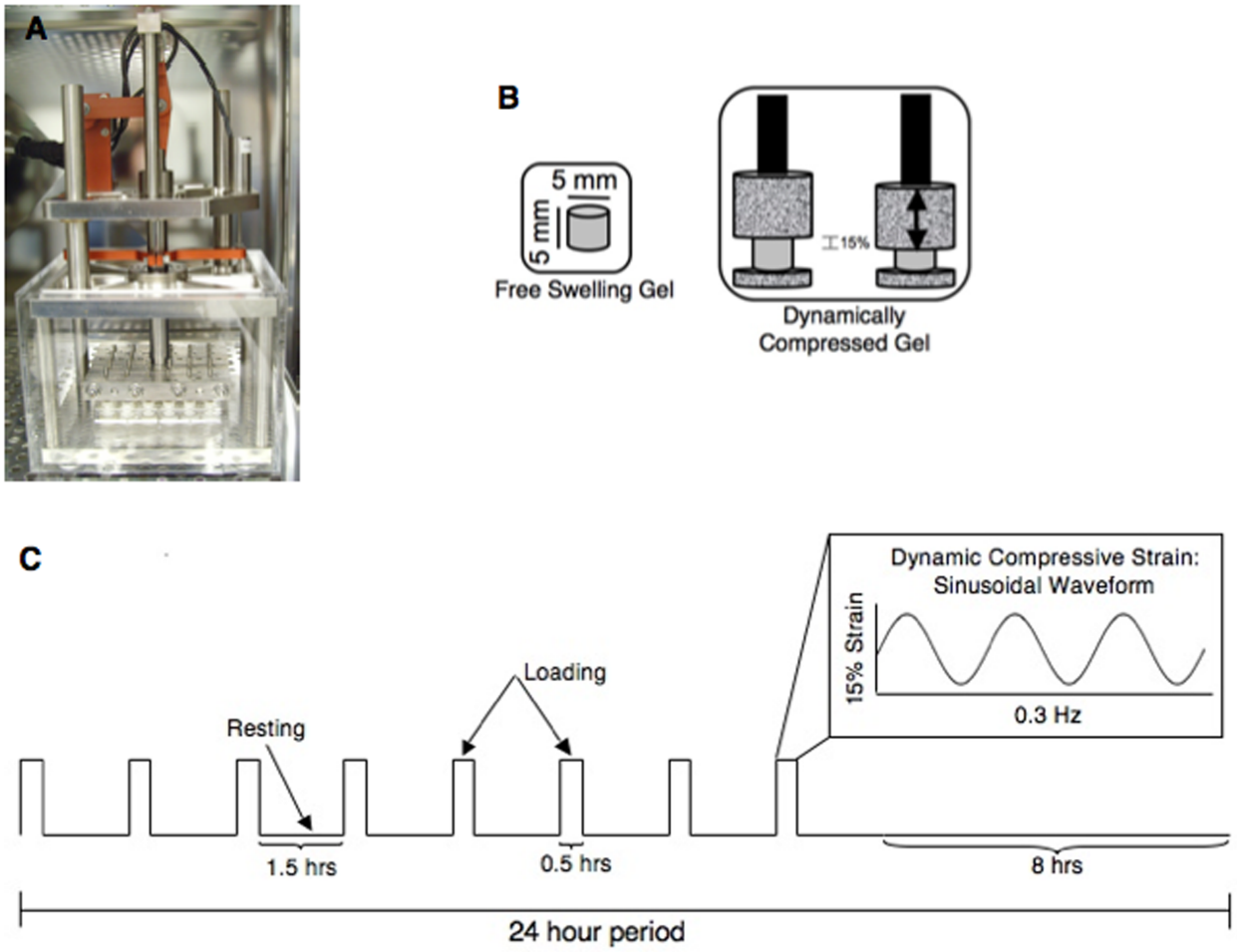

Figure 3.1: (A) Custom built loading bioreactor that applies dynamic compressive strains to individual constructs within a 24-well tissue culture plate. (B) Within each well, each cylindrical hydrogel construct, 5 mm in diameter and 5 mm in height, is placed between a permeable base and a permeable platen and is subjected to a dynamic strain. Free swelling constructs served as controls. (C) A schematic of the daily physiological intermittent dynamic loading regime employed in this study. Intermittent loading (0.5 hrs ON, 1.5 hrs OFF) was applied for 16 hours followed by 8 hours of rest. During the loading period, a dynamic compressive strain was applied from 0 to 15% strain in a sinusoidal waveform and at a frequency of 0.3 Hz while the resting period experienced no strained.

expression for RUNX2, an early transcriptional factor involved in osteogenesis, and for bone matrix molecules, alkaline phosphatase (ALP) and type I collagen (Col I) were assessed.

Additionally, type X collagen (Col X) was assessed as it is present in the hypertrophic region of cartilage. Matrix deposition was also assessed histologically by staining for cartilage and bone matrix molecules; type I, II, and X collagens and aggrecan, as well as for mineralization associated with bone-like extracellular matrix deposition.

3.3.1 Cell Viability

Cell viability, as determined semi-quantitatively from confocal microscopy images, for free swelling and loaded conditions (basal, CDM, and ODM) showed an initial drop between day 0 (94±3%) and day 7 (~55%). However, cell viabilities leveled off at or above ~50% for all conditions by day 14. Representative confocal microscopy images of cell viability in constructs under loaded conditions are shown in Fig 3.2. Free swelling conditions exhibited similar viability trends (data not shown).

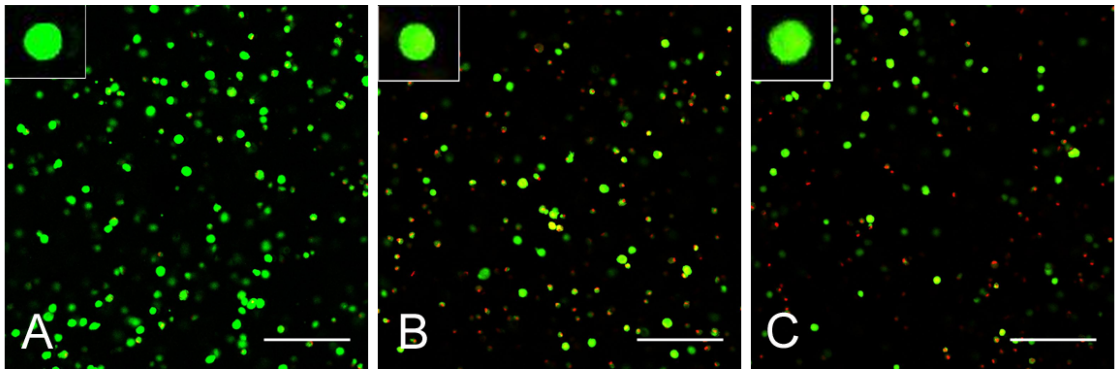

Figure 3.2: Representative Live/Dead images for (A) day 0 (94±3%) (B) intermittent dynamically loaded day 14 CDM (42±8%) and (B) intermittent dynamically loaded day 14 ODM (48±12%) constructs. Original magnification is 100x.

Primer type	Primer Sequence	Primer concentration (nM)/Efficiency
L30 forward reverse	TGGTGTCCATCACTACAGTGGCAA ACCAGTCTGTTCTGGCATGCTTCT	250/99%
SOX9 forward reverse	TGACCTATCCAAGCGCATTACCCA ATCATCCTCCACGCTTGCTCTGAA	250/99%
ACAN forward reverse	ACAATGCCCAAGACTACCAGTGGA TTCTCGTGCCAGATCATCACCACA	250/102%
Col II forward reverse	GGTGGCTTCCATTTCAGCTATG TCTTGCAGTGGTAGGTGATGTTCT	200/97%
Col I forward reverse	TAGGGTCTAGACATGTTCAGCTTTGT CCGTTCTGTACGCAGGTGATT	300/84%
RUNX2 forward reverse	ACCAGTTGAGGTGCACTAAAGGGA AGTTCAGATGAGGACCTGCAGCAT	250/106%
ALP forward reverse	TGCAGTACGAGCTGAACAGGAACA ACTCTCTGCCTGCCCAAGAGAAAT	250/99%
Col X forward reverse	TTTTGCTGCTAGTATCCTTGAACTTG CTGTGTCTTGGTGTTGGGTAGTG	250/100%

Table 3.1: Primer sequences used in qRT-PCR.

3.3.2 Time Dependent hMSC Response in RGD Modified PEG Hydrogels

Gene expression for several chondrogenic and osteogenic markers changed under free swelling and loading conditions as a function of culture time. For chondrogenic genes, culture conditions comprised of basal free swelling, CDM free swelling, and CDM loaded. SOX9 expression increased significantly with culture time up to 7 days for basal ($p=0.001$) and CDM free swelling ($p<0.001$) and then remained constant, but increased significantly for the CDM loaded ($p<0.001$) over the 14 –day culture period (Fig. 3.3A). Mean Col II expression levels increased with culture time in the CDM free swelling ($p=0.05$) and loaded CDM constructs, but was only significant for the former ($p=0.17$), while basal free swelling constructs did not change (Fig. 3.3B). ACAN expression decreased significantly ($p=0.01$ free swelling basal, $p=0.02$ free

swelling CDM, and p=0.001 loaded CDM) (Fig. 3.3C), while Col X expression increased significantly (Fig. 3.3D) for all culture conditions (p=0.005 free swelling basal, p=0.005 free

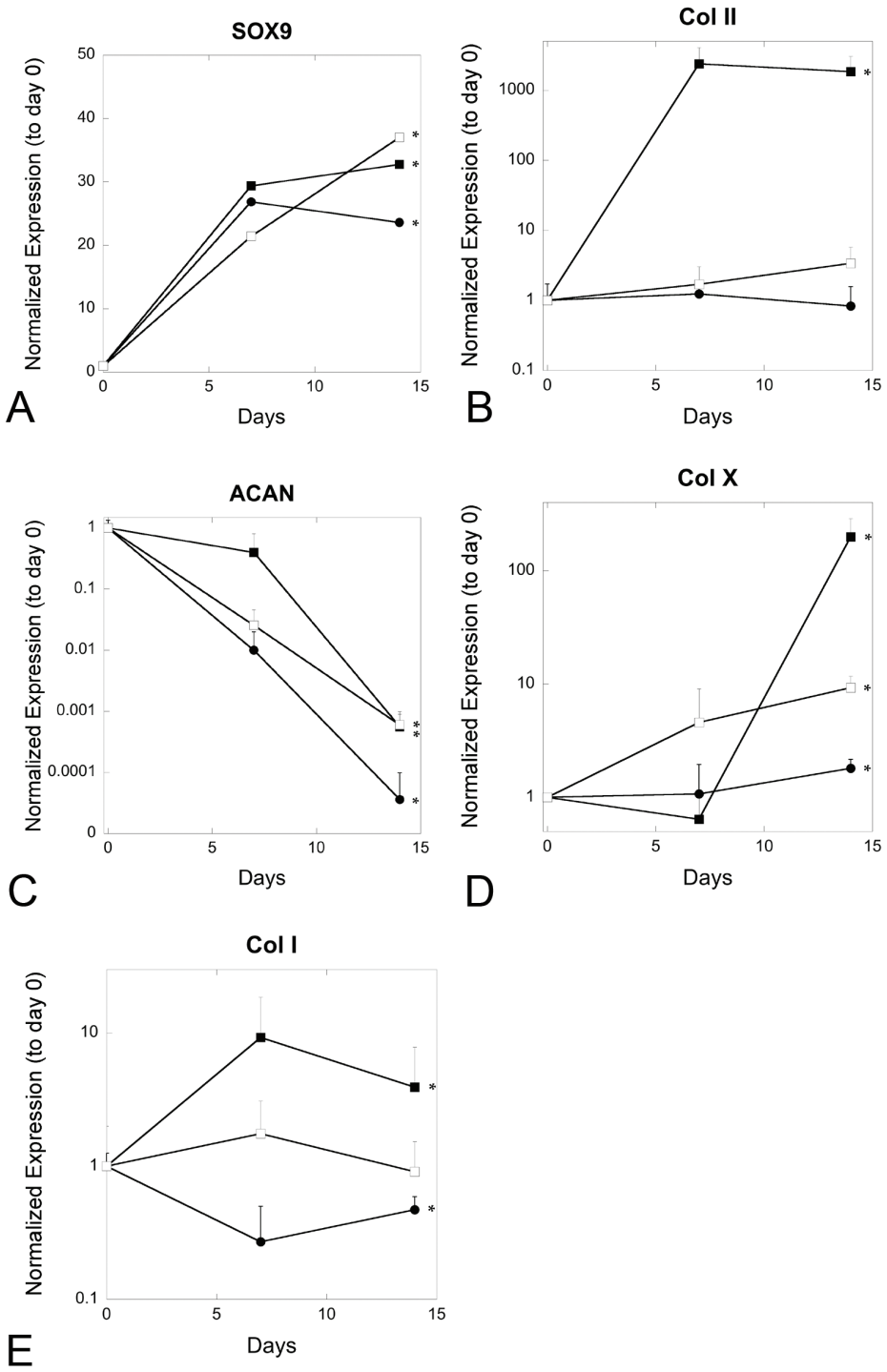

Figure 3.3: Normalized time dependent gene expression for chondrogenic (SOX9, Col II, ACAN) and hypertrophic (Col X) differentiation markers for basal free swelling (●), CDM free swelling (■), and CDM (□) loaded constructs cultured for up to 14 days. Means ± standard deviations are presented as normalized relative expression (to day 0) and are relative to the housekeeping gene L30 (n=3). * $p < 0.05$.

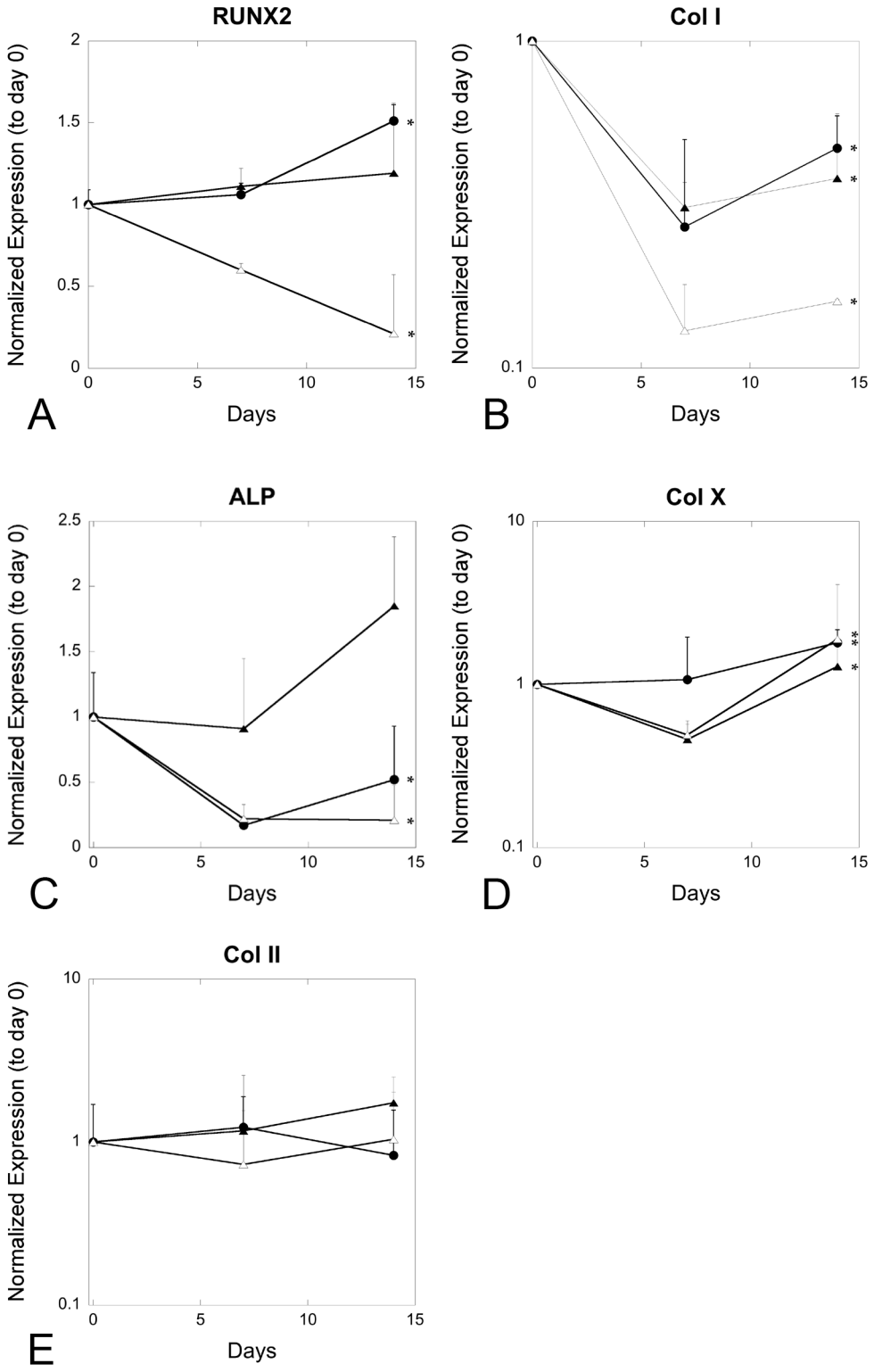

Figure 3.4: Normalized time dependent gene expression for osteogenic (RUNX2, Col I, ALP) and hypertrophic (Col X) differentiation markers for basal free swelling (●), ODM free swelling (▲), and ODM (△) loaded constructs cultured for up to 14 days. Means ± standard deviations are presented as normalized relative expression (to day 0) and are relative to the housekeeping gene L30 (n=3). * $p < 0.05$.

swelling CDM, and p=0.004 loaded CDM). Col I expression increased significantly by day 7 in the CDM free swelling constructs (p=0.001) and then remained constant while the opposite was found in the basal free swelling constructs (p=0.008). Col I expression did not change with culture time for the CDM loaded constructs.

For osteogenic genes, culture conditions comprised of basal free swelling, ODM free swelling, and ODM loaded. For the early osteogenic transcription marker, RUNX2 expression increased in basal free swelling (p=0.001), but decreased in ODM loaded constructs (p=0.01) (Fig. 3.4A). Temporal changes in Col I expression were observed for all culture conditions (p=0.008 free swelling basal, p=0.01 free swelling ODM, and p=0.002 loaded ODM), with a general downregulation as a function of culture time (Fig. 3.4B). ALP expression also changed for all three conditions, it decreased in basal free swelling (p=0.05) and ODM loaded constructs (p=0.02), but increased in the ODM free swelling constructs (p=0.08) (Fig. 3.4C). Temporal changes were also observed in Col X expression with modest, but significant increases in the basal free swelling constructs (p=0.005) with culture time and with an initial downregulation, followed by an upregulation in the ODM free swelling (p=0.03) and loaded constructs (p=0.03) (Fig 3.4D).

3.3.3 hMSC Response in RGD Modified PEG Hydrogels in Chondrogenic and Osteogenic Differentiation Media

In the presence of CDM, hMSC-laden RGD modified PEG constructs cultured under free swelling conditions for 14 days resulted in noticeable increases in Col II (p=0.14), Col I (p=0.06) and ACAN (p=0.08) expressions at day 7 compared to constructs cultured in basal growth medium (Fig. 3.5A). Additionally, SOX9 (p=0.16) and Col X (p=0.02) were upregulated by day

14. Col II increased 1900-fold by day 7 and remained high (2200-fold) at day 14. ACAN increased 70-fold by day 7 and dropped to levels similar to the basal condition by day 14. Col I increased 26-fold by day 7 and remained elevated (8-fold higher) by day 14. SOX 9 and Col X were similar to basal levels at day 7 but increased 1.4-fold and 110-fold by day 14, respectively (Fig. 3.5A).

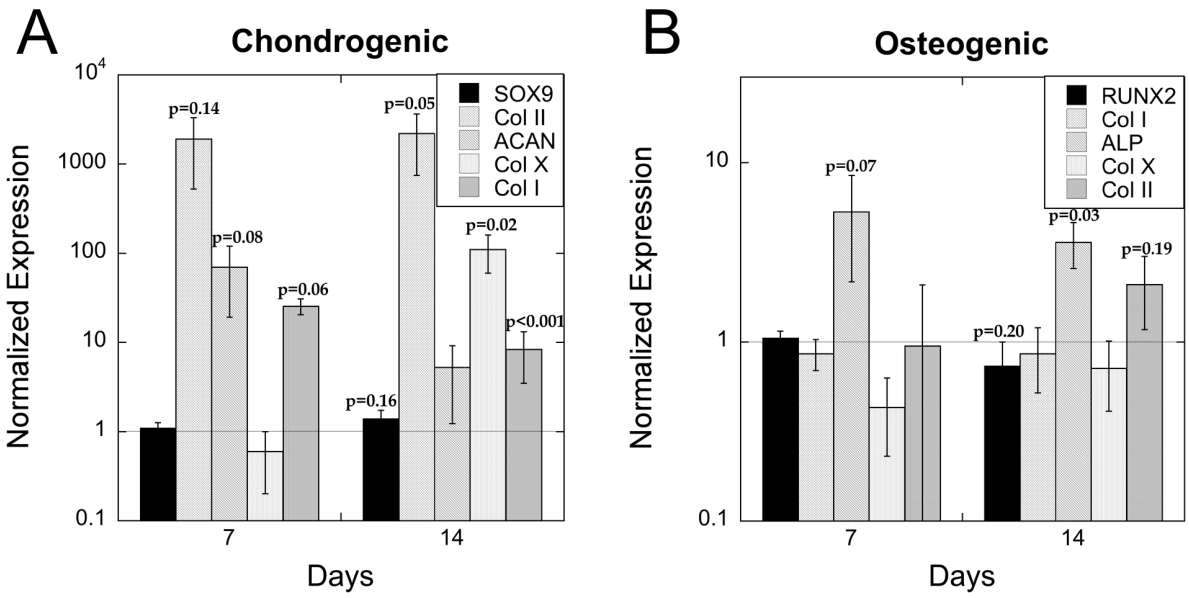

Figure 3.5: Gene expression for chondrogenic (SOX9, Col II, ACAN), osteogenic (RUNX2, Col I, ALP), and hypertrophic (Col X) differentiation markers in free swelling chondrogenic (CDM) (A) and osteogenic (ODM) (B) with constructs normalized to free swelling basal constructs cultured for up to 14 days. Means ± standard deviations are presented as normalized relative expression and are relative to the housekeeping gene L30 (n=3).

When hMSC-laden RGD modified PEG constructs were cultured under free swelling conditions and in the presence of osteogenic differentiation factors, ALP expression increased 5-fold by day 7 (p=0.07) and remained elevated (4-fold higher) compared to basal conditions at day 14 (p=0.03) (Fig. 3.5B). By day 14, the early osteogenic transcriptional factor, RUNX2, expression (p=0.2) was downregulated by 0.3-fold. At day 14, Col II (p=0.19) expression was

upregulated by 2.1-fold. No change in gene expression for Col I or Col X was observed at the time points investigated over the 14-day culture period (Fig. 3.5B).

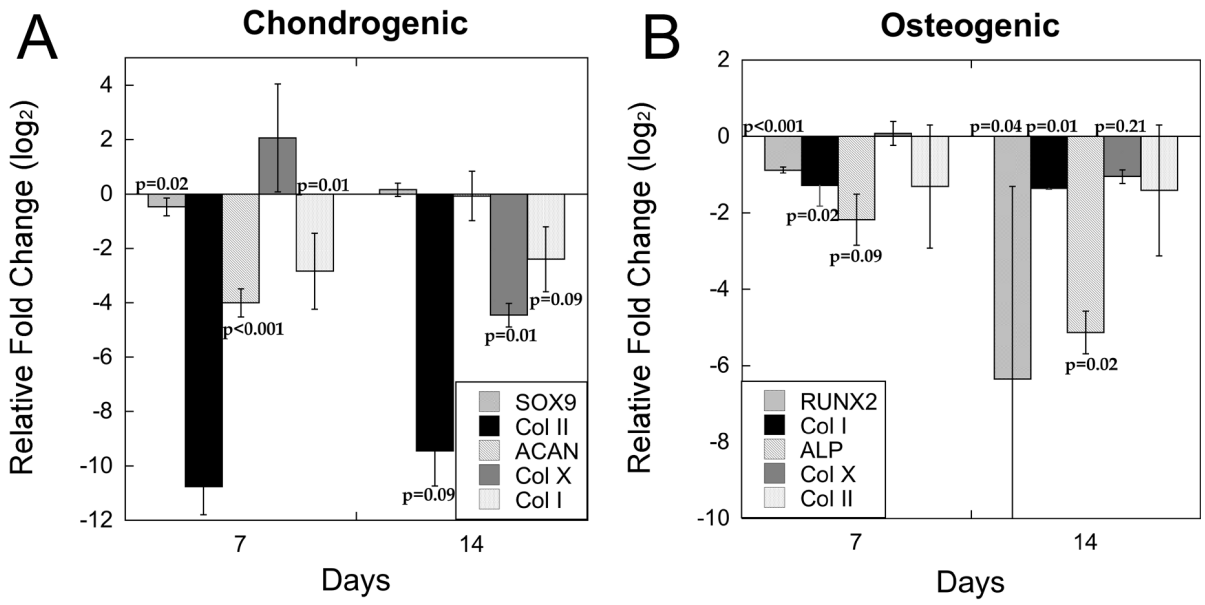

Figure 3.6: (A) Chondrogenic gene expression (SOX9, Col II, ACAN, and Col X) in loaded constructs normalized to free swelling constructs for the same time point cultured for up to 14 days. (B) Osteogenic gene expression (RUNX2, Col I, and ALP) in loaded constructs normalized to free swelling constructs for the same time point cultured for up to 14 days. Means ± standard deviations are presented as normalized $\log_2$ values where values of 0 represent no change in expression, +3 indicates a 8-fold (2^3) increase, and -3 indicates a 8-fold decrease in expression compared to the normalizing factor (same time point free swelling CDM or same time point free swelling ODM, respectively). Data are relative to the housekeeping gene L30 (n=3).

3.3.4 The Effects of Intermittent Dynamic Loading on hMSC Response in the Presence of Chondrogenic Differentiation Medium

The application of loading to CDM constructs downregulated the expression of SOX9 (p=0.02), ACAN (p<0.001), and Col I (p=0.01) by day 7. By day 14, Col II (p=0.09), Col X (p=0.01), and Col I (p=0.09) were also downregulated (Fig. 3.6A). At day 7, SOX9 was slightly downregulated by 0.5-fold and ACAN was downregulated by 4-fold. By day 14 Col II was also

downregulated by 9.5-fold. Additionally, both Col X at day 14 (4.5-fold) and Col I at days 7 and 14 (3-fold and 2.4-fold) were downregulated compared to free swelling constructs in the presence of CDM.

After 14 days, free swelling CDM constructs exhibited positive staining for type II collagen and aggrecan with modest type X collagen staining present (Fig. 3.7G, Q, L). Type II collagen was not detected in the loaded constructs and showed weak aggrecan staining compared to free swelling constructs, whereas dynamically loaded constructs showed reduced staining for type X collagen (Fig. 3.7H, R, M). Additionally, neither free swelling nor loaded CDM constructs showed substantial staining for type I collagen by day 14 and were comparable to the day 0 constructs (Fig. 3.7B, C). Intracellular GAG staining was observed in both day 0 CDM free swelling constructs and day 14 CDM free swelling constructs (Fig. 3.7W). Whereas a drastic reduction in GAG staining was observed in the day 14 dynamically loaded CDM constructs (Fig. 3.7X).

3.3.5 The Effects of Dynamic Loading on hMSC Response in the Presence of Osteogenic Differentiation Medium

When ODM constructs were subjected to loading, inhibition of all three of the osteogenic differentiation markers examined was observed at days 7 and 14 (Fig. 3.6B). RUNX2 was down regulated by 1-fold and 6-fold at days 7 ($p<0.001$) and 14 ($p=0.04$), respectively. Col I was downregulated by 1.3-fold and 1.4-fold at days 7 ($p=0.02$) and 14 ($p=0.01$). Additionally, ALP was downregulated as well at both days 7 ($p=0.09$) and 14 ($p=0.02$) by 2.2-fold and 5.1-fold, respectively, when compared to free swelling constructs. Col X ($p=0.21$) was downregulated by

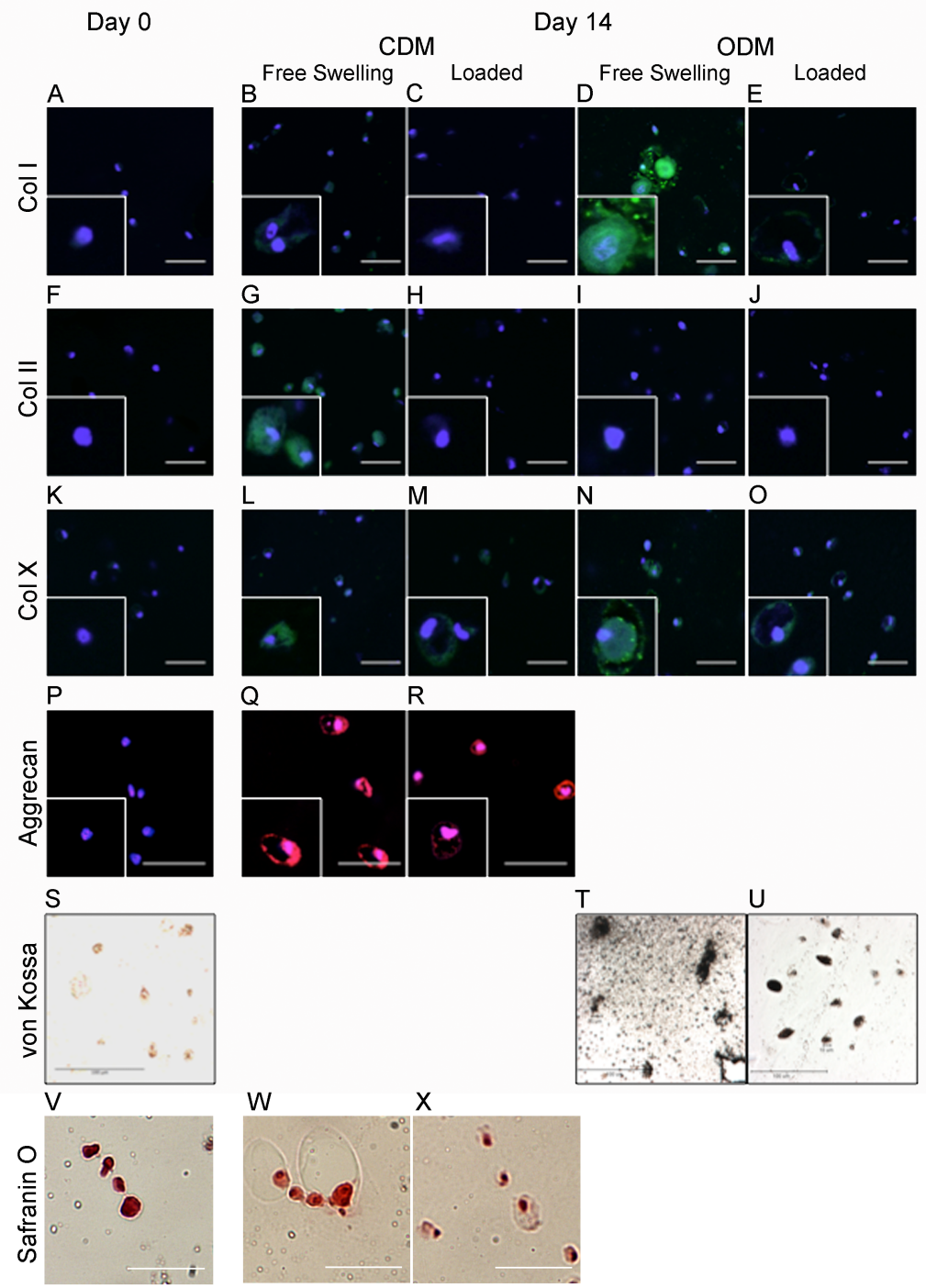

Figure 3.7: Immunohistochemical matrix deposition of bone specific matrix molecules (A-E), cartilage-specific matrix molecules (F-J, P-R), and hypertrophic cartilage matrix molecules (K-O) by hMSCs encapsulated in PEG-RGD constructs, conditioned in CDM or ODM that underwent free swelling and loading conditions and were cultured for up to 14 days. Mineralization was assessed by von Kossa staining in free swelling and loaded ODM constructs (S-U). Glycosaminoglycan deposition was assessed by Safranin O/Fast Green staining in free swelling and loaded CDM constructs (V-X). For A-O, original magnification is 400x, for P-R, original magnification is 630x, and for S-X original magnification is 400x.

1-fold, and Col II expression showed no difference between the loaded and free swelling constructs.

Strong type I collagen staining was observed in the day 14 free swelling osteogenic constructs compared to minimal staining in the loaded constructs (Fig. 3.7D, E). Neither free swelling nor loaded osteogenic constructs stained for type II collagen. Day 14 ODM free swelling constructs showed substantial staining for type X collagen that was markedly decreased in the loaded constructs (Fig. 3.7N, O). Additionally, mineral deposition was observed throughout the extracellular regions of the day 14 ODM free swelling constructs. The application of loading, however, resulted in reduced mineralization with positive staining limited to the pericellular region at day 14 (Fig. 3.7T, U).

3.4 Discussion

The overall goal for this study was to investigate the effects of a physiologically relevant intermittent dynamic compressive loading regime, similar to a regime which has previously been shown to enhance type II collagen expression in chondrocytes encapsulated in PEG based hydrogels [37], on the chondrogenic and osteogenic differentiation of hMSCs when encapsulated in RGD modified PEG hydrogels and when loading was applied at the onset of differentiation. In this system, hMSC differentiation may be influenced by several sources including soluble cues present in the culture medium, their physical attachment to the 3-D PEG hydrogel via the tethered RGD moieties, and biomechanical cues that arise from dynamic compressive loading. While the 3-D culture environment of PEG-RGD hydrogels supported MSC differentiation in the absence of loading, the 4-hour daily loading regime applied intermittently over the course of the day inhibited both chondrogenesis and osteogenesis, contrary to our hypothesis.

The application of an intermittent dynamic compressive strain did not adversely affect hMSC viability within PEG-based hydrogels although viability dropped to ~50% based on a membrane integrity assay within the first week of culture regardless of culture condition. Cell death by day 14 appears to be by a combination of necrosis, as evident by positive staining with ethidium homodimer-I and a lack of staining by calcein AM, and by apoptosis as evident by dual staining with calcein AM and ethidium homodimer-I, which has been suggestive of apoptotic cells [47]. Although it should be noted that ethidium homodimer-I alone may stain cells in the late stages of apoptosis when the cell membrane integrity is lost. Several studies have reported decreases in MSC viability during the initial culture period when uncommitted MSCs are encapsulated in 3-D hydrogels fabricated from PEG [39, 48], alginate [24], agarose [49], or polyglycerol [50], suggesting that the adoption of a rounded phenotype may influence survival for a fraction of the cells prior to their differentiation fate [50]. Nonetheless, the decrease in viability observed has not been detrimental to the MSC's ability to differentiate down chondrogenic or osteogenic lineages [24, 34, 48, 49].

The morphology of MSCs is thought to be an important regulator in MSC differentiation [51]. When encapsulated in RGD modified PEG hydrogels, MSCs maintain a round morphology due to the nature of the covalent and stable crosslinks, exhibiting a mesh size of ~200 Å, which is significantly smaller than the size of a cell and its processes. This tightly crosslinked network provides cells with little room to spread, as indicated by the rounded morphology observed in the Live/Dead and histology images. This observation is consistent with previous work from our group with chondrocytes encapsulated in RGD modified PEG hydrogels [52]. For chondrogenic differentiation, a rounded morphology is important [53]. While it is thought that spreading may be important for osteogenic differentiation of MSCs, particularly in 2D cultures [51], 3D

hydrogel environments promoting a round morphology have been shown to support osteogenic differentiation [34, 54-57] with recent evidence suggesting that cell shape is less of a factor in osteogenic differentiation in 3D [54]. However, once degradable linkages are incorporated into the PEG hydrogels, a prerequisite for long-term cultures, degradation of the hydrogel has been shown to facilitate cell spreading, cell migration, and cell-cell interactions, which will be important in long-term bone formation [58].

Under free swelling conditions, our results are in agreement with findings from others indicating that PEG hydrogels support chondrogenic and osteogenic differentiation of hMSCs when cultured in the presence of soluble differentiation factors [57, 59-61]. Evidence of chondrogenic differentiation is shown by upregulation of several chondrogenic genes, namely Col II, ACAN, and Col X and most notably by the presence of cartilage matrix proteins, type II collagen and aggrecan with a lack of type I collagen staining. Although SOX9 expression, relative to free swelling constructs, was not upregulated with culture time, the expression did increase for both free swelling and loaded CDM constructs, and upregulation can be inferred indirectly since it plays a crucial role in the downstream regulation of Col II expression by encoding a transcription factor that activates a Col II gene enhancer [62]. While ACAN expression, which has been shown to be constitutively expressed in undifferentiated MSCs [63], was downregulated in both CDM free swelling and CDM loaded constructs with culture time, consistent with findings reported by Campbell et al. [24] with hMSCs encapsulated in alginate, deposition of the aggrecan glycoprotein was observed. Evidence of osteogenic differentiation was confirmed by an upregulation in ALP gene expression and the substantially increased presence of type I collagen protein with a lack of type II collagen staining. Additionally, mineral deposition was observed in the constructs. It is important to note that spontaneous mineralization

occurs due to the presence of β-glycerophosphate in the ODM and therefore mineralization may be due to a combination of cellular deposition and the culture medium. Nonetheless, the presence of mineral deposits will enhance the long-term development of a boney tissue. Overall, our findings agree well with the results presented by Yang et al. [57] which showed pericellular mineralization in PEG hydrogels with a similar concentration of RGD tethered in the hydrogel constructs.

When biochemical cues were combined with mechanical stimulation, loading led to a dramatic downregulation in chondrogenesis. Most notably, there was a moderate downregulation of SOX9 expression concomitant with a large downregulation in ACAN and Col II expressions and minimal evidence for the cartilage-specific matrix protein, type II collagen. Additionally, Col X expression, but more notable type X collagen protein, a marker of hypertrophy [64], was also downregulated. The fact that the main chondrocyte marker, type II collagen, as well as the hypertrophic chondrocyte marker, type X collagen, were downregulated at the protein level, strongly points toward an inhibitory effect from loading, at least under the regime employed in this study, on the chondrogenic differentiation of hMSCs in the PEG hydrogel system. These findings suggest that the application of dynamic compression applied at the onset of chondrogenesis may be either delaying or generally inhibiting chondrogenesis. Thorpe et al. [27, 65] have reported similar findings with porcine MSCs in agarose constructs intermittently strained to 10% dynamically, showing reduced chondrogenesis evidenced by decreased sGAG and collagen contents. However, when loading was applied after chondrogenesis, that is after 21 days of free swelling culture in chondrogenic culture conditions, similar sGAG and collagen contents were achieved between the free swelling and the dynamically loaded constructs [65]. Contrarily, Huang et al. [23] have shown that a 4-hour daily, 10% intermittent dynamic load over

an initial 14 day period enhanced the chondrogenesis of rabbit MSCs in agarose constructs. When hMSCs were cultured in hyaluronan-gelatin scaffolds [66] or in fibrin gels [67] and subjected to intermittent dynamic loading, chondrogenesis was either maintained or enhanced. Similarly, intermittent dynamic compressive loading applied at 1 Hz and 10% strains to goat MSCs encapsulated in unmodified PEG hydrogels was shown to have a positive effect on chondrogenic differentiation leading to increased GAG contents after 21 days [26]. When the latter study is compared to our findings, the results together suggest that, the PEG hydrogel environment may be capable of stimulating chondrogenesis in the presence of dynamic loading, but how MSCs respond to loading may be dependent on the specific loading regime (e.g., 15% versus 10%) and/or on the donor species and age (adult human versus adolescent goat). In fact, it has been recently suggested that age plays an important role in how cells sense and respond to mechanical forces [68, 69]. Nonetheless, others have reported enhanced chondrogenesis of hMSCs when subjected to loading, suggesting that the type of scaffold plays an important role in how hMSCS respond to dynamic loading. This observation is supported by finite element models, which have shown that the local biomechanical cues (e.g., peak pressure, radial velocity, and shear stress) produced under dynamic compressive loading, vary greatly depending on the scaffold type, although similar gross strains are applied [43]. Taken together, loading regimes that enhance chondrogenesis of MSCs will likely need to be optimized for cell age and species, but in combination with type of scaffold employed.

Similarly for osteogenic differentiation, when biochemical cues were combined with mechanical stimulation, loading led to a dramatic downregulation in osteogenesis. Specifically, RUNX2, Col I, and ALP expressions were downregulated. Interestingly, Col I gene expression was downregulated with culture time for both ODM free swelling and ODM loaded constructs

relative to day 0 constructs, even though strong type I collagen staining was observed in the day 14 free swelling constructs. Minimal staining for mineralization was observed in the dynamically loaded constructs, which agrees well with the observed decrease in ALP expression, but may also be due to loss of mineralization caused by the increased fluid flow associated with dynamic loading. Although it is well known that mechanical forces have a positive effect on fracture healing, stimulating increased mineralization and fracture stiffness in the healed bone [15], the large compressive strain applied at the onset of differentiation may not be appropriate. Although 10% dynamic compressive strains have been reported to positively effect osteoblasts leading to increased mineralized ECM matrix production, larger strains of 20% were noted to have an inhibitory effect on osteoblast differentiation [15]. Therefore, smaller strains may be necessary to impart a positive effect on osteogenesis for MSCs when cultured in PEG based systems with tethered RGD and subjected to loading.

While the RGD moiety provides a mechanism by which MSCs can interact directly with the hydrogel and which may serve as a mechanoreceptor [70], this peptide is not specific to the cartilage or bone niche, but rather is a ubiquitous cell binding domain found in several common proteins such as fibronectin, collagens, and laminin [41]. Although under free swelling conditions, the presence of RGD promotes MSC differentiation in the presence of soluble cues as shown in this study and several other studies [20, 39], limitations have been noted. For example, the presence of RGD has been shown to inhibit chondrogenesis of bovine MSCs encapsulated in agarose or alginate hydrogels [71, 72]. On the contrary, unpublished findings from our group suggest that unmodified PEG hydrogels are not supportive of hMSC chondrogenesis evidenced by a lack of upregulation in Col II expression and that loading has no further impact. This observation, in conjunction with findings from this study, indicate that RGD is indeed supportive

of chondrogenesis within PEG hydrogels and that loading at the onset of differentiation and/or the loading parameters selected are likely the primary reasons for inhibited chondrogenesis. Long-term, however, the persistent presence of RGD may have inhibitory effects on cartilage development as demonstrated by Salinas et al. [20] who when employed a cleavable RGD peptide motif, showed higher amounts of cartilage-specific ECM by hMSCs encapsulated in PEG hydrogels. Contrarily, other studies have shown that the presence of RGD appears to promote osteogenesis under mechanical loads. For example, Kasten et al. [73] demonstrated that MSCs attached to RGD modified surfaces and cyclically loaded (1Hz, 15 minutes) stimulated type I collagen expression. Additionally, several groups have shown that RGD enhances osteogenic differentiation of MSCs on several different types of biomaterials [73-75], suggesting that the large compressive strain employed in our study is likely the primary reason for inhibited osteogenesis.

We recognize several limitations in our study. First, one loading regime was investigated. While only a few studies have investigated the effects of dynamic compressive loading on chondrogenesis of MSCs in 3-D hydrogels [23, 24, 26, 27, 65], these studies suggest that lower strains [23], higher strain rates [24], or shorter durations of loading [26] are all factors that can favorably influence chondrogenic differentiation of MSCs. Therefore, it is possible that adult hMSCs may respond more favorably to reduced loads, and a loading regime which is different from differentiated chondrocytes, warranting further investigation. A second limitation of our study is the short duration (i.e., 14 days) and the use of non-degrading hydrogels. We chose to investigate the effects of loading at the onset of differentiation in an effort to better understand how a loading environment impacts the differentiation potential of MSCs, such as would be the case for in situ delivery of undifferentiated MSCs into an osteochondral defect within a joint. As

such, the PEG hydrogels employed in this study were non-degrading in order to maintain a consistent 3-D culture environment under loading. Long-term studies, however, will require the incorporation of degradable crosslinks and is the focus of our future efforts.

3.5 Conclusion

Overall our findings indicate that 4-hours of total daily, 15% intermittent dynamic compressive loading applied at the onset of differentiation inhibits both chondrogenesis and osteogenesis in PEG-RGD hydrogels as demonstrated through both qRT-PCR and (immuno)histochemistry. It is possible that loading applied at relatively large compressive strains, prior to differentiation and the development of a protective pericellular matrix, [76] may be perceived as overloading leading to the observed inhibition in differentiation. Additionally, while not the focus of this study, it is possible that the loading regime applied may have impacted the fate of the MSCs down other differentiation pathways, which were not explored in this study. These observations suggest that either reduced loading (e.g., lower strains) and/or delaying the application of loading may be important to the differentiation potential of MSCs. Nonetheless, it is important to recognize that there are a number of factors to consider when selecting a loading regime (e.g., timing of the initiation, frequency, strain, and durations of loading), which will impact the magnitude and duration of the biomechanical cues such as fluid flow and cellular strains. The combination of loading and the hydrogel environment (structure and chemistry) will further impact the biomechanical cues perceived by the cells. Therefore, given the findings for this study in combination with the wide-ranging compilation of results from other groups combining different scaffolds, types of mechanical stimuli, and diverse loading regimes, as reported by Babalola et al., it seems unlikely that there exists one loading

regime that will serve as the ideal regime for all scaffolds being developed for chondrogenic or osteogenic differentiation. As such, additional studies are needed to gain more insight into the role of loading on MSC differentiation. Identifying the optimal loading regime to guide MSC differentiation and enhance matrix deposition in PEG-based hydrogels is still to be realized.

3.6 Acknowledgments

This study was in part supported by a NSF CAREER Award and a research grant from the NIH (K22 DE016608). The authors would like to thank Dr. Garret Nicodemus for his technical assistance with RT-PCR and immunohistochemistry. The type X collagen monoclonal antibody developed by Thomas F. Linsenmayer was obtained from the Developmental Studies Hybridoma Bank developed under the auspices of the NICHD and maintained by The University of Iowa.

3.7 References

[1] Ehrlich PJ, Lanyon LE. Mechanical strain and bone cell function: A review. Osteoporosis International 2002;13:688.

[2] Grodzinsky AJ, Levenston ME, Jin M, Frank EH. Cartilage tissue remodeling in response to mechanical forces. Annual Review of Biomedical Engineering 2000;2:691.

[3] Mauck RL, Nicoll SB, Seyhan SL, Ateshian GA, Hung CT. Synergistic action of growth factors and dynamic loading for articular cartilage tissue engineering. Tissue Engineering 2003;9:597.

[4] Skerry TM. The response of bone to mechanical loading and disuse: Fundamental principles and influences on osteoblast/osteocyte homeostasis. Archives of Biochemistry and Biophysics 2008;473:117.
s
[5] Sarraf CE, Otto WR, Eastwood M. In vitro mesenchymal stem cell differentiation after mechanical stimulation. Cell Proliferat 2011;44:99.

[6] Bikle DD, Halloran BP. The response of bone to unloading. Journal of Bone and Mineral Metabolism 1999;17:233.

[7] Mullender M, El Haj AJ, Yang Y, van Duin MA, Burger EH, Klein-Nulend J. Mechanotransduction of bone cells in vitro: mechanobiology of bone tissue. Medical & Biological Engineering & Computing 2004;42:14.

[8] Sandell LJ, Aigner T. Articular cartilage and changes in arthritis - An introduction: Cell biology of osteoarthritis. Arthritis Research 2001;3:107.

[9] Damsky CH. Extracellular matrix-integrin interactions in osteoblast function and tissue remodeling. Bone 1999;25:95.

[10] Mauck RL, Seyhan SL, Ateshian GA, Hung CT. Influence of seeding density and dynamic deformational loading on the developing structure/function relationships of chondrocyte-seeded agarose hydrogels. Ann Biomed Eng 2002;30:1046.

[11] Davisson T, Kunig S, Chen A, Sah R, Ratcliffe A. Static and dynamic compression modulate matrix metabolism in tissue engineered cartilage. J. Orthop. Res. 2002;20:842.

[12] Lima EG, Bian L, Ng KW, Mauck RL, Byers BA, Tuan RS, Ateshian GA, Hung CT. The beneficial effect of delayed compressive loading on tissue-engineered cartilage constructs cultured with TGF-beta 3. Osteoarthr Cartilage 2007;15:1025.

[13] Sikavitsas VI, Temenoff JS, Mikos AG. Biomaterials and bone mechanotransduction. Biomaterials 2001;22:2581.

[14] Yanagisawa M, Suzuki N, Mitsui N, Koyama Y, Otsuka K, Shimizu N. Compressive force stimulates the expression of osteogenesis-related transcription factors in ROS 17/2.8 cells. Archives Of Oral Biology 2008;53:214.

[15] Rath B, Nam J, Knobloch TJ, Lannutti JJ, Agarwal S. Compressive forces induce osteogenic gene expression in calvarial osteoblasts. J Biomech 2008;41:1095.

[16] Pittenger MF, Mackay AM, Beck SC, Jaiswal RK, Douglas R, Mosca JD, Moorman MA, Simonetti DW, Craig S, Marshak DR. Multilineage potential of adult human mesenchymal stem cells. Science 1999;284:143.

[17] Meinel L, Karageorgiou V, Fajardo R, Snyder B, Shinde-Patil V, Zichner L, Kaplan D, Langer R, Vunjak-Novakovic G. Bone tissue engineering using human mesenchymal stem cells: Effects of scaffold material and medium flow. Ann Biomed Eng 2004;32:112.

[18] Martino MM, Mochizuki M, Rothenfluh DA, Rempel SA, Hubbell JA, Barker TH. Controlling integrin specificity and stem cell differentiation in 2D and 3D environments through regulation of fibronectin domain stability. Biomaterials 2009;30:1089.

[19] Temenoff JS, Park H, Jabbari E, Conway DE, Sheffield TL, Ambrose CG, Mikos AG. Thermally cross-linked oligo(poly(ethylene glycol) fumarate) hydrogels support osteogenic differentiation of encapsulated marrow stromal cells in vitro. Biomacromolecules 2004;5:5.

[20] Salinas CN, Cole BB, Kasko AM, Anseth KS. Chondrogenic differentiation potential of human mesenchymal stem cells photoencapsulated within poly(ethylene glycol)-arginine-glycine-aspartic acid-serine thiol-methacrylate mixed-mode networks. Tissue Engineering 2007;13:1025.

[21] Mauck RL, Yuan X, Tuan RS. Chondrogenic differentiation and functional maturation of bovine mesenchymal stem cells in long-term agarose culture. Osteoarthr Cartilage 2006;14:179.

[22] Kelly DJ, Jacobs CR. The Role of Mechanical Signals in Regulating Chondrogenesis and Osteogenesis of Mesenchymal Stem Cells. Birth Defects Research Part C-Embryo Today-Reviews 2010;90:75.

[23] Huang CYC, Hagar KL, Frost LE, Sun YB, Cheung HS. Effects of cyclic compressive loading on chondrogenesis of rabbit bone-marrow derived mesenchymal stem cells. Stem Cells 2004;22:313.

[24] Campbell JJ, Lee DA, Bader DL. Dynamic compressive strain influences chondrogenic gene expression in human mesenchymal stem cells. Biorheology 2006;43:455.

[25] Kisiday JD, Frisbie DD, McIlwraith CW, Grodzinsky AJ. Dynamic Compression Stimulates Proteoglycan Synthesis by Mesenchymal Stem Cells in the Absence of Chondrogenic Cytokines. Tissue Eng Pt A 2009;15:2817.

[26] Terraciano V, Hwang N, Moroni L, Park HB, Zhang Z, Mizrahi J, Seliktar D, Elisseeff J. Differential response of adult and embryonic mesenchymal progenitor cells to mechanical compression in hydrogels. Stem Cells 2007;25:2730.

[27] Thorpe SD, Buckley CT, Vinardell T, O'Brien FJ, Campbell VA, Kelly DJ. Dynamic compression can inhibit chondrogenesis of mesenchymal stem cells. Biochemical and Biophysical Research Communications 2008;377:458.

[28] Qi MC, Hu J, Zou SJ, Chen HQ, Zhou HX, Han LC. Mechanical strain induces osteogenic differentiation: Cbfa1 and Ets-1 expression in stretched rat mesenchymal stem cells. International Journal of Oral and Maxillofacial Surgery 2008;37:453.

[29] Zhao HB, Lu TD, Ma J, Ma H, Zhang XZ. Mechanotransduction in differentiation of osteogenic from mesenchymal stem cells. Progress In Biochemistry And Biophysics 2007;34:718.

[30] Sumanasinghe RD, Bernacki SH, Loboa EG. Osteogenic differentiation of human mesenchymal stem cells in collagen matrices: Effect of uniaxial cyclic tensile strain on bone morphogenetic protein (BMP-2) mRNA expression. Tissue Engineering 2006;12:3459.

[31] Byrne EM, Farrell E, McMahon LA, Haugh MG, O'Brien FJ, Campbell VA, Prendergast PJ, O'Connell BC. Gene expression by marrow stromal cells in a porous collagen-glycosaminoglycan scaffold is affected by pore size and mechanical stimulation. Journal of Materials Science-Materials in Medicine 2008;19:3455.

[32] Bryant SJ, Anseth KS. Hydrogel properties influence ECM production by chondrocytes photoencapsulated in poly(ethylene glycol) hydrogels. Journal of Biomedical Materials Research 2002;59:63.

[33] Hern DL, Hubbell JA. Incorporation of adhesion peptides into nonadhesive hydrogels useful for tissue resurfacing. Journal of Biomedical Materials Research 1998;39:266.

[34] Nuttelman CR, Tripodi MC, Anseth KS. In vitro osteogenic differentiation of human mesenchymal stem cells photoencapsulated in PEG hydrogels. J Biomed Mater Res A 2004;68A:773.

[35] Benoit DSW, Anseth KS. Heparin functionalized PEG gels that modulate protein adsorption for hMSC adhesion and differentiation. Acta Biomater 2005;1:461.

[36] Buxton AN, Zhu J, Marchant R, West JL, Yoo JU, Johnstone B. Design and characterization of poly(ethylene glycol) photopolymerizable semi-interpenetrating networks for chondrogenesis of human mesenchymal stem cells. Tissue Engineering 2007;13:2549.

[37] Nicodemus GD, Bryant SJ. Mechanical loading regimes affect the anabolic and catabolic activities by chondrocytes encapsulated in PEG hydrogels. Osteoarthr Cartilage 2010;18:126.

[38] Bryant SJ, Durand KL, Anseth KS. Manipulations in hydrogel chemistry control photoencapsulated chondrocyte behavior and their extracellular matrix production. J Biomed Mater Res A 2003;67A:1430.

[39] Nuttelman CR, Tripodi MC, Anseth KS. Synthetic hydrogel niches that promote hMSC viability. Matrix Biology 2005;24:208.

[40] Bryant SJ, Chowdhury TT, Lee DA, Bader DL, Anseth KS. Crosslinking density influences chondrocyte metabolism in dynamically loaded photocrosslinked poly(ethylene glycol) hydrogels. Ann Biomed Eng 2004;32:407.

[41] Ruoslahti E, Pierschbacher MD. New Perspectives in Cell-Adhesion - Rgd and Integrins. Science 1987;238:491.

[42] Ruoslahti E, Reed JC. ANCHORAGE DEPENDENCE, INTEGRINS, AND APOPTOSIS. Cell 1994;77:477.

[43] Babalola OM, Bonassar LJ. Parametric Finite Element Analysis of Physical Stimuli Resulting From Mechanical Stimulation of Tissue Engineered Cartilage. Journal of Biomechanical Engineering-Transactions of the Asme 2009;131.

[44] Nicodemus GD, Bryant SJ. The role of hydrogel structure and dynamic loading on chondrocyte gene expression and matrix formation. J Biomech 2008;41:1528.

[45] Villanueva I, Hauschulz DS, Mejic D, Bryant SJ. Static and dynamic compressive strains influence nitric oxide production and chondrocyte bioactivity when encapsulated in PEG hydrogels of different crosslinking densities. Osteoarthr Cartilage 2008;16:909.

[46] Pfaffl MW. A new mathematical model for relative quantification in real-time RT-PCR. Nucleic Acids Research 2001;29.

[47] Palma PFR, Baggio GL, Spada C, da Silva R, Ferreira S, Treitinger A. Evaluation of annexin V and calcein-AM as markers of mononuclear cell apoptosis during human immunodeficiency virus infection. Braz. J. Infect. Dis. 2008;12:108.

[48] Salinas CN, Anseth KS. The influence of the RGD peptide motif and its contextual presentation in PEG gels on human mesenchymal stem cell viability. J Tissue Eng Regen Med 2008;2:296.

[49] Coleman RM, Case ND, Guldberg RE. Hydrogel effects on bone marrow stromal cell response to chondrogenic growth factors. Biomaterials 2007;28:2077.

[50] Fedorovich NE, Oudshoorn MH, van Geemen D, Hennink WE, Alblas J, Dhert WJA. The effect of photopolymerization on stem cells embedded in hydrogels. Biomaterials 2009;30:344.

[51] McBeath R, Pirone DM, Nelson CM, Bhadriraju K, Chen CS. Cell shape, cytoskeletal tension, and RhoA regulate stem cell lineage commitment. Dev. Cell 2004;6:483.

[52] Villanueva I, Weigel CA, Bryant SJ. Cell-matrix interactions and dynamic mechanical loading influence chondrocyte gene expression and bioactivity in PEG-RGD hydrogels. Acta Biomater 2009;5:2832.

[53] Gao L, McBeath R, Chen CS. Stem Cell Shape Regulates a Chondrogenic Versus Myogenic Fate Through Rac1 and N-Cadherin. Stem Cells 2010;28:564.

[54] Huebsch N, Arany PR, Mao AS, Shvartsman D, Ali OA, Bencherif SA, Rivera-Feliciano J, Mooney DJ. Harnessing traction-mediated manipulation of the cell/matrix interface to control stem-cell fate. Nature Materials 2010;9:518.

[55] Temenoff JS, Park H, Jabbari E, Sheffield TL, LeBaron RG, Ambrose CG, Mikos AG. In vitro osteogenic differentiation of marrow stromal cells encapsulated in biodegradable hydrogels. J Biomed Mater Res A 2004;70A:235.

[56] Hsiong SX, Boontheekul T, Huebsch N, Mooney DJ. Cyclic Arginine-Glycine-Aspartate Peptides Enhance Three-Dimensional Stem Cell Osteogenic Differentiation. Tissue Eng Pt A 2009;15:263.

[57] Yang F, Williams CG, Wang DA, Lee H, Manson PN, Elisseeff J. The effect of incorporating RGD adhesive peptide in polyethylene glycol diacrylate hydrogel on osteogenesis of bone marrow stromal cells. Biomaterials 2005;26:5991.

[58] Cushing MC, Anseth KS. Hydrogel cell cultures. Science 2007;316:1133.

[59] Sharma B, Williams CG, Khan M, Manson P, Elisseeff JH. In vivo chondrogenesis of mesenchymal stem cells in a photopolymerized hydrogel. Plastic and Reconstructive Surgery 2007;119:112.

[60] Nuttelman CR, Benoit DSW, Tripodi MC, Anseth KS. The effect of ethylene glycol methacrylate phosphate in PEG hydrogels on mineralization and viability of encapsulated hMSCs. Biomaterials 2006;27:1377.

[61] Salinas CN, Anseth KS. The enhancement of chondrogenic differentiation of human mesenchymal stem cells by enzymatically regulated RGD functionalities. Biomaterials 2008;29:2370.

[62] Lefebvre V, Huang WD, Harley VR, Goodfellow PN, deCrombrugghe B. SOX9 is a potent activator of the chondrocyte-specific enhancer of the pro alpha 1(II) collagen gene. Mol. Cell. Biol. 1997;17:2336.

[63] Mwale F, Stachura D, Roughley P, Antoniou J. Limitations of using aggrecan and type X collagen as markers of chondrogenesis in mesenchymal stem cell differentiation. J. Orthop. Res. 2006;24:1791.

[64] Djouad F, Tuan RS. Fundamentals of Tissue Engineering and Regenerative Medicine, 2009.

[65] Thorpe SD, Buckley CT, Vinardell T, O'Brien FJ, Campbell VA, Kelly DJ. The Response of Bone Marrow-Derived Mesenchymal Stem Cells to Dynamic Compression Following TGF-beta 3 Induced Chondrogenic Differentiation. Ann Biomed Eng 2010;38:2896.

[66] Angele P, Schumann D, Angele M, Kinner B, Englert C, Hente R, Fuchtmeier B, Nerlich M, Neumann C, Kujat R. Cyclic, mechanical compression enhances chondrogenesis of mesenchymal progenitor cells in tissue engineering scaffolds. Biorheology 2004;41:335.

[67] Pelaez D, Huang CYC, Cheung HS. Cyclic Compression Maintains Viability and Induces Chondrogenesis of Human Mesenchymal Stem Cells in Fibrin Gel Scaffolds. Stem Cells Dev 2009;18:93.

[68] Crolet JM, Stroe MC, Racila M. Decreasing of mechanotransduction process with age. Comput Method Biomec 2010;13:43.

[69] Wu MZ, Fannin J, Rice KM, Wang B, Blough ER. Effect of aging on cellular mechanotransduction. Ageing Res Rev 2011;10:1.

[70] Le Maitre CL, Frain J, Millward-Sadler J, Fotheringham AP, Freemont AJ, Hoyland JA. Altered integrin mechanotransduction in human nucleus pulposus cells derived from degenerated discs. Arthritis Rheum 2009;60:460.

[71] Connelly JT, Garcia AJ, Levenston ME. Interactions between integrin ligand density and cytoskeletal integrity regulate BMSC chondrogenesis. Journal of Cellular Physiology 2008;217:145.

[72] Connelly JT, Garcia AJ, Levenston ME. Inhibition of in vitro chondrogenesis in RGD-modified three-dimensional alginate gels. Biomaterials 2007;28:1071.

[73] Kasten A, Muller P, Bulnheim U, Groll J, Bruellhoff K, Beck U, Steinhoff G, Moller M, Rychly J. Mechanical Integrin Stress and Magnetic Forces Induce Biological Responses in Mesenchymal Stem Cells Which Depend on Environmental Factors. Journal of Cellular Biochemistry 2010;111:1586.

[74] Chun C, Lim HJ, Hong KY, Park KH, Song SC. The use of injectable, thermosensitive poly(organophosphazene)-RGD conjugates for the enhancement of mesenchymal stem cell osteogenic differentiation. Biomaterials 2009;30:6295.

[75] Hosseinkhani H, Hosseinkhani M, Tian F, Kobayashi H, Tabata Y. Osteogenic differentiation of mesenchymal stem cells in self-assembled peptide-amphiphile nanofibers. Biomaterials 2006;27:4079.

[76] Guilak F, Alexopoulos LG, Upton ML, Youn I, Choi JB, Cao L, Setton LA, Haider MA. The pericellular matrix as a transducer of biomechanical and biochemical signals in articular cartilage. Ann Ny Acad Sci 2006;1068:498.

Chapter 4

Chondroitin sulfate and dynamic loading alter chondrogenesis of human MSCs in PEG hydrogels

(Submitted)

While biochemical and biomechanical cues are known to play important roles in directing stem cell differentiation, there remains little known regarding how these inextricably linked biological cues impact the differentiation fate of human marrow stromal cells (hMSCs). This study investigates the chondrogenic differentiation potential of hMSCs when encapsulated in a three dimensional (3D) hydrogel and exposed to a biochemical cue, chondroitin sulfate, a biomechanical cue, dynamic loading, and their combination. hMSCs were encapsulated in bioinert poly(ethylene glycol) (PEG) hydrogels only, PEG hydrogels modified with covalently incorporated methacrylated chondroitin sulfate (ChS) and cultured under free swelling conditions or subjected to delayed intermittent dynamic loading for two weeks. The 3D hydrogel environment led to the expression of chondrogenic genes (SOX9) and proteins (aggrecan and collagen II), but also upregulated hypertrophic genes (RUNX2 and Col X mRNA) and proteins (collagen X), while the application of loading generally led to a downregulation in chondrogenic proteins (collagen II). The presence of ChS led to elevated levels of aggrecan, but also collagen I, protein expression and when combined with dynamic loading downregulated, but did not suppress, hypertrophic genes (Col X and RUNX2) and collagen I protein expression. Taken together, this study demonstrates that while the 3D environment induces early terminal differentiation during chondrogenesis of hMSCs, the incorporation of chondroitin sulfate into

PEG hydrogels may slow the terminal differentiation process down the hypertrophic lineage particularly when dynamic loading is applied.

4.1 Introduction

Millions of people suffer pain and loss of joint mobility due to degenerative cartilage disorders, whether from a specific injury incurred or an unknown cause resulting in osteoarthritis (OA) [1-3]. With the U.S. healthcare system alone spending $186 billion annually on OA [4] and the poor ability of cartilage to heal on its own due to low cell densities and avascularity, significant efforts have turned to cartilage tissue engineering. Regenerating cartilage through tissue engineering holds great promise for health care prevention and management of cartilage damage and OA.

Tissue engineering strategies often combine an appropriate cell source with a 3D scaffold and introduce biological cues such as (in)soluble biochemical cues and/or biophysical cues to enhance stem cell differentiation or behavior of tissue-specific cells. Human adult mesenchymal stem cells or marrow stromal cells (MSCs) offer a promising cell source that overcomes many of the limitations associated with autologous primary chondrocyte (i.e., cartilage) cells, and can easily be expanded in culture and differentiate into multiple cell lineages including chondrocytes [5]. While a number of studies have investigated MSCs for cartilage regeneration, most studies employ non-human MSCs. With evidence in the literature pointing towards specie-dependent MSC differentiation potential as reviewed by [6], a need exists to better characterize human MSC differentiation in response to biological cues.

One promising platform for cartilage tissue engineering is poly(ethylene glycol) (PEG) based hydrogels. When cells are encapsulated, this three dimensional environment helps to maintain a round cell morphology, which is thought to be important in chondrogenesis [7]. PEG-based hydrogels offer a high degree of tailorability including the resultant mechanical properties [8], which is important for applications when mechanical forces are applied and ease with which

to incorporate a variety of biomimetic moieties. In particular, chondroitin sulfate (ChS) has been modified with methacrylates enabling its incorporation into PEG hydrogels in a controlled and robust manner [9, 10]. ChS is a negatively charged sulfated glycosaminoglycan, which is a major matrix component of cartilage [11] and has been shown to be chondro-protective acting in an anti-inflammatory role [12-14]. The incorporation of ChS into PEG based hydrogels has been shown to improve chondrogenic differentiation of goat MSCs [15] and when combined with dynamic compressive loading enhances matrix synthesis by primary bovine chondrocytes [16]. Modifying the bioinert PEG hydrogel with a molecule such as ChS presents an attractive strategy to create a local cartilage-like microenvironment, providing native biological cues to the encapsulated cells.

Based on promising evidence in the literature, this study set out to test the hypothesis that a PEG hydrogel covalently modified with ChS combined with dynamic loading would enhance hMSC chondrogenic differentiation and subsequently lead to cartilage specific matrix protein production. hMSC differentiation, through qRT-PCR and immunohistochemistry, was investigated in PEG/ChS hydrogels in the absence and presence of dynamic loading and in the absence and presence of soluble chondrogenic differentiation factors and compared to PEG hydrogels without ChS over two weeks. Overall findings from this study indicate that the PEG and PEG/ChS hydrogel environments enhance terminal differentiation of human MSCs and the application of loading generally led to an inhibitory effect on chondrogenesis. However, the presence of ChS appears to reduce, but not suppress, terminal differentiation, in the presence of loading. These findings suggest that biological cues will need to be optimized specifically for human MSCs.

4.2 **Methods**

hMSC Cell Culture and Aggregate Pellet Culture

Adult hMSCs (24 year old male, Texas A&M Health Science Center College of Medicine Institute for Regenerative Medicine) were cultured in basal stem cell medium (20% fetal bovine serum (FBS, Atlanta Biologicals), 1mg/mL amphotericin B, PSG (50 U/mL penicillin, 50 mg/mL streptomycin, and 20 mg/mL gentamicin) in low glucose Dulbecco's modified Eagle medium (αMEM, Invitrogen)). Cells were plated at ~60 cells/cm^2 till passage 2 (P2, 1:10), grown to 80% confluency, and frozen until use. P3 cells were thawed, plated at ~4500 cells/cm^2, and cultured to Passage 5 (P5) (1:5 for P3-P4, 1:6 for P4-P5). Pellet cell cultures were formed following [17] where 2.5x10^5 hMSCs were pelleted by centrifugation in individual 15 ml conical vials, and basal medium replaced with chondrogenic differentiation media (CDM: 1ml/100 ml media ITS+ Premix (BD), 100 nM dexamethasone, 10 ng/mL TGFβ3 (Peprotech), 50 mg/ml l-ascorbic acid 2-phosphate trisodium salt, 100 mg/ml sodium pyruvate, 1mg/mL amphotericin B, and PSG in high glucose DMEM (Invitrogen)). Aggregate samples were cultured for up to 14 days in a standard incubator. Medium was replaced every 2-3 days.

Macromer Synthesis, Hydrogel Formation and Their Characterization

Microwave methacrylation, described by [18], was used to synthesize poly(ethylene glycol) dimethacrylate (PEGDM) macromolecular monomers. Briefly, 4600 g/mol poly(ethylene glycol) (PEG) (Sigma-Aldrich) was reacted with excess methacrylic anhydride (Sigma-Aldrich) in the presence of hydroquinone (Sigma-Aldrich). The resultant product was purified by precipitations with ethyl ether, filtered, and dried under vacuum. The degree of methacrylation was determined to be 93% via ^{1}HNMR (Varian VYR-500), where the area under the curve for

the vinyl resonance peaks (d= 5.7 ppm, d = 6.1 ppm) was compared to the area under the curve for the methylene peaks in the PEG backbone (d =4.3 ppm). Methacrylated chondroitin sulfate (ChSMA) was synthesized [16, 19]. Briefly, 25% (w/v) chondroitin sulfate A (Sigma), containing ~30% chondroitin-6-sulfate and ~70% chondroitin-4 sulfate, in deionized water (dI-H_2O) was reacted in a 1:8 ratio with methacrylic anhydride at pH of 8 and 4º C for 24 hrs. The resultant product was precipitated in chilled methanol, dialyzed in dI-H_2O and recovered via lyophilization. ^{1}H NMR (Varian VYR-500), indicated that on average, there were 23 methacrylate groups per ChSMA molecule, where the area under the curve for the vinyl resonance peaks (d= 5.5-6.2 ppm) was compared to the area for the acetyl groups (d =1.7-2.0 ppm).

Hydrogels were formed from 10% (g/g) macromer solutions of 100% PEGDM (PEG) or 80:20 PEGDM:ChSMA (PEG/ChS), 0.05 wt% (g/g) photoinitiator (Irgacure 2959, Ciba Specialty Chemical) in PBS with photopolymerization (365 nm light at ~5 mW/cm^2, 10 minutes). Cylindrical hydrogels (height: ~5 mm; Ø: 5 mm) were swollen in PBS for 24 hrs at 37°C. The soluble fraction after 24 hours was assayed for ChS using the dimethylmethylene blue assay (DMMB) [20]. It was determined that ~80% of ChS in the precursor solution was incorporated into the hydrogel. The fixed charge density of PEG/ChS hydrogels was estimated from the true amount of ChSMA incorporated into the hydrogels, assuming 2 mol of equivalent charge per repeat unit with an average ChS molecular weight ~48,700 Da [19]. Swollen hydrogels were subjected to unconfined compression applied at a constant rate of 0.03mm/sec using nonporous platens (Bose LM1 Test Bench). The tangent compressive modulus was determined from the linear region of the stress/strain curve (n=4). The equilibrium volumetric

swelling ratio (Q) was estimated from the swollen hydrogel mass (M_s) dry polymer mass (M_d), and the densities of water and unmodified polymer (n=4) [21].

Cell Encapsulation

hMSCs were combined at a concentration of $10x10^6$ cells/mL macromer solution dissolved in either basal or CDM. Medium osmolarity was measured using a freezing point Osmometer (Precision Systems Inc, Natick, MA). Cell/macromer solutions were polymerized as described above. Cylindrical hMSC-laden hydrogels (height ~2.5mm; Ø=5 mm) were cultured in their respective culture medium for the duration of the study in standard culture conditions. Medium was replaced every two days.

Mechanical Loading

Custom-built bioreactors [22, 23] were employed to apply intermittent dynamic unconfined compressive strains to hMSC-laden hydrogels. Hydrogels were cultured under free swelling conditions for one week and then subjected to loading applied from 0 to 15% amplitude strain in a sinusoidal waveform at a frequency of 0.3 Hz (0.5hr on, 1.5hr off, repeated for 16 hours followed by 8hr off) for one week. This loading regime was selected because it has been shown to enhance Col 2 expression in primary bovine chondrocytes in similar PEG hydrogels [24]. A delayed application of dynamic loading was selected to allow hMSCs to begin chondrogenically differentiating, as immediate application of dynamic loading has been shown to inhibit chondrogenesis [25, 26]. Constructs were cultured in separate wells with 2 mL of medium changed every two days. Free swelling constructs were analyzed at days 7 and 14.

Loaded constructs were analyzed after 14 days (7 days free swelling followed by 7 days of loading) immediately following the 16-hour loading cycle.

Gene Expression

Total RNA was extracted from constructs (n=4) and purified using Total RNA Mini Kit (Omega Biotek) per manufacturer and quantified on a Nanodrop 1000 Spectrophotometer (Thermo Scientific). RNA (11.0 to 78.5 ng/μl) was transcribed to cDNA with a High Capacity Reverse Transcription Kit (Applied Biosystems). Primers were designed in Primer Express 3.0 (Applied Biosystems) and purchased from Integrated DNA Technologies (Table SI). Real-time polymerase chain reactions (RT-PCR) was performed with Fast SYBR® Green Master Mix (Applied Biosystems) on a 7500 Fast Real-Time PCR Machine (Applied Biosystems). All genes were normalized to the housekeeping gene, L30, and relative expression levels were calculated from a modified ΔΔCt method with true primer efficiencies (Table SI) [27].

Total DNA Content

Constructs (n=4) were homogenized and digested in 0.125 mg/ml of papain (Worthington). Double stranded DNA was measured with the PicoGreen® assay (Invitrogen).

Immunohistochemistry

Constructs (n=2) were fixed overnight in 4% paraformaldehyde, embedded, flash frozen. Sections (20 μm) were pretreated with Chondroitanase-ABC (500 mU/mL) (Sigma-Aldrich), then with protease (from *streptomyces griseus*, Sigma-Aldrich) for anti-collagen I and II or with pepsin for anti-collagen X. After permeabilization (0.25% Triton-X 100™) and blocking (10%

normal goat serum), sections were treated with anti-aggrecan (US Biologicals, 1:5), anti-type I collagen (Abcam; Cambridge, MA, 1:400), anti-type II collagen (Abcam, 1:100), and anti-type X collagen (Developmental Studies Hybridoma Bank, 1:2) followed by goat anti-mouse IgG labeled with Alexa Fluor® 546 or 488 (Invitrogen, 1:200) and counterstained with DAPI. Sections were stained with Leukocyte Alkaline Phosphatase (ALP) Kit, per manufacturer (Sigma-Aldrich) and with Oil Red O to assess for lipids (Sigma-Aldrich). Sections were imaged on a laser scanning confocal microscope (Zeiss LSM 510). Using Image J, grayscale images for the two channels (405 nm, DAPI and either 546 or 488 nm Alexa Flour®) were separated and inverted. The 16_color lookup table was applied to the Alexa Flour® channel and the images re-merged. Staining intensity is converted to a color spectrum scale from red (low) to violet (high).

Cell Straining

Cell-laden hydrogels were treated with 2μM calcein-AM (Invitrogen). Hydrogels were placed in a custom-built cell straining device which sits on the stage of an inverted confocal microscope [28]. Hydrogels were subjected to 0% or 15% static compressive strains. Cells were imaged at half height maximum width. A diameter ratio (x/y) was determined where x and y are cell diameters in the axes parallel and perpendicular to the applied strain, respectively. ~30-45 cells per hydrogel (n=3) were imaged.

Statistical analysis

Data were analyzed using One Way ANOVA with a Tukey HSD Post Hoc with $p < 0.05$ considered significant. Data are reported as the mean ± standard deviation of the mean.

4.3 Results

Characterization of Acellular Constructs and the Media

The macroscopic properties for PEG and PEG/ChS hydrogels are given in Table I. The volumetric swelling ratio, Q, which is a measure of the amount of water the hydrogel imbibes, was similar for PEG and PEG/ChS in the range 11-12. The tangent compressive modulus was also similar for PEG and PEG/ChS at 72 and 83 kPa, respectively. For the PEG/ChS hydrogels, the fixed charge density was estimated to be 0.130 mEq/ml, which falls in the range reported for human cartilage [29]. The osmolarity for the basal and chondrogenic media was determined to be 290 and 330 mOsm, respectively.

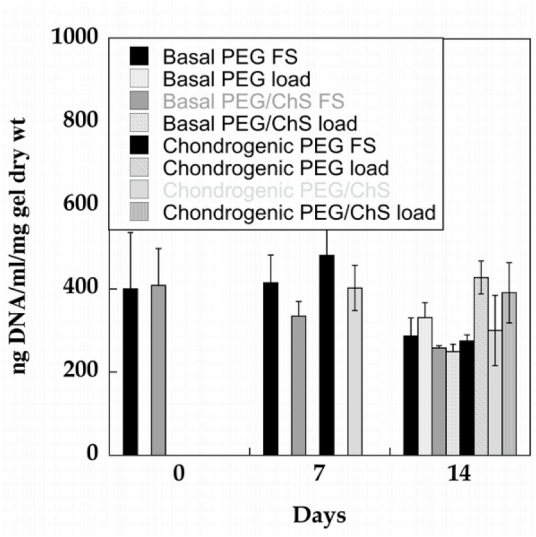

Figure S4.1: Total DNA for each condition type over the 14 day study.

	Fixed Charge Density (mEq/ml)	Q[b]	K[c] (kPa)
PEG	n/a	11.4 ±0.43	71.9±7.8
PEG/ChS	0.130 ± 0.0012	12.03 ±0.48	83.4±14.4
Human cartilage	0.1-0.28[a]	n/a	n/a

Table 4.1: [a]Depth dependent fixed charge density of human articular cartilage (mEq/ g tissue water) reported by Chen et al. 2001, [b]volume swelling ratio (Q), [c]unconfined tangent compressive modulus (K).

hMSC Deformation

Cell deformation was measured for hMSCs encapsulated in PEG and PEG/ChS gels under the application of a 15% static strain, which is the maximum strain applied to the hydrogels in the dynamic loading study. The cytosol of encapsulated hMSCs was fluorescently stained to visualize the cells and their morphology was measured prior to, and after the application of the strain. Prior to the application of strain, cell shape was generally round. After the application of the strain, cell shape became ellipsoidal. Representative images of cells in each hydrogel strained and unstrained are in Fig. 1A-D. Diameter ratios were significantly reduced under the applied strain and were similar for both hydrogels at 0.84.

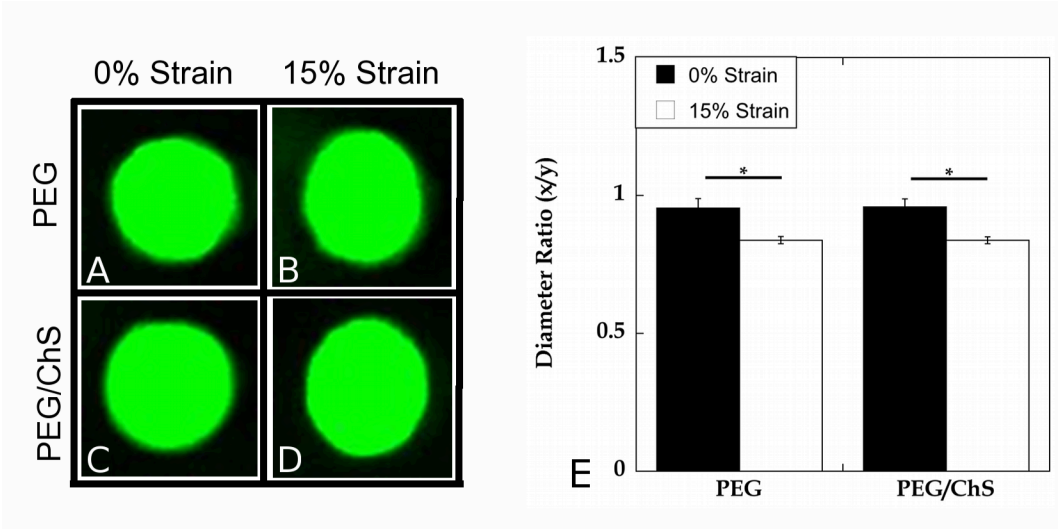

Figure 4.1: A-D) Representative confocal microscopy images of hMSCs encapsulated in PEG only (A-B) and PEG/ChS (C-D) constructs subjected to no strain (A, C) or 15% gross static strain (B, D). Original magnification is 200x. E) hMSC deformation was quantitatively assessed in each construct under 0% (black) and 15% (white) gross strains, means ± standard mean of the error are presented with * $p < 0.05$.

Temporal gene expression in hMSCs-laden hydrogels and pellet cultures

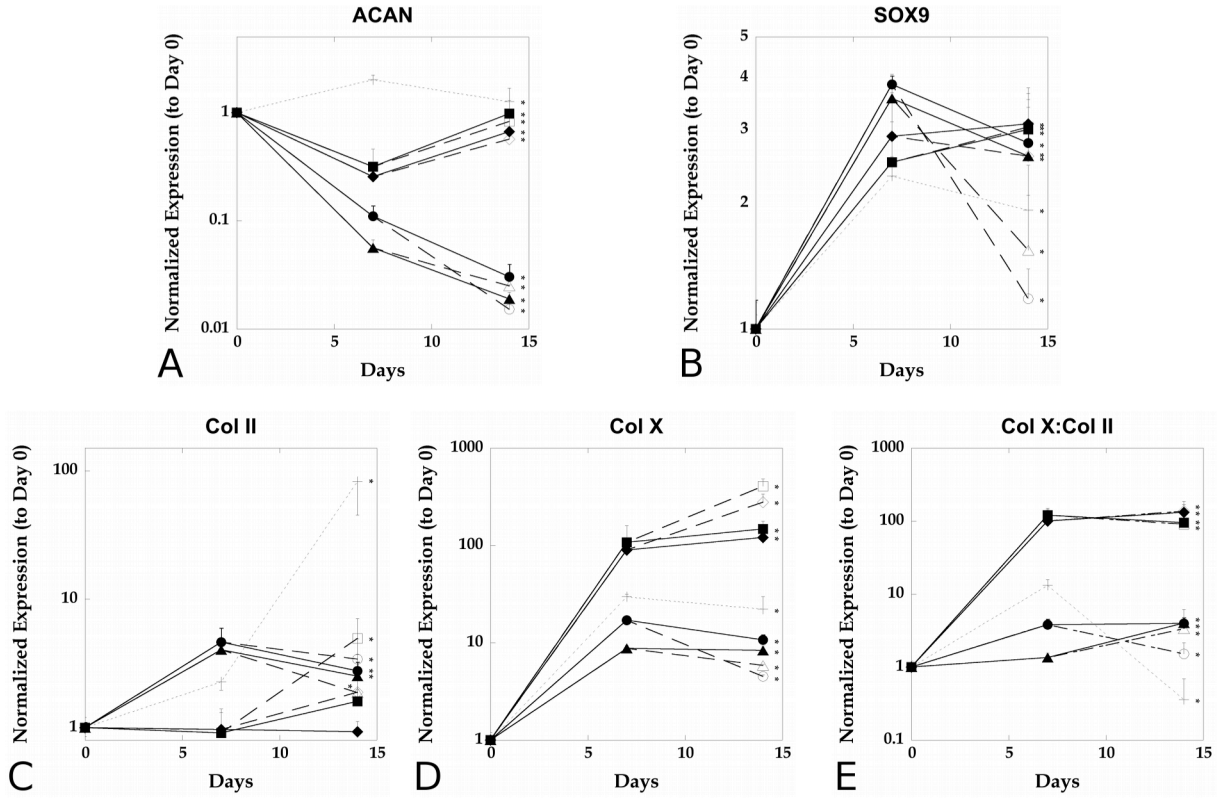

Figure 4.2: Normalized temporal gene expression for chondrogenic (SOX9, Col II, ACAN, and ColX) differentiation markers for basal PEG free swelling (●), basal PEG/ChS free swelling (▲), chondrogenic PEG free swelling (■), chondrogenic PEG/ChS free swelling (◆), basal PEG loaded (○), basal PEG/ChS loaded (△), chondrogenic PEG loaded (□), chondrogenic PEG/ChS loaded (◇), pellet control (+) cultured for up to 14 days. Means ± standard deviations are presented as normalized relative expression (to day 0) and are relative to the housekeeping gene L30 (n=4), * $p < 0.05$.

In general, gene expression for several chondrogenic (aggrecan, SOX9, Col II), hypertrophic (Col X, Col X/Col II), and osteogenic (RUNX2, ALP, Col I, Osteocalcin) markers changed over the course of two weeks in hMSC-laden PEG and PEG/ChS hydrogels and in hMSC pellet cultures when cultured either in basal growth media or CDM. In all hydrogel conditions, aggrecan expression (Fig. 2A) decreased during week one. During week two, aggrecan expression in CDM returned to initial levels while expression in basal medium

continued to drop. In pellet culture, aggrecan expression increased during the first week, but returned to initial levels by day 14. SOX9 expression (Fig. 2B), an early chondrogenic transcription factor, increased significantly during week one for all conditions. During week two, SOX9 expression decreased with loading in PEG and PEG/ChS basal constructs, but was not affected in the CDM and pellet constructs. Mean Col II expression (Fig. 2C) did not change for free swelling CDM constructs over two weeks, while in all other conditions expression increased over time with the highest expression being in the pellet culture at day 14. All conditions upregulated Col X expression (Fig 2D) during week one, with the highest expression being in the CDM hydrogel constructs. During week two, loading further increased Col X expression in CDM hydrogel constructs, but decreased Col X expression under basal conditions. During week one, Col X/Col II (Fig 2E) increased for all CDM conditions and to a lesser extent for basal constructs. During week two, Col X/Col II decreased significantly in pellet culture, but remained constant for all hydrogel conditions.

RUNX2 expression (Fig. 3A), an early osteogenic transcription factor, increased significantly for all hydrogel conditions and to a lesser extent pellet cultures during week one. During week 2, RUNX2 expression decreased for all hydrogel conditions except for CDM free swelling PEG and PEG/ChS and loaded PEG constructs. ALP expression (Fig. 3B) was

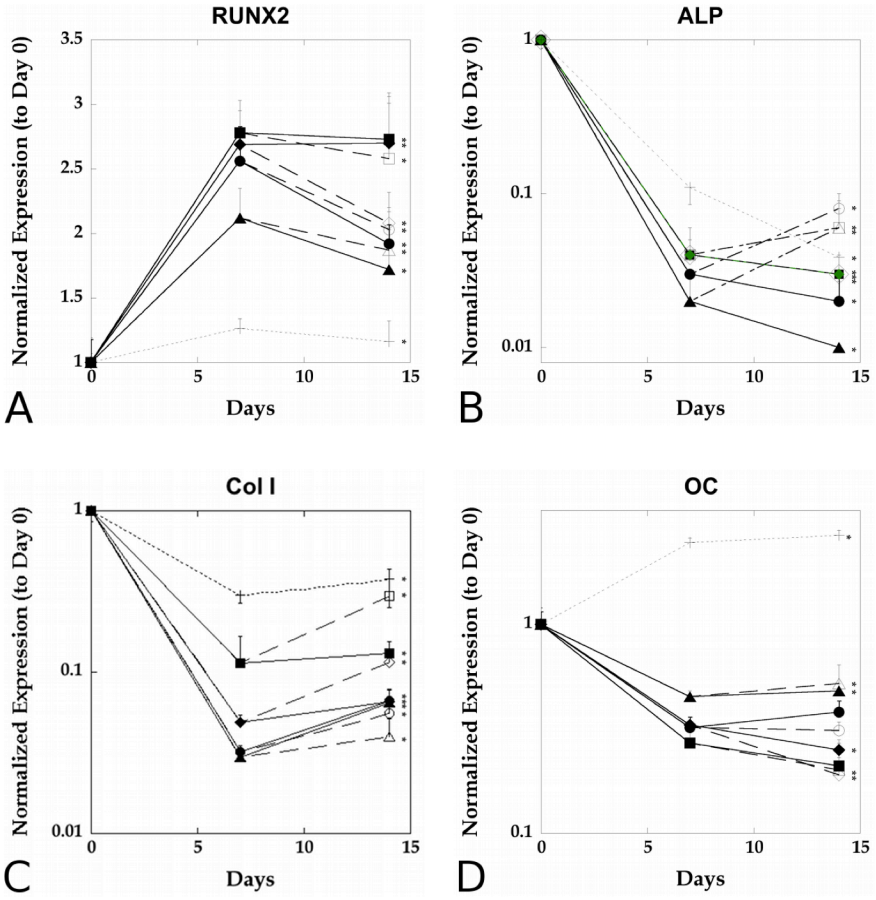

Figure 4.3: Normalized temporal gene expression for osteogenic (RUNX2, ALP, Col 1 and OC) differentiation markers for basal PEG free swelling (●), basal PEG/ChS free swelling (▲), chondrogenic PEG free swelling (■), chondrogenic PEG/ChS free swelling (◆), basal PEG loaded (○), basal PEG/ChS loaded (△), chondrogenic PEG loaded (□), chondrogenic PEG/ChS loaded (◇), pellet control (+) cultured for up to 14 days. Means ± standard deviations are presented as normalized relative expression (to day 0) and are relative to the housekeeping gene L30 (n=4), * $p < 0.05$.

significantly downregulated over time in all conditions. Col I expression (Fig. 3C) decreased for all conditions during week one. In week two, loading plus CDM increased Col I expression, while free swelling conditions remained constant. Overall, pellet cultures had the highest Col I expression. Osteocalcin expression (Fig. 3D) was significantly downregulated for all hydrogel conditions but significantly upregulated in pellet culture over time.

Cell Content and ECM Molecule Expression by Encapsulated hMSCs

Initial cell content, based on total DNA, was similar for both PEG and PEG/ChS hydrogels (Fig. S1). At day 7, cell content remained high for PEG and PEG/ChS in basal and CDM. By day 14, cell content was reduced by ~25-35% in the free swelling constructs and basal loaded constructs, but remained at ~100% of day 0 values in the loaded CDM constructs.

Representative histology images are shown in Figures 4-7 for aggrecan, collagen II, X and I, respectively, with general qualitative observations given in Table II. All staining appears to be primarily intracellular. Aggrecan was the most prominent ECM protein expressed. By day 7, all hydrogels stained positive for aggrecan with CDM PEG/ChS hydrogels staining the strongest. There was a qualitative increase in staining for aggrecan in all conditions at day 14, with a further increase in staining due to loading in the CDM PEG constructs. Only CDM PEG and PEG/ChS free swelling conditions stained positive for collagen II at day 14. Loading inhibited collagen II protein expression, with no detectable staining present in the CDM loaded hydrogels. Collagen X protein was present in all conditions at day 7. By day 14, collagen X expression increased in all conditions except the loaded basal constructs which showed no qualitative change. Collagen I protein expression was only present in the CDM PEG/ChS hydrogels at day 7, which remained at day 14 under free swelling conditions. Slight collagen I was observed at day 14 for the other conditions under free swelling. Qualitatively, loading appears to inhibit collagen I in both CDM conditions while enhancing its expression in the basal PEG/ChS condition. All conditions stained negatively for lipids (Oil Red O) and for alkaline phosphatase activity (data not shown).

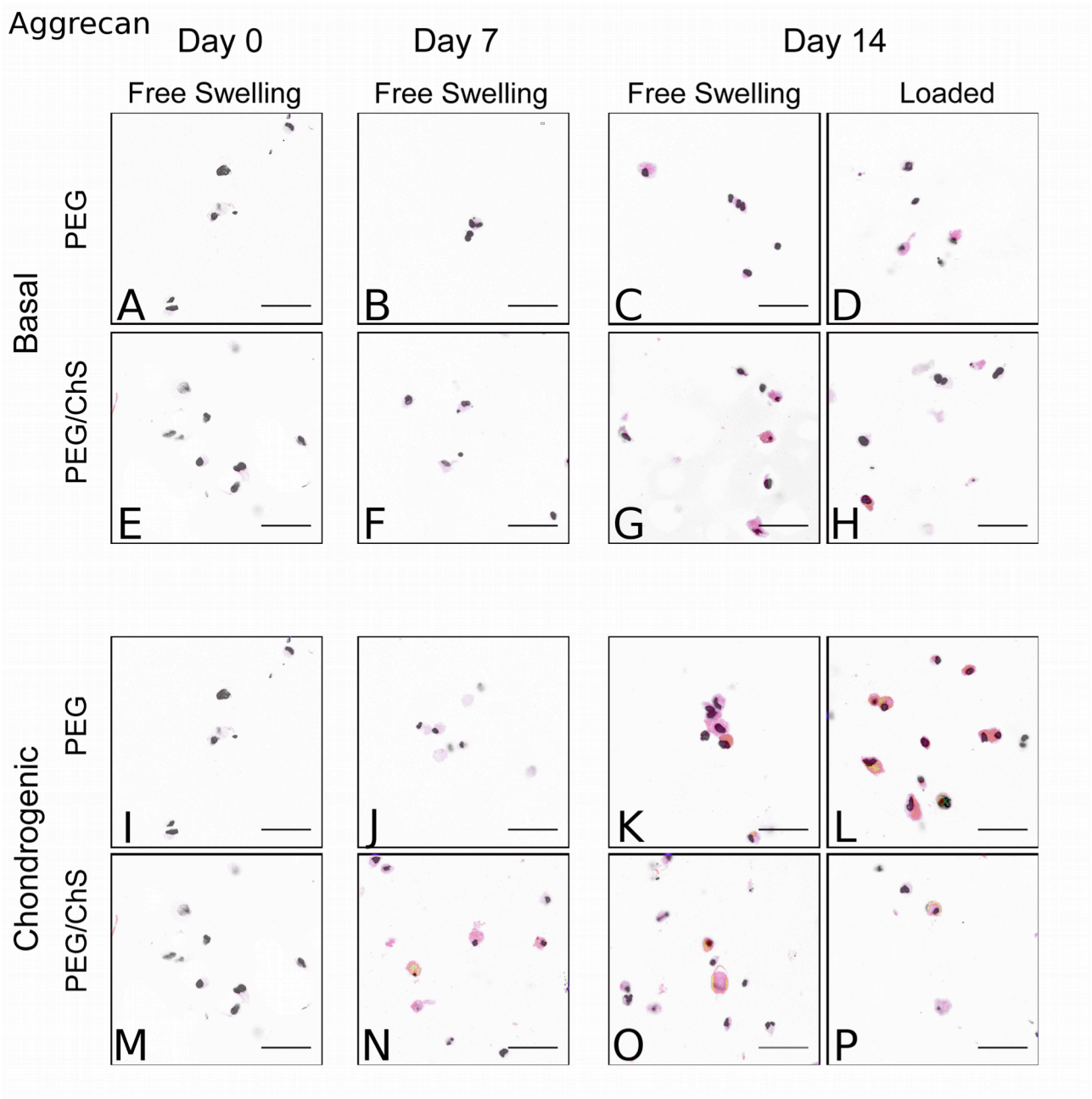

Figure 4.4: Immunohistochemical deposition of aggrecan by hMSCs encapsulated in PEG constructs (A-D, I-L), PEG/ChS constructs (E-H, M-P), conditioned in basal media (A-H) or CDM (I-P) that underwent free swelling and loading conditions and were cultured for up to 14 days. Original magnification is 400x. Staining intensity is visualized with a color spectrum scale from red to violet, with red indicating low intensity and violet indicating high intensity.

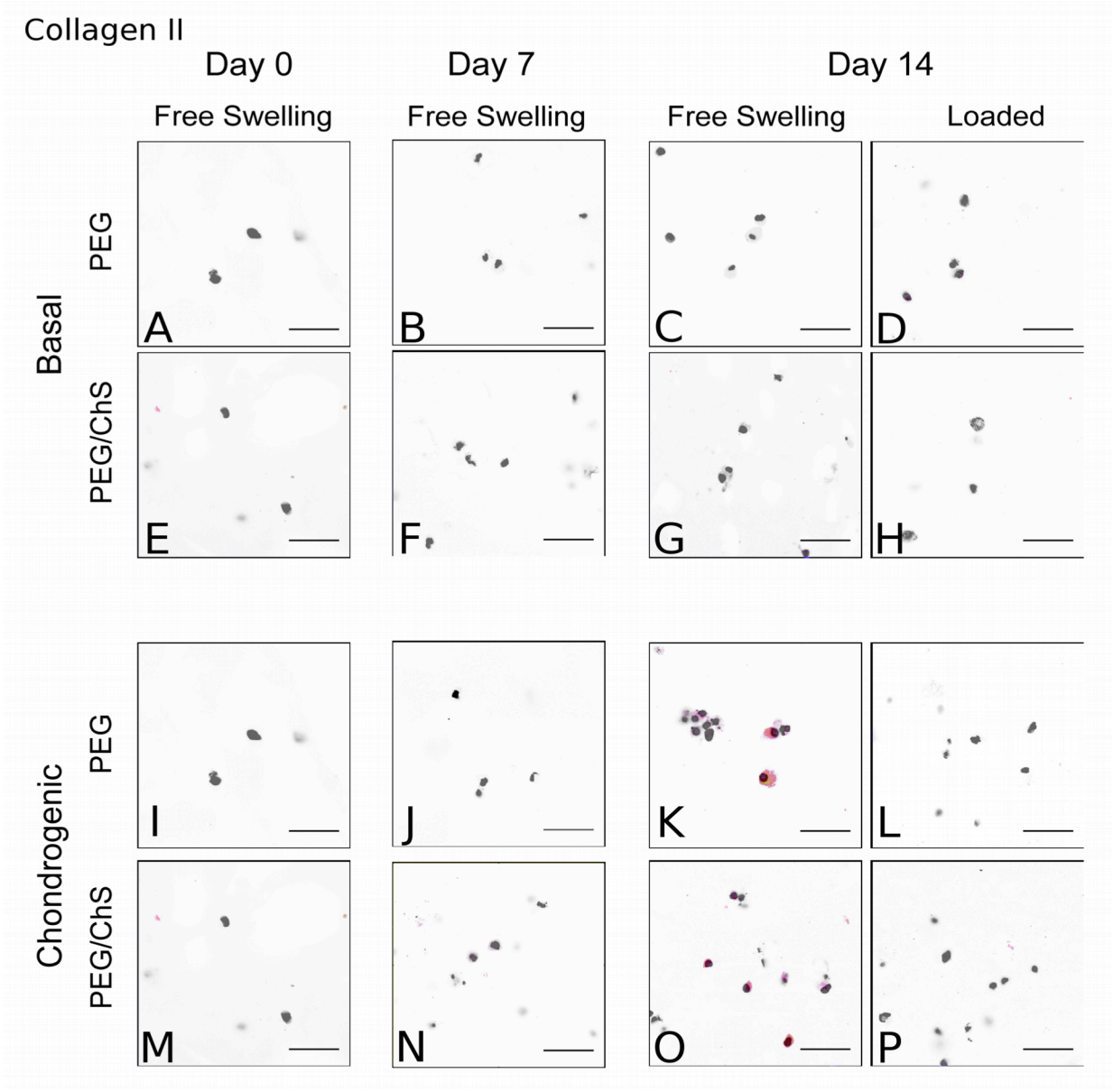

Figure 4.5: Immunohistochemical deposition of type II collagen by hMSCs encapsulated in PEG constructs (A-D, I-L), PEG/ChS constructs (E-H, M-P), conditioned in basal media (A-H) or CDM (I-P) that underwent free swelling and loading conditions and were cultured for up to 14 days. Original magnification is 400x. Staining intensity is visualized with a color spectrum scale from red to violet, with red indicating low intensity and violet indicating high intensity.

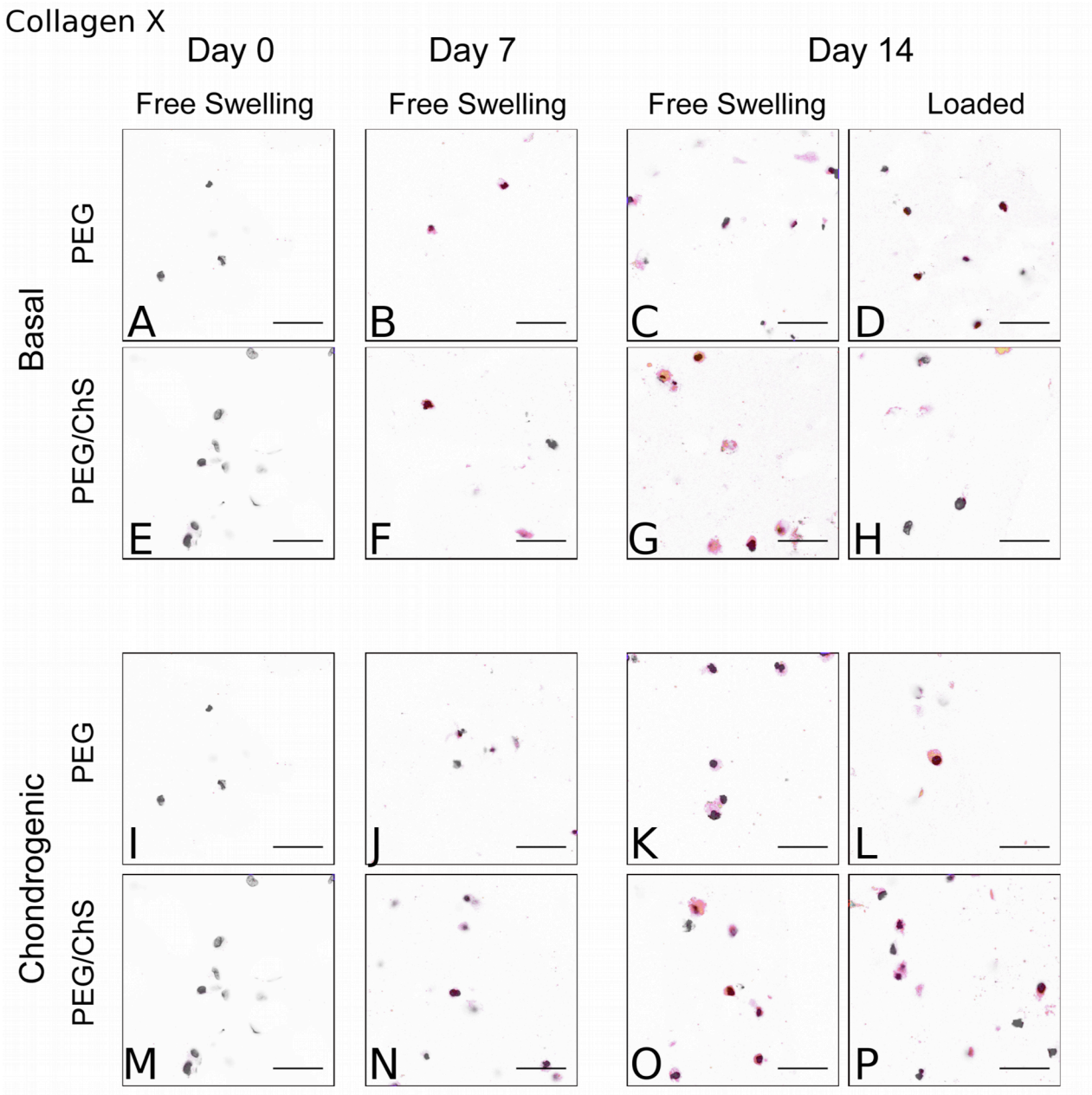

Figure 4.6: Immunohistochemical deposition of type X collagen by hMSCs encapsulated in PEG constructs (A-D, I-L), PEG/ChS constructs (E-H, M-P), conditioned in basal media (A-H) or CDM (I-P) that underwent free swelling and loading conditions and were cultured for up to 14 days. Original magnification is 400x. Staining intensity is visualized with a color spectrum scale from red to violet, with red indicating low intensity and violet indicating high intensity.

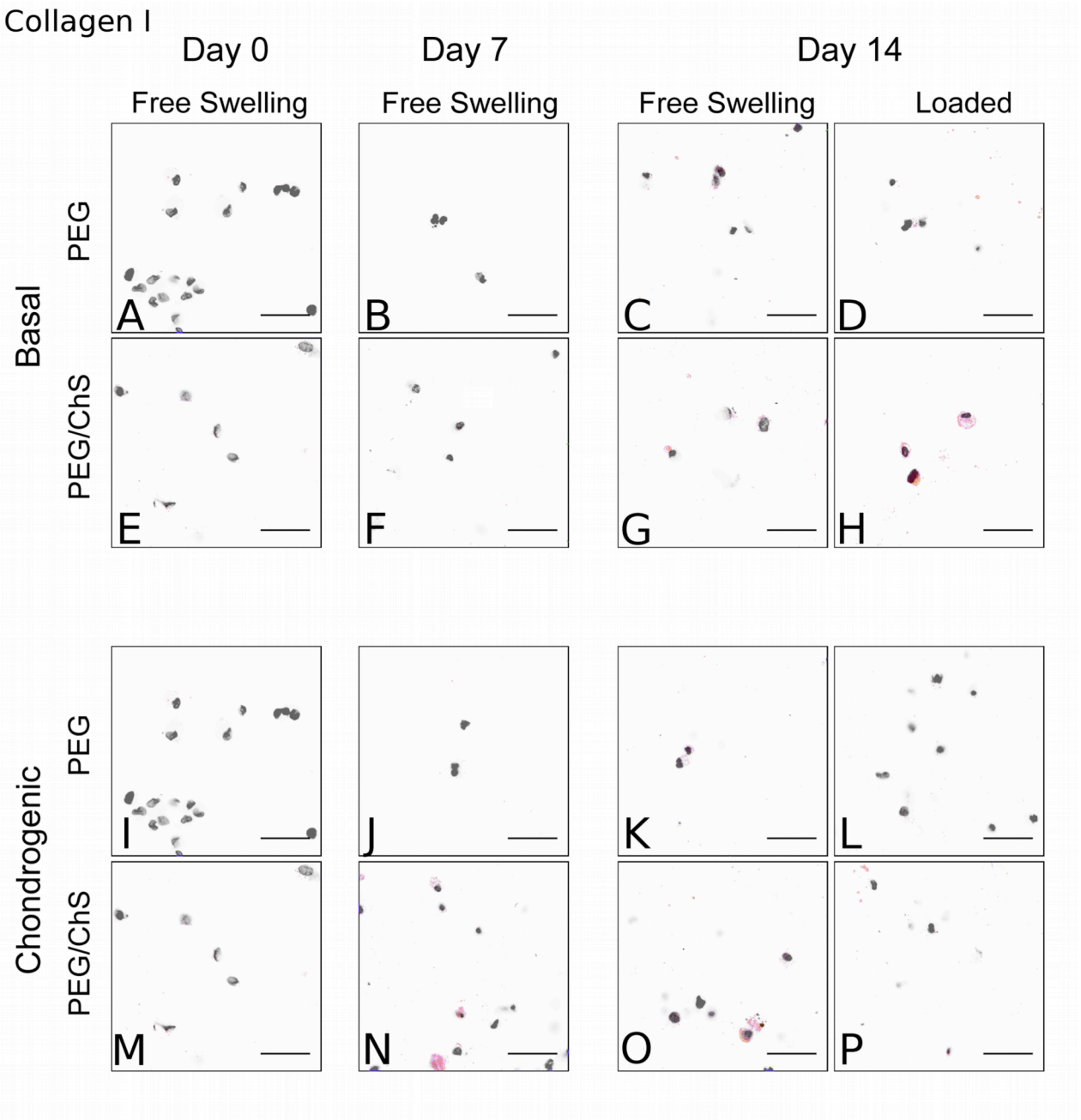

Figure 4.7: Immunohistochemical deposition of type I collagen by hMSCs encapsulated in PEG constructs (A-D, I-L), PEG/ChS constructs (E-H, M-P), conditioned in basal media (A-H) or CDM (I-P) that underwent free swelling and loading conditions and were cultured for up to 14 days. Original magnification is 400x. Staining intensity is visualized with a color spectrum scale from red to violet, with red indicating low intensity and violet indicating high intensity.

	Day 0-FS	Day 7-FS	Day 14-FS	Day 14, load	load effect
Aggrecan					
Basal PEG	X	+	++	++	ne
Basal PEG/ChS	X	+	++	++	ne
Chondrogenic PEG	X	+	++	+++	#
Chondrogenic PEG/ChS	X	++	++	++	ne
Collagen II					
Basal PEG	X	X	X	X	ne
Basal PEG/ChS	X	X	X	X	ne
Chondrogenic PEG	X	X	+	X	-
Chondrogenic PEG/ChS	X	X	+	X	-
Collagen X					
Basal PEG	X	+	++	+	-
Basal PEG/ChS	X	+	++	+	-
Chondrogenic PEG	X	+	++	++	ne
Chondrogenic PEG/ChS	X	+	++	++	ne
Collagen I					
Basal PEG	X	X	+	+	ne
Basal PEG/ChS	X	X	+	++	#
Chondrogenic PEG	X	X	+	X	-
Chondrogenic PEG/ChS	X	++	++	+	-

Table 4.2: Denotation of qualitative observations for IHC staining in Figure 5 (n=2). X denotes no detected staining, + denotes weak staining, ++ denotes stronger staining, +++ denotes strongest staining in free swelling and loaded samples. # denotes an increase in staining with the application of load, - denotes a reduction in staining with load, and "ne" denotes no effect from load.

4.4 Discussion

The main findings from this study are that during early chondrogenesis of hMSCs i) a three-dimensional culture environment neutral or charged enhances terminal differentiation during chondrogenesis in human MSCs, ii) the application of dynamic unconfined compressive loading, at least under the conditions investigated in this study, hinders stable chondrogenesis while simultaneously enhancing terminal differentiation, and iii) the presence of negatively charged chondroitin sulfate promotes production of aggrecan and collagen I, but under loading appears to have a positive effect by reducing terminal differentiation and collagen I expression.

One of the challenges in using MSCs for cartilage tissue engineering is that their natural pathway *in vivo* is endochondral ossification; where MSCs normally follow a terminal differentiation fate during chondrogenesis. It has been shown that in the *in vitro* pellet culture model, pellets supplemented with dexamethasone and TGF-β lead to chondrogenesis evidenced by increased Col II mRNA and protein expression. However, this invariably is followed by up-regulations in Col X and ALP activity, indicating terminal differentiation of MSCs [17], and leads to calcification when implanted *in vivo*, further supporting a pathway to endochondral ossification [30, 31]. Strategies to suppress terminal differentiation have only had marginal success, largely due to the fact that pathways involved in terminal differentiation *in vivo* remain unclear and pathways that regulate *in vitro* chondrogenesis appear to be markedly different [32]. However, chondrogenic differentiation of human MSCs in hydrogels (e.g., Matrigel™) has shown reduced Col X expression *in vitro* and reduced calcification *in vivo*, suggesting a role for hydrogels in controlling hypertrophy and terminal differentiation of MSCs [33].

In this study, comparison to pellet cultures revealed that PEG or PEG/ChS hydrogels appear to induce terminal differentiation earlier than pellet cultures, in the presence of

chondrogenic medium under free swelling conditions [34]. This was apparent by lower levels of aggrecan and Col II mRNA concomitant with higher mRNA levels of RUNX2 and Col X/Col II mRNA in the hydrogels over pellet cultures. Gene expression in the hydrogels was corroborated at the protein level, where both aggrecan and collagen II proteins were expressed, but collagen X protein expression was notably higher. It is important to note that aggrecan and collagen X proteins were expressed before collagen II, which agrees with findings from others [32]. Interestingly, late markers of terminal differentiation (ALP and osteocalcin mRNA), and Col I mRNA decreased with time in the hydrogels, which were similar or lower to pellet cultures, with no ALP protein expression detected in the hydrogels. It has been suggested that *in vitro*, Col X is regulated independent of ALP, where collagen X is not sufficient to induce mineralization in the absence of ALP [35]. Therefore, it is possible that the hydrogel environments, which maintain a round cell morphology, may suppress the late stages of hypertrophy. However, others have reported that ALP activity in hMSC pellets does not appear until three weeks [32]. Therefore, longer culture times are required to determine the long-term fate of hMSCs in PEG and PEG/ChS hydrogels. It is important to recognize that the mesh size of the hydrogels will impact diffusion of larger molecules (e.g., TGFβ) [36] and may delay the onset of chondrogenic differentiation when compared to pellet cultures.

It is interesting to note that in the absence of differentiation cues, both PEG and PEG/ChS hydrogels support expression of aggrecan and collagen X as early as day 7 suggesting that the preferred rounded morphology alone may be capable of inducing hMSC chondrogenesis. Although these systems did not induce the expression of collagen II, this could be due to the relatively short duration of this study. Previous work had demonstrated that goat MSCs

encapsulated in PEG based hydrogels expressed collagen II protein after six weeks of culture in the absence of chondrogenic differentiation cues [37].

One of the goals of this study was to investigate whether the incorporation of a cartilage biomimetic matrix component, specifically negatively charged chondroitin sulfate into a hydrogel, could favorably impact chondrogenesis of hMSCs over a bioinert and neutral hydrogel. Our results indicate that ChS indeed has an effect on hMSCs. Under free swelling conditions, ChS led to a stronger early response in aggrecan and collagen I protein expression, possibly indicating a fibrocartilage pathway [38]. Most interesting is that under dynamic loading, the presence of ChS downregulated Col X ($p<0.05$) and RUNX2 ($p<0.05$) by ~30% as well as collagen I protein expression. Interestingly, Col II does not appear to be impacted by ChS showing similar mRNA levels and protein expression with PEG hydrogels; although it was hindered by dynamic loading. The effect of ChS is largely attributed to the presence of charge because PEG and PEG/ChS hydrogels had similar volumetric swelling ratios, compressive moduli, and resulted in similar local strains experienced by cells under loading. The presence of fixed negative charges can impact cells by interacting with positively charged molecules. ChS will bind positively charged TGFβ [39] and may bind other positively charged signaling molecules (e.g., serum proteins), potentially enhancing the contextual presentation of these molecules to cells or alternatively reducing their availability to cells. Additionally, the fixed negative charges will attract positive ions from the media creating a hyperosmotic environment, which will be dynamic under loading [16, 40]. Hyperosmolarity has been shown to effect negatively MSC cells leading to apoptosis [41] and decreasing cartilage matrix protein expression [42] but has had a positive effect on total GAG production by chondrogenically differentiating adipose derived stem cells [43]. We recently demonstrated that chondrocytes

responded more favorably to a hyperosmotic environment under dynamic loading [16, 44]. Taken together, we hypothesize the favorable results observed with dynamic loading may be a result of the dynamic hyperosmotic environment. Additional studies are necessary to confirm this hypothesis.

A few studies report on the effect of chondroitin sulfate on MSCs in 3D scaffolds [15, 45-47], with even fewer studies focusing on clinically relevant human MSCs [45], and none to the best of our knowledge, combined with mechanical stimulation. Our findings differ from reports with goat MSCs encapsulated in ChS modified PEG gels under free swelling, where collagen II protein expression was detected with a notable lack of collagen X after 6 weeks [15]. The differences are likely due to a combination of specie-dependent differentiation potential and the duration of the studies (2 vs. 6 weeks), during which time it was noted that the encapsulated cells began degrading the ChS modified hydrogels which led to the formation of nodules of macroscopic tissue elaboration. Interestingly, Vargehese *et al*. incorporated higher amounts of ChS which would lead to an even higher local osmolarity. It is possible that adult human MSCs may respond markedly different to the osmotic environment that younger goat MSCs. Given that collagen II protein expression was observed at day 14, it is also possible with long term studies and a degradable system a more stable chondrogenic phenotype may arise.

Regardless of the hydrogel environment, PEG or PEG/ChS, dynamic loading hindered collagen II deposition. This finding is consistent with our previous work utilizing PEG/RGD hydrogels [25]. We hypothesize that dynamic loading may delay the onset of chondrogenesis. Others [26] have reported inhibition of chondrogenesis with the application of loading to MSCs-laden hydrogels, however, if cells were chondrogenically differentiated first, loading was no longer inhibitory [48]. Although, a one week chondrogenic differentiation period was employed

in this study, hMSCs had not yet produced collagen II protein, suggesting that cells may need to become more stably differentiated before mechanical stimulation is applied.

In summary, PEG and the PEG/ChS hydrogels were found to induce an early terminal chondrogenic differentiation response based on elevated aggrecan protein expression in combination with elevated gene and protein expression of the hypertrophic protein, collagen X. The presence of charge may slow terminal differentiation in the presence of loading; however loading appears to have a general inhibitory effect on collagen II protein expression. This suggests that additional studies are necessary to define optimal cues, ChS concentration and loading regimes, which together support stable chondrogenic differentiation of human MSCs. Under the conditions investigated in this study, hMSCs in the PEG/ChS hydrogel subjected to mechanical stimulation express aggrecan, collagen X, and collagen I proteins, a combination which represents key ECM molecules that are present in the interfacial region between cartilage and bone, i.e. osteochondral interface [49]. Cartilage tissue engineering strategies will require the engineered cartilage to successfully integrate with the underlying subchondral bone through the osteochondral interface. Therefore the ChS and loading regimes employed in this study may be a good candidate for use in osteochondral tissue engineering applications where a successful interfacial region between bone and cartilage is required; however additional studies are needed to define biological cues for regenerating stable cartilage.

4.5 Acknowledgements

This study was supported by a NSF CAREER Award. Human MSCs were obtained from the Texas A&M Health Science Center College of Medicine Institute for Regenerative Medicine at Scott & White through a grant from NCRR of the NIH, Grant #P40RR017447. Collagen X

monoclonal antibody developed by Thomas F. Linsenmayer was obtained from the Developmental Studies Hybridoma Bank developed under the auspices of the NICHD and maintained by The University of Iowa. Confocal microscopy was performed at the Nanomaterials Characterization Facility at the University of Colorado.

Primer type	Primer Sequence	Primer concentration (nM)/Efficiency
L30 forward	TGGTGTCCATCACTACAGTGGCAA	250/99%
reverse	ACCAGTCTGTTCTGGCATGCTTCT	
SOX9 forward	TGACCTATCCAAGCGCATTACCCA	250/99%
reverse	ATCATCCTCCACGCTTGCTCTGAA	
ACAN forward	ACAATGCCCAAGACTACCAGTGGA	350/84.5%
reverse	TTCTCGTGCCAGATCATCACCACA	
Col II forward	GGTGGCTTCCATTTCAGCTATG	250/92%
reverse	TCTTGCAGTGGTAGGTGATGTTCT	
Col X forward	TTTTGCTGCTAGTATCCTTGAACTTG	200/87.5%
reverse	CTGTGTCTTGGTGTTGGGTAGTG	
Col I forward	TAGGGTCTAGACATGTTCAGCTTTGT	300/99.8%
reverse	CCGTTCTGTACGCAGGTGATT	
RUNX2 forward	ACCAGTTGAGGTGCACTAAAGGGA	250/100.8%
reverse	AGTTCAGATGAGGACCTGCAGCAT	
ALP forward	TGCAGTACGAGCTGAACAGGAACA	250/100%
reverse	ACTCTCTGCCTGCCCAAGAGAAAT	
OC forward	GGGAGGTGTGTGAGCTCAATC	250/108%
reverse	GCCGTAGAAGCGCCGATAG	

Table Supplemental 4.1: Primer sequences used in qRT-PCR.

4.6 References

[1] Mirzayan R. Cartilage Injury in the Athlete. New York, NY: Thieme Medical Publishers; 2006.

[2] Clifford R. Wheeless III M. Wheeless' Textbook of Orthopaedics. In: Clifford R. Wheeless III M, editor. Articular Cartilage. Durham, NC: Data Trace Internet Publishing, LLC; 2011.

[3] Nordin M, Frankel VH. Basic biomechanics of the musculoskeletal system. In: Butler J, editor. Baltimore, MD: Lippincott Williams & Wilkins; 2001.

[4] Kotlarz H, Gunnarsson CL, Fang H, Rizzo JA. Insurer and Out-of-Pocket Costs of Osteoarthritis in the US Evidence From National Survey Data. Arthritis Rheum 2009;60:3546-53.

[5] Caplan AI. Mesenchyman stem cells. J Orthop Res 1991;9:641-50.

[6] Bosnakovski D, Mizuno M, Kim G, Ishiguro T, Okumura M, Iwanaga T, et al. Chondrogenic differentiation of bovine bone marrow mesenchymal stem cells in pellet cultural system. Experimental Hematology 2004;32:502-9.

[7] Gao L, McBeath R, Chen CS. Stem Cell Shape Regulates a Chondrogenic Versus Myogenic Fate Through Rac1 and N-Cadherin. Stem Cells 2010;28:564-72.

[8] Bryant SJ, Anseth KS. Hydrogel properties influence ECM production by chondrocytes photoencapsulated in poly(ethylene glycol) hydrogels. Journal of Biomedical Materials Research 2002;59:63-72.

[9] Bryant SJ, Arthur JA, Anseth KS. Incorporation of tissue-specific molecules alters chondrocyte metabolism and gene expression in photocrosslinked hydrogels. Acta Biomaterialia 2005;1:243-52.

[10] Li Q, Wang DA, Elisseeff JH. Heterogeneous-phase reaction of glycidyl methacrylate and chondroitin sulfate: Mechanism of ring-opening-transesterification competition. Macromolecules 2003;36:2556-62.

[11] Dziewiatkowski DD. Isolation of chondroitin sulfate-S-35 from articular cartilage of rats. J Biol Chem 1951;189:187-90.

[12] Bassleer C, Rovati L, Franchimont P. Stimulation of proteoglycan production by glucosamine sulfate in chondrocytes isolated from human osteoarthritic articular cartilage in vitro. Osteoarthritis Cartilage 1998;6:427-34.

[13] Pipitone VR. Chondroprotecition with chondroitin sulfate. Drugs under Experimental and Clinical Research 1991;17:3-7.

[14] Ronca F, Palmieri L, Panicucci P, Ronca G. Anti-inflammatory activity of chondroitin sulfate. Osteoarthritis Cartilage 1998;6:14-21.

[15] Varghese S, Hwang NS, Canver AC, Theprungsirikul P, Lin DW, Elisseeff J. Chondroitin sulfate based niches for chondrogenic differentiation of mesenchymal stem cells. Matrix Biology 2008;27:12-21.

[16] Villanueva I, Gladem SK, Kessler J, Bryant SJ. Dynamic loading stimulates chondrocyte biosynthesis when encapsulated in charged hydrogels prepared from poly(ethylene glycol) and chondroitin sulfate. Matrix Biology 2010;29:51-62.

[17] Johnstone B, Hering TM, Caplan AI, Goldberg VM, Yoo JU. In vitro chondrogenesis of bone marrow-derived mesenchymal progenitor cells. Exp Cell Res 1998;238:265-72.

[18] Lin-Gibson S, Bencherif S, Cooper JA, Wetzel SJ, Antonucci JM, Vogel BM, et al. Synthesis and characterization of PEG dimethacrylates and their hydrogels. Biomacromolecules 2004;5:1280-7.

[19] Bryant SJ, Davis-Arehart KA, Luo N, Shoemaker RK, Arthur JA, Anseth KS. Synthesis and characterization of photopolymerized multifunctional hydrogels: Water-soluble poly(vinyl alcohol) and chondroitin sulfate macromers for chondrocyte encapsulation. Macromolecules 2004;37:6726-33.

[20] Barbosa I, Garcia S, Barbier-Chassefiere V, Caruelle JP, Martelly I, Papy-Garcia D. Improved and simple micro assay for sulfated glycosaminoglycans quantification in biological extracts and its use in skin and muscle tissue studies. Glycobiology 2003;13:647-53.

[21] Metters AT, Anseth KS, Bowman CN. Fundamental studies of a novel, biodegradable PEG-b-PLA hydrogel. Polymer 2000;41:3993-4004.

[22] Nicodemus GD, Bryant SJ. The role of hydrogel structure and dynamic loading on chondrocyte gene expression and matrix formation. J Biomech 2008;41:1528-36.

[23] Villanueva I, Hauschulz DS, Mejic D, Bryant SJ. Static and dynamic compressive strains influence nitric oxide production and chondrocyte bioactivity when encapsulated in PEG hydrogels of different crosslinking densities. Osteoarthritis Cartilage 2008;16:909-18.

[24] Nicodemus GD, Bryant SJ. Mechanical loading regimes affect the anabolic and catabolic activities by chondrocytes encapsulated in PEG hydrogels. Osteoarthritis Cartilage 2010;18:126-37.

[25] Steinmetz NJ, Bryant SJ. The Effects of Intermittent Dynamic Loading on Chondrogenic and Osteogenic Differentiation of Human Marrow Stromal Cells Encapsulated in RGD Modified PEG Hydrogels Acta Biomaterialia 2011;7:3829-40.

[26] Thorpe SD, Buckley CT, Vinardell T, O'Brien FJ, Campbell VA, Kelly DJ. Dynamic compression can inhibit chondrogenesis of mesenchymal stem cells. Biochemical and Biophysical Research Communications 2008;377:458-62.

[27] Pfaffl MW. A new mathematical model for relative quantification in real-time RT-PCR. Nucleic Acids Research 2001;29:-.

[28] Knight MM, Ghori SA, Lee DA, Bader DL. Measurement of the deformation of isolated chondrocytes in agarose subjected to cyclic compression. Medical Engineering & Physics 1998;20:684-8.

[29] Chen SS, Falcovitz YH, Schneiderman R, Maroudas A, Sah RL. Depth-dependent compressive properties of normal aged human femoral head articular cartilage: relationship to fixed charge density. Osteoarthritis Cartilage 2001;9:561-9.

[30] Dickhut A, Pelttari K, Janicki P, Wagner W, Eckstein V, Egermann M, et al. Calcification or Dedifferentiation: Requirement to Lock Mesenchymal Stem Cells in a Desired Differentiation Stage. J Cell Physiol 2009;219:219-26.

[31] Dickhut A, Pelttari K, Janicki P, Wagner W, Eckstein V, Egermann M, et al. Low ALP Activity and Reduced In Vivo Calcification after In Vitro Chondrogenesis of Human Synovium Derived Mesenchymal Stem Cells. Tissue Engineering Part A 2009;15:704-.

[32] Pelttari K, Winter A, Steck E, Goetzke K, Hennig T, Ochs BG, et al. Premature induction of hypertrophy during in vitro chondrogenesis of human mesenchymal stem cells correlates with calcification and vascular invasion after ectopic transplantation in SCID mice. Arthritis Rheum 2006;54:3254-66.

[33] Dickhut A, Gottwald E, Steck E, Heisel C, Richter W. Chondrogenesis of mesenchymal stem cells in gel-like biomaterials in vitro and in vivo. Frontiers in Bioscience 2008;13:4517-28.

[34] Barry F, Boynton RE, Liu BS, Murphy JM. Chondrogenic differentiation of mesenchymal stem cells from bone marrow: Differentiation-dependent gene expression of matrix components. Exp Cell Res 2001;268:189-200.

[35] Bahrami S, Plate U, Dreier R, DuChesne A, Willital GH, Bruckner P. Endochondral ossification of costal cartilage is arrested after chondrocytes have reached hypertrophic stage of late differentiation. Matrix Biology 2001;19:707-15.

[36] Weber LM, Lopez CG, Anseth KS. Effects of PEG hydrogel crosslinking density on protein diffusion and encapsulated islet survival and function. Journal of Biomedical Materials Research Part A 2009;90A:720-9.

[37] Williams CG, Kim TK, Taboas A, Malik A, Manson P, Elisseeff J. In vitro chondrogenesis of bone marrow-derived mesenchymal stem cells in a photopolymerizing hydrogel. Tissue Eng 2003;9:679-88.

[38] Eyre DR, Wu JJ. Collagen of fibrocartilage - A distinctive molecular phenotype in bovine meniscus. Febs Letters 1983;158:265-70.

[39] Lozito TP, Kolf CM, Tuan RS. Regulatory Networks in Stem Cells. In: Rajasekhar VK, Vemuri MC, editors. Regulatory Networks in Stem Cells. New York City: Humana Press; 2009. p. 185-210.

[40] Mow VC, Wang CC, Hung CT. The extracellular matrix, interstitial fluid and ions as a mechanical signal transducer in articular cartilage. Osteoarthritis Cartilage 1999;7:41-58.

[41] Li YM, Schilling T, Benisch P, Zeck S, Meissner-Weigl J, Schneider D, et al. Effects of high glucose on mesenchymal stem cell proliferation and differentiation. Biochemical and Biophysical Research Communications 2007;363:209-15.

[42] Wuertz K, Godburn K, Neidlinger-Wilke C, Urban J, Iatridis JC. Behavior of mesenchymal stem cells in the chemical microenvironment of the intervertebral disc. Spine 2008;33:1843-9.

[43] Jurgens WJFM, Lu Z, Zandieh-Doulabi B, Kuik DJ, Ritt MJPF, Helder MN. Hyperosmolarity and hypoxia induce chondrogenesis of adipose-derived stem cells in a collagen type 2 hydrogel. J Tissue Eng Regen M 2011.

[44] Hung CT. Transient Receptor Potential Vanilloid 4 Channel as an Important Modulator of Chondrocyte Mechanotransduction of Osmotic Loading. Arthritis Rheum 2010;62:2850-1.

[45] Chen WC, Yao CL, Chu IM, Wei YH. Compare the effects of chondrogenesis by culture of human mesenchymal stem cells with various type of the chondroitin sulfate C. Journal of Bioscience and Bioengineering 2011;111:226-31.

[46] Nguyen LH, Kudva AK, Guckert NL, Linse KD, Roy K. Unique biomaterial compositions direct bone marrow stem cells into specific chondrocytic phenotypes corresponding to the various zones of articular cartilage. Biomaterials 2011;32:1327-38.

[47] Park JS, Yang HJ, Woo DG, Yang HN, Na K, Park KH. Chondrogenic differentiation of mesenchymal stem cells embedded in a scaffold by long-term release of TGF-beta 3 complexed with chondroitin sulfate. Journal of Biomedical Materials Research Part A 2010;92A:806-16.

[48] Thorpe SD, Buckley CT, Vinardell T, O'Brien FJ, Campbell VA, Kelly DJ. The Response of Bone Marrow-Derived Mesenchymal Stem Cells to Dynamic Compression Following TGF-beta 3 Induced Chondrogenic Differentiation. Ann Biomed Eng 2010;38:2896-909.

[49] Lu HH, Subramony SD, Boushell MK, Zhang XZ. Tissue Engineering Strategies for the Regeneration of Orthopedic Interfaces. Ann Biomed Eng 2010;38:2142-54.

Chapter 5

Effect of poly(ethylene glycol) based scaffolds modified with a bone mimetic peptide on hMSC attachment and osteogenic biomarker molecule synthesis

5.1 Introduction

Efficacious bone tissue engineering can play a critical role in developing successful osteochondral and cartilage tissue engineering strategies. Articular cartilage integrates with the underlying subchondral bone through the osteochondral interface [1] and as such, the successful implementation of engineered cartilage will require a means by which to anchor the engineered cartilage, i.e. through the osteochondral interface to the subchondral bone, with the ultimate goal of restoring joint function. Successful osteochondral tissue engineering strategies are complex, involving engineering three distinctly different tissues (bone, cartilage, and the osteochondral interface) with varying mechanical properties and extra cellular matrix (ECM) compositions. With the long-term goal of this research focused on developing an osteochondral tissue engineering strategy, a first step is to identify individual biochemical constituents that can be incorporated into the boney region to support osteogenic differentiation.

Bone tissue engineering strategies often involve a combination of several important factors: selecting an appropriate cell source, designing a suitable scaffold, and the delivery of appropriate physiological cues. Human mesenchymal stromal cells (hMSCs) are an excellent cell source due to their ability to differentiate down several lineages including the chondrogenic and osteogenic lineages as well as for their use in clinical applications. Poly(ethylene glycol) based hydrogels have been used in bone tissue engineering strategies for several years now [2-9], and provide an attractive basis for scaffold design. These hydrogels have many attractive qualities including the ability to covalently incorporate molecules such as tissue specific biomimetic cues [10, 11] and cell-binding ligands such as the ubiquitous cell-binding domain, RGD [12].

The ECM of bone is primarily comprised of inorganic mineral matrix (hydroxyapatite) and organic matrix [13]. Collagen I is the most abundant organic component of bone and serves to provide important extracellular signals to MSCs [14, 15] through several cell-binding domains in the protein that interact with different MSC surface integrins. These binding domains include the ubiquitous RGD domain(s), a DGEA domain, and the GIAG domain found in the 15 amino acid sequence known as P-15 (GTPGPQGIAGQRDVV) [16]. The RGD domain, found in several ECM molecules, has been widely utilized as a generic cell-binding domain in MSC laden hydrogels [12, 17-19]. However, RGD requires additional signals to induce osteogenesis of MSCs [16]. Alternatively, the P-15 peptide sequence has been shown to promote osteogenesis of MSCs [20].

The overall objective of this study was to investigate the response of hMSCs to a P-15 modified PEG based scaffold. P-15 has previously been shown to promote cell attachment when the peptide is adsorbed on anorganic bone mineral (ABM) particles [21] and enhance the osteogenic potential of osteoblasts [22] as well as promote osteogenic differentiation of MSCs [20]. The specific aims of this study were twofold: 1) to investigate the attachment and differentiation of the hMSCs to the PEG hydrogels with immobilized P-15, in 2D and 2) to investigate the effect of the 3D PEG/P-15 environment on the viability and osteogenic biomarker molecule synthesis of encapsulated hMSCs. In these studies, the P-15 peptide motif was covalently bound to the PEG based hydrogel and hMSCs were either seeded on (2D) or encapsulated in (3D) either a tightly or loosely crosslinked PEG/P-15 system and cultured under basal or osteogenic medium conditions. We hypothesized that the incorporation of the P-15 peptide motif into PEG based hydrogels promotes hMSC attachment and adhesion to PEG hydrogels (in 2D) and enhances the production of osteogenic biomarker molecules and the

deposition of osteogenic ECM molecules (in 3D). Our findings demonstrate that hMSCs attach to P-15 modified PEG based hydrogels in 2D and express osteonectin, a bone specific osteogenic biomarker molecule that selectively binds both hydroxyapatite and collagen I, but the 3D P-15 modified environment does not appear to enhance the viability of these cells or the production of osteogenic biomarker molecules by hMSCs over unmodified environments.

5.2 Materials and Methods

hMSC cell culture

Adult hMSCs (24 year old male) were purchased from Texas A&M Health Science Center College of Medicine Institute for Regenerative Medicine and cultured with basal stem cell medium (BM) (20% fetal bovine serum (FBS, Atlanta Biologicals, Atlanta, GA), 1mg/mL amphotericin B, 50 U/mL penicillin, 50 mg/mL streptomycin, and 20 mg/mL gentamicin in low glucose Dulbecco's modified Eagle medium (αMEM, Invitrogen; Carlsbad, CA) containing 1g/L glucose). The cells were grown under standard cell culture conditions (in a regulated incubator at 37ºC with 5% CO_2 conditions) and were plated at ~60 cells/cm^2 till passage 2 (P2, 1:10) and allowed to grow to 80% confluency before being frozen down.

P3 cells were thawed and plated at approximately 4500 cells/cm^2 in T-275 tissue culture polystyrene flasks. Media was changed twice weekly and cells were cultured until Passage 5 (P5) (1:3 for P3-P4, 1:10 for P4-P5).

Macromolecular Monomer Synthesis

Poly(ethylene glycol) dimethacrylate (PEGMA) macromolecular monomers were synthesized via microwave synthesis, described elsewhere [23]. Briefly, 4600 g/mol

poly(ethylene glycol) (PEG) (Fluka, Sigma-Aldrich; St. Loius, MO) was allowed to react with 10x molar excess methacrylic anhydride in a molten reaction for 5 minutes. The reaction mixture was purified by precipitations with ethyl ether, filtered, and allowed to dry under vacuum.

Acryloyl-PEG-N-hydroxysuccinimide (acryloyl-PEG-SCM, 3400 Da; Laysan Bio, Inc.; Arab, AL) was reacted with either GTPGPQGIAGQRGVV (P15) (Cerapedics) or YRGDS (Genscript; Piscataway, NJ) in a 1:1.1 molar ratio (excess acryloly-PEG-SCM) in 50 mM sodium bicarboate buffer (pH 8.2) overnight at room temperature. The P-15 degree of attachment was determined to be 92% and the RGD degree of attachment was determined to be 94% using the spectroscopic Fluoraldehyde™ o-Phthalaldehyde (Pierce) method of detection. The product, acryloyl-PEG-P15 or acryloyl-PEG-RGD, was dialysed with 1000 MWCO cellulose ester dialysis tubing (Spectra/Por® Biotech; Rancho Dominguez, CA) in de-ionized water with three water changes for 24 hrs. The conjugated acryloyl-PEG-P-15 and acryloyl-PEG-RGD were lyophilized and stored at 4ºC.

hMSC Seeding on 2D Hydrogel Discs

2D photopolymerized hydrogel discs were fabricated. Briefly, a 20% (g/g) PEGDM (4600 MW) solution containing either 0 peptide, 2.8 mM acryloyl-PEG-P15, or 2.8 mM acryloyl-PEG-RGD and 0.05 wt% photoinitiator Irgacure 2959 (Ciba Specialty Chemicals; Tarrytown, NY) dissolved in phosphate buffered saline (PBS, pH 7.4). Hydrogel sheets of each of the macromer formulations previously described were polymerized between two glass slides with a 1 mm Teflon spacer under 365 nm light with an intensity of ~5 mW/cm^2 for 10 minutes (Black Ray XX-20BLB UV Bench Lamp, Upland, CA). 5 mm disks were punched out of the sheets using a 5 mm biopsy punch. The disks were sterilized in 70% ethanol overnight followed

by multiple rinses in sterile PBS over three days to sterilize the disks and remove any unreacted polymerization reactants. The disks were secured to the bottom of non tissue culture treated 96 well plates using a minimal amount of sterile vacuum grease.

2000 cells/well were seeded on the disks with serum free basal medium and allowed to attach for six hours before medium was replaced with either basal (described previously) or osteogenic differentiation medium (osteogenic differentiation medium: 10 nM dexamethasone, 50 mM l-Ascorbic acid 2-Phosphate trisodium Salt, 10 mM β-glycerophosphate, 20% fetal bovine serum (FBS, Atlanta Biologicals), 1mg/mL amphotericin B, 50 U/mL penicillin, 50 mg/mL streptomycin, and 20 mg/mL gentamicin in low glucose alpha modified Eagle medium (aMEM, Invitrogen) containing 1g/L glucose). Cells were cultured for up to seven days in standard incubator conditions with media changes every two to three days.

3D hMSC Photoencapsulation

hMSCs were combined at a cell concentration of $10x10^6$ cells/mL with a sterile 20% (g/g) macromer solution PEGDM (either 4600 MW PEG (tightly crosslinked) or 10,000 MW PEG (loosely crosslinked)) solution containing either 0 or 10 mM acryloyl-PEG-P15 and 0.05 wt% photoinitiator Irgacure 2959 dissolved in basal or osteogenic differentiation medium. The cell/macromer solution was polymerized under 365 nm light with an intensity of ~5 mW/cm^2 for 10 minutes. Cylindrical hMSC-laden hydrogel constructs (~2.5mm in height and 5 mm in diameter) were allowed to free swell in their respective culture media for the duration of the study in standard incubator conditions.

Cell Morphology and Immunohistochemistry

2D hydrogel constructs were fixed for 1 hour in 4% paraformaldehyde and transferred to a 15% sucrose solution for storage (n=3). After permeabilization and blocking, the attached cells were stained for the presence of osteonectin (ON, 1:2, Iowa Hybridoma) for 2 hrs at room temperature, rinsed with PBS, and treated for 2 hr with goat anti-mouse IgG labeled Alexa Flour 546 (1:200, Invitrogen). Additionally, the same samples were stained with Alexa Flour 488 phalloidin (1:40, Invitrogen) for 20 minutes and the nuclei were counterstained with DAPI (Invitrogen) for 5 minutes. Samples were imaged using scanning laser confocal microscopy (Zeiss LSM 510) using a 40x water objective.

Cell Viability

Cell viability throughout the duration of the 3D study was assessed using the LIVE/DEAD Viability/Cytotoxicity Kit (Invitrogen). Cell seeded constructs were imaged with a Zeiss LSM 510 confocal microscope. At each time point (days 0, 7, 14, and 21) constructs were removed, rinsed with PBS and allowed to incubate for 30 minutes in a solution of 2mM calcein and 2mM ethidium homodimer. After incubation, the constructs were removed and rinsed before imaging. Two to four images were taken for each construct (n=2) and 50-100 cells were counted for each image using Cell Counter with Image J software.

Biochemical Analysis

Samples were homogenized in dionized water and taken through three freeze (-80ºC)/thaw (at room temperature)/sonicate cycles. DNA content was measured with a spectrophotomoter using the PicoGreen dsDNA Reagent (Invitrogen). The amount of alkaline

phosphatase (ALP) produced by the cells was measured using Sigma Diagnostic Kit #104 (Sigma), modified for osteogenic ALP applications, as previously described [24]. The amount of total calcium incorporation into the scaffolds was measured with the Total Calcium Liquicolor Assay (Stanbio).

Statistical analysis

Statistical analysis was performed using One Way ANOVA with a Tukey HSD Post Hoc assessment to determine differences between experimental variables. p values < 0.05 were considered significant. Data are reported as the mean ± standard deviation of the mean unless stated otherwise.

5.3 Results

5.3.1 Effect of PEG/P-15 hydrogels on hMSC attachment and osteogenic biomarker molecule expression in 2D

2D PEGDM hydrogels modified with either P-15 or RGD, which served as a positive control for cell adhesion, or no peptide were fabricated and undifferentiated hMSCs were seeded on the gels and cultured under free swelling conditions for 7 days in either basal medium or osteogenic differentiation medium. Cells attached to both the RGD modified and P-15 modified surfaces as demonstrated by the F-actin staining in Fig. 5.1. No cells were detected on the unmodified PEGDM hydrogels. Additionally, attached cells were stained for osteonectin through immunohistochemistry. hMSCS on both RGD and P-15 modified hydrogels cultured in osteogenic medium stained positively for ON (Fig. 5.1) whereas hMSCs cultured on P-15 modified hydrogels, but not RGD in basal medium stained positively for ON (Fig. 5.1).

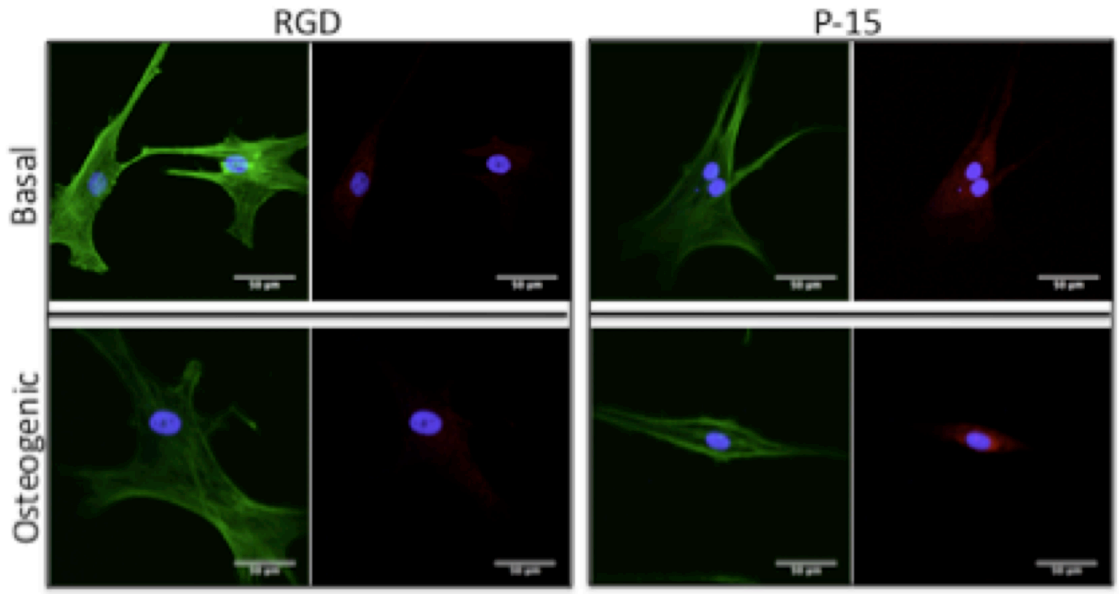

Figure 5.1: Day 7 staining of hMSCs attached to PEG hydrogels modified with either RGD or P-15 peptide motifs cultured in either basal (top) or osteogenic differentiation medium (bottom). Columns 1 and 3, green staining of actin filaments using fluorescently conjugated phalloidin. Columns 2 and 4, red staining of osteonectin (ON) in the same samples as columns 1 and 3. Samples are counterstained with the nuclear stain DAPI. 400x original magnification with scale bars=50μm.

5.3.2 Effect of PEG/P-15 hydrogels on hMSC viability and osteogenic biomarker molecule expression in 3D

5.3.2.1 Viability and survivability

hMSCs were encapsulated in either tightly crosslinked or loosely crosslinked PEGDM hydrogels. The tightly crosslinked macromer was synthesized from PEG with MW=4600 g/mol and 20% (g/g) gels had a volumetric swelling ratio of ~7 and the loosely crosslinked macromer was synthesized from PEG with MW = 10,000 g/mol and had a volumetric swelling raio of ~21. The hydrogels were either plain PEGDM or modified with 10 mM P-15. Cell-laden hydrogels of each condition were cultured for up to 21 days in either basal or osteogenic differentiation media. Cell viability, based on visualization of a membrane integrity assay, was assessed semi-

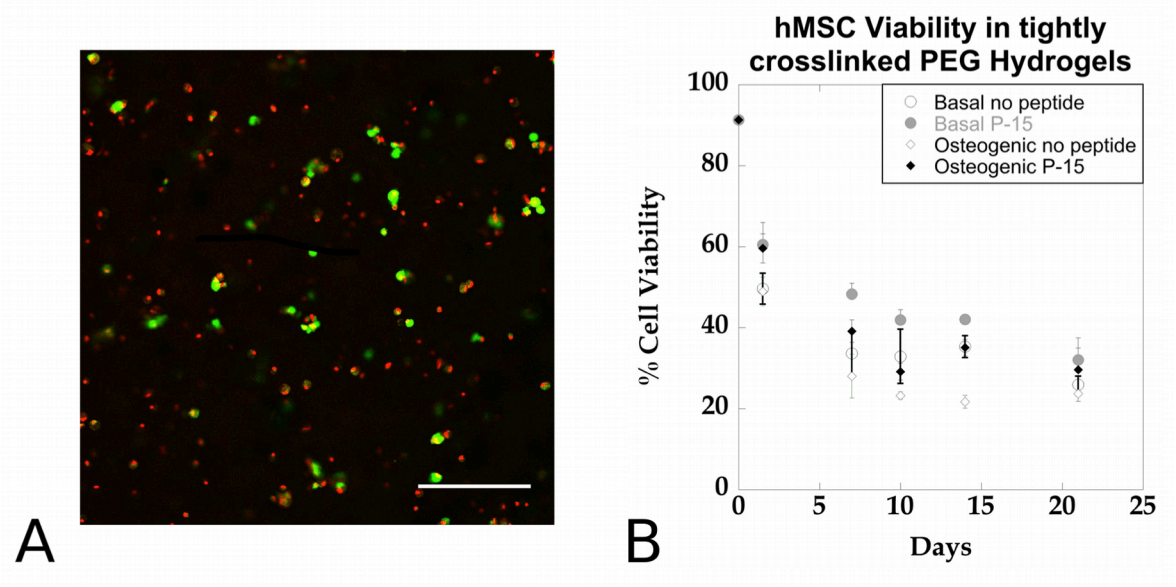

Figure 5.2: A) Representative Live/Dead image of hMSCs encapsulated in a tightly crosslinked P-15 modified scaffold cultured in basal medium for 21 days. Original magnification is 100x and scale bar = 200 μm. B) Semi-quantitative hMSC cell viability assessed over 21 days in tightly crosslinked P-15 modified and unmodified PEGDM scaffolds.

qualitatively from confocal microscopy images, for basal and osteogenic medium conditions in the more tightly crosslinked P-15 modified hydrogels over the course of the 21 study and a representative confocal image is shown in Fig. 52A. Viability dropped off sharply to ~30-50% by day 7 in all conditions and leveled off at 25-35% by day 21 (Fig. 52B).

Total DNA content was assessed in the hydrogels as a function of peptide and culture medium. DNA content in the P-15 modfied hydrogels was normalized to the DNA content in unmodified hydrogels in the same respective culture medium (Fig. 5.3). This ratio was used as a measure of cell survivability as a result of the P-15. In the more tightly crosslinked hydrogels, cells in P-15 modified hydrogels, on average survived better than the no peptide conditions in both basal and osteogenic medium (Fig. 5.3). However, in the more loosely crosslinked hydrogels, the survivability of the hMSCs was better, for both basal and osteogenic medium, in the unmodified hydrogels (Fig. 5.3).

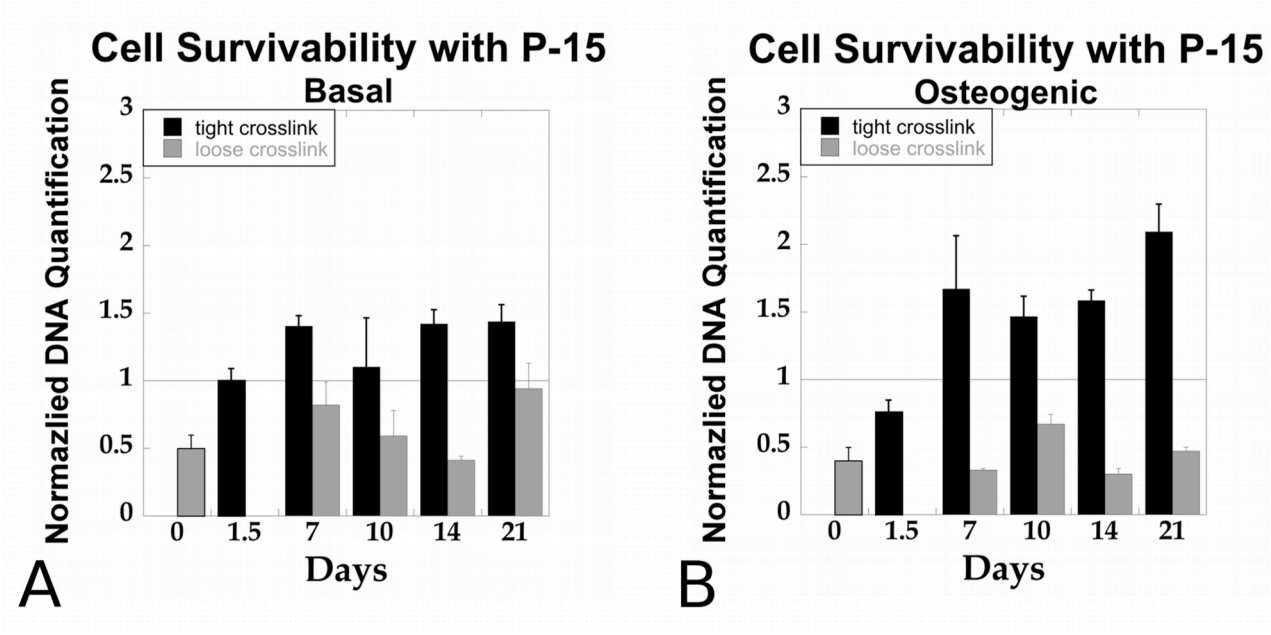

Figure 5.3: Cell survivability in P-15 modified scaffolds normalized to unmodified scaffolds (survivability in unmodified scaffolds = 1) in A) basal medium and B) osteogenic differentiation medium.

5.3.2.2 Osteogenic biomarkers: Alkaline phosphatase production and mineral deposition

A general increase in the production of ALP for all hydrogel conditions was observed compared to day 0 (loosely crosslinked) and day 1.5 (tightly crosslinked) levels with an overall increasing trend enzyme production over the course of the study (Fig. 5.4). Higher levels of ALP were detected in both the basal and osteogenic loosely crosslinked conditions as compared to their respective tightly crosslinked counterparts. Interestingly, absolute production of ALP was similar in corresponding basal and osteogenic conditions. It is also interesting to note that the condition that exhibited the highest production of ALP was the no peptide/loosely crosslinked scaffold in basal media (Day 21) (Fig. 5.4A).

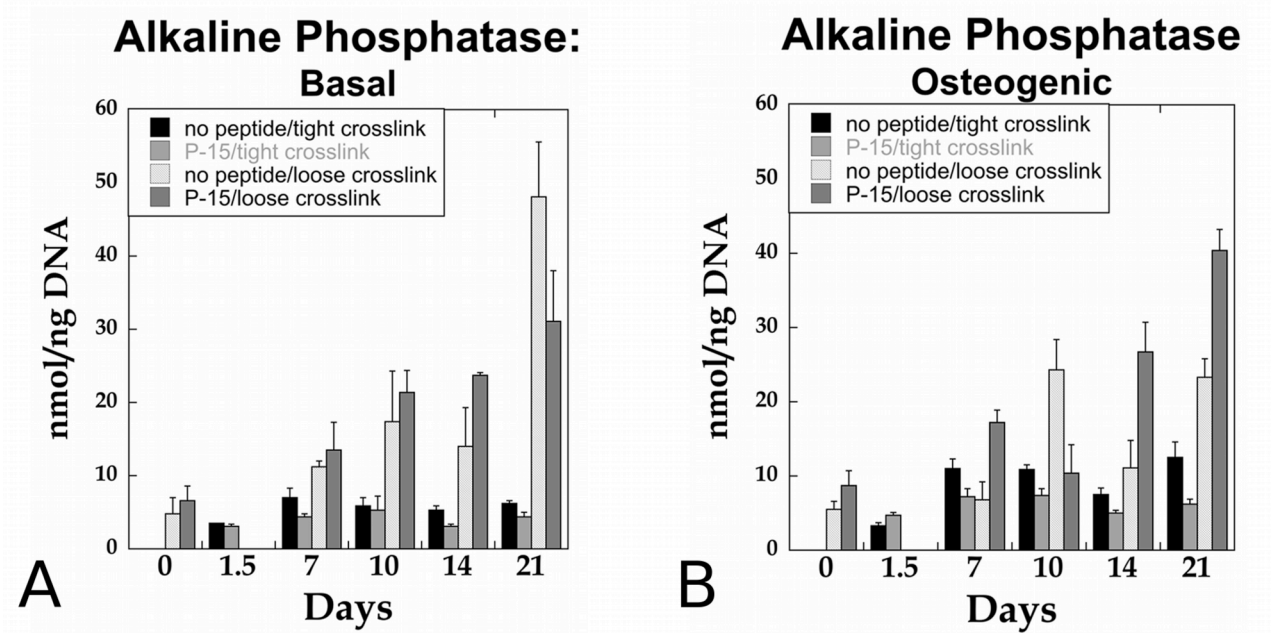

Figure 5.4: Alkaline phosphatase enzyme production in unmodified and P-15 modified scaffolds :A) basal medium and B) osteogenic differentiation medium.

Total calcium levels also increased for all samples investigated over the course of the 21 day study (Fig. 5.5). Calcium levels for all basal conditions were similar, with no observed differences among either the unmodified and P-15 modified or the tightly and loosely crosslinked conditions (Fig. 5.5A). The calcium levels in all osteogenic conditions also increased temporally (Fig. 5.5B). Beginning at day 10, the levels of calcium were slightly higher in the

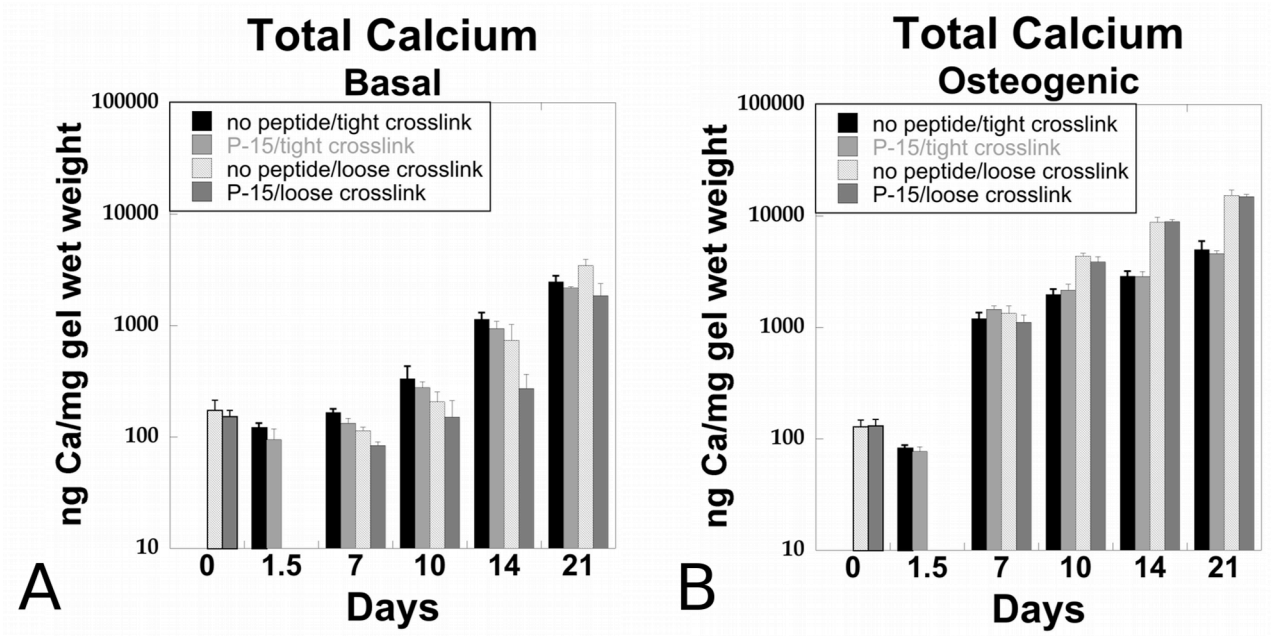

Figure 5.5: Total calcium production in unmodified and P-15 modified scaffolds :A) basal medium and B) osteogenic differentiation medium.

loosely crosslinked conditions as compared to the tightly crosslinked samples, but there was no difference between the unmodified and P-15 modified samples within each type of crosslinking. The absolute amount of calcium in the scaffolds was approximately an order of magnitude higher in the osteogenic samples as compared to the basal samples.

5.4 Discussion

The overall goal of this study was to investigate the response of hMSCs to the collagen I analog, P-15, to determine whether it would be a suitable biomimetic constituent in a "boney" layer of a multi-layered scaffold for osteochondral tissue engineering applications. Typically, studies incorporate RGD into bioinert PEG based hydrogels to provide a generic attachment domain for MSCs [8, 12, 18, 19, 25, 26]. However, RGD is a ubiquitous binding domain found in several ECM molecules [16] and as such does not serve to provide a specific biomimetic cue

to the encapsulated cells within the hydrogel scaffold. The 15 amino acid collagen I analog, P-15, however, is also a cell-binding domain and has been previously shown to enhance osteogenesis in MSCs [20].

In this study, we confirmed that P-15 does serve as a cell binding ligand for MSCs when these cells are seeded on 2D P-15 modified hydrogels similar to the response seen in RGD control gels. Additionally, undifferentiated hMSCs seeded on these P-15 modified scaffolds, in the absence of osteogenic differentiation cues, expressed a bone specific protein that assists in binding mineralized matrix to collagen I [27]. Although, the expression of this osteogenic biomarker alone does not confirm the ability of P-15 to induce osteogenesis in hMSCs, the 2D results did encourage further investigation in a 3D system. hMSCs will bind to the RGD and P-15 peptide domains through different cell surface receptors [16] where RGD is typically thought to bind to the $\alpha5\beta1$ integrin and it has been suggested that P-15 binds to the $\alpha2\beta1$ integrin [28, 29]. We hypothesize that MSCs may have more $\alpha5\beta1$ integrins available, or may upregulate the expression of these integrins, over the $\alpha2\beta1$ counterparts, potentially leading to a stronger binding effect from RGD over P-15. PEG based scaffolds containing both RGD and P-15 could take advantage of both the strong adhesive behavior of RGD while investigating the potential of P-15 to enhance osteogenic differentiation of hMSCs.

We hypothesized that nutrient diffusion could be limited in the tightly crosslinked ($Q =\sim7$) hydrogels potentially impacting cell viability and osteogenic biomarker molecule synthesis. As such, two different hydrogel crosslinking densities were investigated, to potentially rule out these nutrient diffusion limitations [30] and to enhance fluid flow within the gel scaffolds, as data in the literature suggests that interstitial fluid flow is beneficial for bone cells [31]. One important difference between the two crosslinking density studies is that the loosely crosslinked

scaffolds were placed on an orbital shaker for the duration of the study to maximize the nutrient diffusion and fluid flow within the scaffolds after very low viabilities were observed in the tightly crosslinked scaffold study. Incorporating the P-15 into the scaffolds did appear to modestly enhance the survivability of the hMSCs, although, interestingly, this was only observed in the tightly crosslinked and potentially nutrient diffusion limited systems for both basal and osteogenic medium conditions. Although the cell survivability was enhanced, the actual cell viability was still very low (<35%) in all of the systems investigated. In previous work by this group [25], we observed substantially higher (>50%) hMSC viability in RGD modified PEG based hydrogels. It has been suggested that hMSCs may attach to P-15 [32] in combination with binding sites in other ECM molecules [16] to be most effective, potentially creating a positive feedback loop for synthesis of collagen by MSCs [16]. This further supports the idea that a combination of RGD and P-15 may provide the most efficacious local environment for encapsulated hMSCs.

Both of the osteogenic biomarker molecules that were explored in this study were produced in all of the conditions investigated and increased over the course of the study. It was interesting that the conditions that produced the most ALP in both the basal and the osteogenic conditions were in the loosely crosslinked scaffolds, although there was no evidence that the presence of P-15 enhanced the production of ALP. It was also interesting that in the absence of osteogenic differentiation cues, hMSCs produced ALP, a biomarker typically thought as an osteogenic biomarker molecule. Findings in Chapter 4 of this thesis suggest that the PEG hydrogel environment may induce terminal chondrogenic differentiation. Here we hypothesize that the production of ALP in the basal system is actually indicative of terminal chondrogenic differentiation [33] as a result of being encapsulated in the PEG based system, whether inclusive

of P-15 or not, in the absence of differentiation cues, rather than an osteogenic lineage. Additional studies investigating the production of more specific hypertrophic ECM molecule production (type X collagen) would be needed to test this hypothesis.

Additionally, the conditions that were most promising for mineralized matrix deposition were the unmodified and modified osteogenic loosely crosslinked scaffolds. While mineralization in the presence of osteogenic differentiation medium (containing β-glycerophspate) has previously been observed in both acellular and dead cell control scaffolds we have not observed this behavior in similar constructs cultured in basal media. Given those results, the most interesting of the total calcium results are the basal conditions where both the unmodified and P-15 modified conditions (in both the tightly and loosely crosslinked conditions) exhibited greater than a 10-fold increase in total calcium by day 21. Although, the calcium results are interesting, they do not suggest that incorporating P-15 into the PEG based scaffolds enhances the production of osteogenic biomarker molecules.

Several studies have been published presenting evidence that P-15 enhances osteogenesis in osteoblasts [20, 34] and/or enhances MSC osteogenic differentiation [20]. However, to date, most studies reporting beneficial effects of P-15 have investigated the effect of P-15 on these cells in a "local" 2D environment, where the P-15 is either adsorbed onto ABM particles [20-22, 35-37] or coupled to poly(l-lactide-co-ε-caprolactone) microshperes [38]. Both the ABM particle systems and the microsphere system provide an environment, where locally, the cells attach and spread onto the surface that has been modified with P-15, similar to the 2D system reported in this study where the P-15 modified PEG hydrogel appears to direct hMSCs down an osteogenic lineage, based on the detection of the expression of ostenectin in the absence of osteogenic differentiation cues. Additionally, osteogenic differentiation of MSCs in tissue culture is done in

2D [39], in contrast to the 3D cell pellet environment required for chondrogenic differentiation of MSCs [40]. We hypothesize that hMSCs differentiating down an osteogenic lineage prefer a spread morphology, similar to that obtained in a "local" 2D environment, to the rounded morphology adopted in the current PEG systems. Investigating the behavior of hMSCs in a PEG based system with incorporated P-15 modified and unmodified ABM particles would be an interesting means to test this hypothesis.

5.5 Conclusions

Overall our findings indicate that P-15 can serve as an alternative to RGD as a covalently incorporated binding peptide for hMSCs in PEG based hydrogels, however the efficiency of the P-15 peptide to bind the cells may be lower than the efficiency of RGD. Additionally, the collagen I based peptide may be able to serve as an insoluble differentiation cue for hMSCs, although evidence of this behavior in 3D remains to be seen. In 3D, although P-15 appears to increase the survivability of encapsulated hMSCs as compared to unmodified scaffolds, cell viability in these systems is still very low. These observations, in combination with previous work with RGD modified PEG based hydrogels in this group [25], suggest that a better approach to investigate the response of encapsulated hMSCs to incorporated P-15 may be to include both P-15 and RGD in the PEG hydrogel system, as cells encapsulated with RGD maintain a substantially higher viability than unmodified or P-15 modified scaffolds and have been shown to produce both collagen I and mineralized matrix in a similar PEG based system [25] and may work in concert with P-15 [16] to further enhance the production of osteogenic biomarker molecules.

5.6 Acknowledgements

The authors would like to thank Katherine Walline for her guidance and support on this project and Cerapedics, Inc. for the donation of P-15 for these studies.

5.7 References

[1] Lu HH, Subramony SD, Boushell MK, Zhang XZ. Tissue Engineering Strategies for the Regeneration of Orthopedic Interfaces. Ann Biomed Eng 2010;38:2142-54.

[2] Benoit DSW, Nuttelman CR, Collins SD, Anseth KS. Synthesis and characterization of a fluvastatin-releasing hydrogel delivery system to modulate hMSC differentiation and function for bone regeneration. Biomaterials 2006;27:6102-10.

[3] Nuttelman CR, Tripodi MC, Anseth KS. Dexamethasone-functionalized gels induce osteogenic differentiation of encapsulated hMSCs. Journal of Biomedical Materials Research Part A 2006;76A:183-95.

[4] Nuttelman CR, Tripodi MC, Anseth KS. In vitro osteogenic differentiation of human mesenchymal stem cells photoencapsulated in PEG hydrogels. Journal of Biomedical Materials Research Part A 2004;68A:773-82.

[5] Burdick JA, Mason MN, Hinman AD, Thorne K, Anseth KS. Delivery of osteoinductive growth factors from degradable PEG hydrogels influences osteoblast differentiation and mineralization. J Control Release 2002;83:53-63.

[6] Burdick JA, Anseth KS. Photoencapsulation of osteoblasts in injectable RGD-modified PEG hydrogels for bone tissue engineering. Biomaterials 2002;23:4315-23.

[7] Pratt AB, Weber FE, Schmoekel HG, Muller R, Hubbell JA. Synthetic extracellular matrices for in situ tissue engineering. Biotechnology and Bioengineering 2004;86:27-36.

[8] Gurav N, Lutolf MP, Raeber GP, Hubbell JA, Di Silvio L. Differentiation of human bone marrow stem cells within RGD functionalised, proteolytically sensitive PEG gels. Tissue Eng 2007;13:1675-.

[9] Ehrbar M, Lutolf MP, Rizzi SC, Hubbell JA, Weber FE. Artificial extracellular matrices for bone tissue engineering. Bone 2008;42:S72-S.

[10] Bryant SJ, Arthur JA, Anseth KS. Incorporation of tissue-specific molecules alters chondrocyte metabolism and gene expression in photocrosslinked hydrogels. Acta Biomaterialia 2005;1:243-52.

[11] Nuttelman CR, Rice MA, Rydholm AE, Salinas CN, Shah DN, Anseth KS. Macromolecular monomers for the synthesis of hydrogel niches and their application in cell encapsulation and tissue engineering. Progress in Polymer Science 2008;33:167-79.

[12] Nuttelman CR, Tripodi MC, Anseth KS. Synthetic hydrogel niches that promote hMSC viability. Matrix Biology 2005;24:208-18.

[13] Gentili C, Cancedda R. Cartilage and Bone Extracellular Matrix. Current Pharmaceutical Design 2009;15:1334-48.

[14] Gelse K, Poschl E, Aigner T. Collagens - structure, function, and biosynthesis. Advanced Drug Delivery Reviews 2003;55:1531-46.

[15] Heng BC, Cao T, Stanton LW, Robson P, Olsen B. Strategies for directing the differentiation of stem cells into the osteogenic lineage in vitro. Journal of Bone and Mineral Research 2004;19:1379-94.

[16] Lozito TP, Kolf CM, Tuan RS. Regulatory Networks in Stem Cells. In: Rajasekhar VK, Vemuri MC, editors. Regulatory Networks in Stem Cells. New York City: Humana Press; 2009. p. 185-210.

[17] Salinas CN, Cole BB, Kasko AM, Anseth KS. Chondrogenic differentiation potential of human mesenchymal stem cells photoencapsulated within poly(ethylene glycol)-arginine-glycine-aspartic acid-serine thiol-methacrylate mixed-mode networks. Tissue Eng 2007;13:1025-34.

[18] Yang F, Williams CG, Wang DA, Lee H, Manson PN, Elisseeff J. The effect of incorporating RGD adhesive peptide in polyethylene glycol diacrylate hydrogel on osteogenesis of bone marrow stromal cells. Biomaterials 2005;26:5991-8.

[19] Hern DL, Hubbell JA. Incorporation of adhesion peptides into nonadhesive hydrogels useful for tissue resurfacing. Journal of Biomedical Materials Research 1998;39:266-76.

[20] Yang XBB, Bhatnagar RS, Li S, Oreffo ROC. Biomimetic collagen scaffolds for human bone cell growth and differentiation. Tissue Eng 2004;10:1148-59.

[21] Qian JJ, Bhatnagar RS. Enhanced cell attachment to anorganic bone mineral in the presence of a synthetic peptide related to collagen. Journal of Biomedical Materials Research 1996;31:545-54.

[22] Nguyen H, Qian JJ, Bhatnagar RS, Li S. Enhanced cell attachment and osteoblastic activity by P-15 peptide-coated matrix in hydrogels. Biochemical and Biophysical Research Communications 2003;311:179-86.

[23] Lin-Gibson S, Bencherif S, Cooper JA, Wetzel SJ, Antonucci JM, Vogel BM, et al. Synthesis and characterization of PEG dimethacrylates and their hydrogels. Biomacromolecules 2004;5:1280-7.

[24] van den Dolder J, Bancroft GN, Sikavitsas VI, Spauwen PHM, Jansen JA, Mikos AG. Flow perfusion culture of marrow stromal osteoblasts in titanium fiber mesh. Journal of Biomedical Materials Research Part A 2003;64A:235-41.

[25] Steinmetz NJ, Bryant SJ. The Effects of Intermittent Dynamic Loading on Chondrogenic and Osteogenic Differentiation of Human Marrow Stromal Cells Encapsulated in RGD Modified PEG Hydrogels Acta Biomaterialia 2011;7:3829-40.

[26] Salinas CN, Anseth KS. The influence of the RGD peptide motif and its contextual presentation in PEG gels on human mesenchymal stem cell viability. J Tissue Eng Regen Med 2008;2:296-304.

[27] Termine JD, Kleinman HK, Whitson SW, Conn KM, McGarvey ML, Martin GR. Osteonectin, a bone-specific protein linking mineral to collagen. Cell 1981;26:99-105.

[28] Knight CG, Morton LF, Onley DJ, Peachey AR, Messent AJ, Smethurst PA, et al. Identification in collagen type I of an integrin alpha(2)beta(1)-binding site containing an essential GER sequence. J Biol Chem 1998;273:33287-94.

[29] Morton LF, Peachey AR, Knight CG, Farndale RW, Barnes MJ. The platelet reactivity of synthetic peptides based on collagen III fragment alpha 1(III)CB4 - Evidence for an integrin alpha(2)beta(1) recognition site involving residues 522-528 of the alpha 1(III) collagen chain. J Biol Chem 1997;272:11044-8.

[30] Weber LM, Lopez CG, Anseth KS. Effects of PEG hydrogel crosslinking density on protein diffusion and encapsulated islet survival and function. Journal of Biomedical Materials Research Part A 2009;90A:720-9.

[31] Sikavitsas VI, Temenoff JS, Mikos AG. Biomaterials and bone mechanotransduction. Biomaterials 2001;22:2581-93.

[32] Di Lullo GA, Sweeney SM, Korkko J, Ala-Kokko L, San Antonio JD. Mapping the ligand-binding sites and disease-associated mutations on the most abundant protein in the human, type I collagen. J Biol Chem 2002;277:4223-31.

[33] Pelttari K, Winter A, Steck E, Goetzke K, Hennig T, Ochs BG, et al. Premature induction of hypertrophy during in vitro chondrogenesis of human mesenchymal stem cells correlates with calcification and vascular invasion after ectopic transplantation in SCID mice. Arthritis Rheum 2006;54:3254-66.

[34] Suaid FA, Macedo GO, Novaes AB, Borges GJ, Souza SLS, Taba M, et al. The Bone Formation Capabilities of the Anorganic Bone Matrix-Synthetic Cell-Binding Peptide 15 Grafts in an Animal Periodontal Model: A Histologic and Histomorphometric Study in Dogs. Journal of Periodontology 2010;81:594-603.

[35] Bhatnagar RS, Qian JJ, Wedrychowska A, Sadeghi M, Wu YM, Smith N. Design of biomimetic habitats for tissue engineering with P-15, a synthetic peptide analogue of collagen. Tissue Eng 1999;5:53-65.

[36] Lindley EM, Guerra FA, Krauser JT, Matos SM, Burger EL, Patel VV. Small peptide (P-15) bone substitute efficacy in a rabbit cancellous bone model. Journal of Biomedical Materials Research Part B-Applied Biomaterials 2010;94B:463-8.

[37] Lutz R, Srour S, Nonhoff J, Weisel T, Damien CJ, Schlegel Ka. Biofunctionalization of titanium implants with a biomimetic active peptide (P-15) promotes early osseointegration. Clinical oral implants research 2010;21:726-34.

[38] Garkhal K, Mittal A, Verma S, Kumar N. P-15 functionalized porous microspheres as biomimetic habitats for bone tissue engineering applications. Polymers for Advanced Technologies 2011;22:190-8.

[39] Jaiswal N, Haynesworth SE, Caplan AI, Bruder SP. Osteogenic differentiation of purified, culture-expanded human mesenchymal stem cells in vitro. Journal of Cellular Biochemistry 1997;64:295-312.

[40] Johnstone B, Hering TM, Caplan AI, Goldberg VM, Yoo JU. In vitro chondrogenesis of bone marrow-derived mesenchymal progenitor cells. Exp Cell Res 1998;238:265-72.

Chapter 6

Property-Function Characterization of a Multi-layered Hydrogel for Interfacial Tissue Engineering Applications

(Submitted)

Tissue interfaces are complex junctions between two distinctly different tissues that vary in biochemical composition and often have very dissimilar mechanical properties. Interfaces are critical to overall function and their complexity presents unique challenges in tissue engineering. This study describes the development and characterization of the property-function relationships of multi-layered biomimetic hydrogels with spatially controlled biochemical and mechanical properties, with a particular emphasis on the local mechanical cues that are perceived by cells. As a proof of concept, tri-layered hydrogels were designed specifically for an osteochondral interface, the interfacial region between bone and cartilage, where the cartilage-niche was designed from compliant crosslinked poly(ethylene glycol) (PEG) with chondroitin sulfate, the bone-niche was designed from stiff PEG with RGD, and the interface was a hybrid of the two. Spatially controlling the local mechanical properties gave rise to characteristically different levels of cell deformation in all layers under static gross strains, which correlated with local strains determined from finite element models. When undifferentiated human mesenchymal stromal cells (hMSCs) were encapsulated in multi-layered hydrogels and cultured under free swelling or subjected to dynamic loading in osteochondral differentiation medium, the spatial presentation of biochemical and mechanical cues gave rise to characteristically different cartilage and bone protein expressions in hMSCs in each layer. In summary, this study demonstrates that

property-function relationships that arise in a multi-layered scaffold with distinctly varied biochemical and mechanical properties influence the local strains sensed by the cells and differentially affect the fate of encapsulated undifferentiated hMSCs.

6.1 Introduction

Interfaces in biological tissues are junctions that exist between two distinctly different tissues. They are biologically complex where their composition and structure are unique, giving rise to important property-function relationships [1-3]. For example, the dentin-enamel junction in teeth is the interface between two distinct calcified tissues, the outer rigid enamel and the softer underlying boney dentin. This interface provides resistance to crack propagation to the underlying bone, thus serving to minimize tooth fractures [4]. Musculoskeletal tissue interfaces include several distinct interfaces, tendon/ligament to bone (enthesis), muscle to tendon (myotendinous), and cartilage to bone (osteochondral) [5]. These interfaces are characterized by a gradation in their mechanical properties enabling the transfer of loads between two mechanically different tissues while minimizing stress concentration, reducing failure, and overall enabling the joint to function properly [6]. To achieve their functional properties, each interface has a unique biochemical make-up, which in some cases is described by a transition in extracellular matrix composition from one tissue to the other, e.g. osteochondral interface [6], or by a distinctly different composition, e.g. fibrocartilage of the enthesis interface [1].

Developing strategies to engineer tissues that span two distinct tissues connected by a complex junction is challenging, yet critical to restoring function. To date, the majority of studies focus on creating scaffolds that capture the two distinct tissues, through bi-layer designs. This strategy enables distinct layers to be engineered and tailored to each specific tissue. For example, the chemistry and/or structure of each layer have been designed to mimic aspects of the two tissues [7-9]. In addition, different tissue-specific cells have been seeded into each layer [7, 10-13]. The most prolific area of research in interfacial tissue engineering is in osteochondral tissue engineering [14]. Strategies often combine a form of inorganic mineralized matrix such as

tricalcium phosphate or decellularized trabecular bone, to represent the stiff boney region, with compliant hydrogel polymers such as poly(lactic-co-glycolic acid), poly(lactic acid), or agarose to represent the cartilage region [15-19]. Bi-layered hydrogels have also been explored, which enable cell encapsulation and have the added benefit of being able to be formed *in situ* [20, 21]. For example, layers of poly(ethylene glycol)-based hydrogels have been formed from the same structure, but with different cell types and growth factors for osteochondral tissue engineering [21]. A few strategies have investigated more complex multi-layered structures [7, 12, 15]. For example, Park *et al.* [12] created multi-layered porous scaffolds using solid free-form technology for engineering the dentin-peridontal ligament-bone complex in teeth. Taken together, these studies among others have demonstrated that it is possible to grow two distinctly different tissues within a single scaffold.

To engineer an interface that can provide function, strategies will also need to focus on ways to engineer the interfacial region, which in and of itself composes a unique cell phenotype and extracellular matrix with distinct mechanical properties, *and* focus on the connection to function. The bi-layer design approach has enabled advancements in interfacial tissue engineering, but the interface is largely characterized by an abrupt change in material properties created between the scaffold layers. Although the osteochondral interface exhibits a distinct tidemark separating non-mineralized cartilage matrix from mineralized matrix, there exists an interfacial region that is characterized as calcified cartilage having properties that are between cartilage and bone. Recently Harley *et al.* [22] developed a multi-layered osteochondral scaffold with varying composition of collagen, glycosaminoglycan and mineral, and was able to create an interfacial region that better captured the mineral composition of the osteochondral interface; however, the impact on cells was not tested. In addition to tailoring scaffold composition and

structure, the mechanical environment must also be incorporated as many of these junctions are subjected to external forces. Because cells respond very differently when external loads are applied, a better understanding of how mechanical forces are translated through these complex materials and how the local forces ultimately impact cells within the scaffold is needed. A few studies have utilized finite element modeling as a means to predict the local mechanical stresses and strains that are present in complex multi-layered osteochondral scaffolds [17, 23-25]. However, the impact on cells remains under-studied.

The overall objective for this study was to characterize the property-function relationships of multi-layered hydrogels, particularly with respect to local mechanical cues that are perceived by cells. This study investigates multi-layered biomimetic hydrogels laden with undifferentiated human marrow stromal cells (MSCs) for interfacial tissue engineering. Synthetically derived hydrogels were chosen because biological moieties can readily be incorporated in a controlled manner while independently tuning the mechanical properties [26-28]. Human MSCs were chosen because they offer an exciting clinically relevant cell source for engineering a range of interfaces and exhibit a multipotency to differentiate into cells with phenotypes that span interfacial tissues. In this study, we focus on one particular interface, the osteochondral interface because of the importance of the mechanical environment and the clinical prevalence of osteoarthritis that affects cartilage and the osteochondral interface [29, 30]. The specific aims of this study were twofold: 1) to characterize through experiments and finite element modeling, the property-function relationships of cell-laden multi-layered hydrogels fabricated with spatially controlled presentation of biochemical and mechanical cues that capture three regions, bone, cartilage, and the distinct interface and 2) to investigate whether the local

cues presented by a multi-layered hydrogel under the application of intermittent dynamic compression differentially impacts the fate of undifferentiated human hMSCs.

6.2 Results

Multi-layer Hydrogel Fabrication and Characterization

Initially the formation of multi-layered hydrogels with spatially controlled crosslinked structures was investigated. Three-dimensional tri-layered hydrogels were fabricated by sequential photopolymerization of two macromolecular monomer (macromer) solutions of 10% (g/g) and 30% (g/g) poly(ethylene glycol dimethacrylate) (PEGDM)) to produce layered hydrogels whereby the chemistry remained constant but the structure, via crosslinking density, was varied. To create an interfacial region, the hydrogels were fabricated by partially polymerizing the bottom, more stiff, layer (30% PEGDM) followed by the addition of the second monomer solution (10% PEGDM) and subsequent polymerization to produce the less stiff top layer. This process yielded a middle layer as a result of mixing between the two monomer solutions, which defined the interfacial region. The thickness of the interfacial region was controlled by varying the polymerization times for the bottom layer from 0 to 10 minutes prior to adding the top layer macromer solution (Fig. 6.1). Qualitatively, the formation of a distinct boundary between the top and bottom layers became apparent with polymerization times for the bottom layer exceeding 2.5 minutes (Fig. 6.1G-I), whereas hydrogels fabricated with a bottom layer polymerization time of 2.5 minutes or less resulted in the formation of a continuous and more substantial interfacial region (Fig 6.1 A-C). Semi-quantitative analysis of the interface revealed interface thicknesses that ranged from 2.7 to 0.5 mm or ~45 to ~10% of the total scaffold height with increasing polymerization times for the bottom layer (Fig. 6.1M).

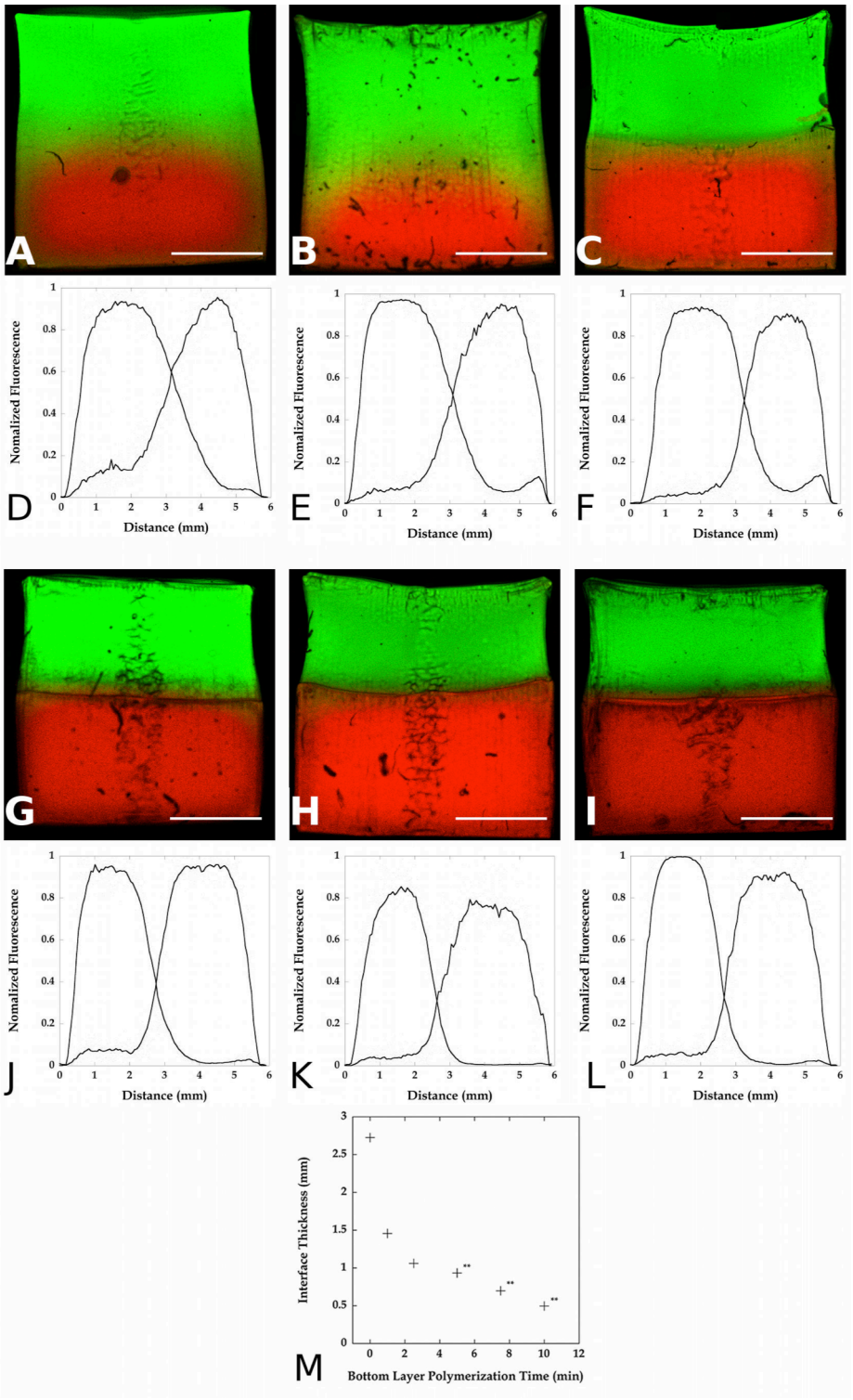

Figure 6.1: A-L) Representative microscopy images of dually fluorescent tri-layered hydrogels (green, top; red, bottom) and the corresponding normalized fluorescence intensity plots. The hydrogels were fabricated using a range of bottom layer (red) polymerization times: 0 min. (A, D), 1 min. (B, E), 2.5 min. (C, F), 5 min. (G, J), 7.5 min. (H, K), and 10 min. (J, L), with the top layer polymerization time held constant at 10 min. Original magnification is 25x. Scale bar = 1 mm. M) Interface thickness measured by the thickness of overlapping fluorescence intensities as a function of bottom layer polymerization time. **denotes that interface shearing occurred under a compressive force.

We selected one hydrogel fabrication scheme to explore spatially controlling both biochemical composition *and* mechanical properties in the different layers. We chose the formulation, bottom layer, polymerization time: 1 minute, and top layer, polymerization time: 10 minutes (Fig. 6.1B), because it yielded a measurable and mechanically robust interface, which would enable its characterization. The local biochemical composition was varied by introducing different extracellular matrix (ECM) moieties into each monomer solution. The bottom layer was fabricated by co-polymerizing 30% (g/g) PEGDM macromers with 2.8 mM acryloyl-PEG-RGD as the boney niche, while the top layer was fabricated by co-polymerizing PEGDM with

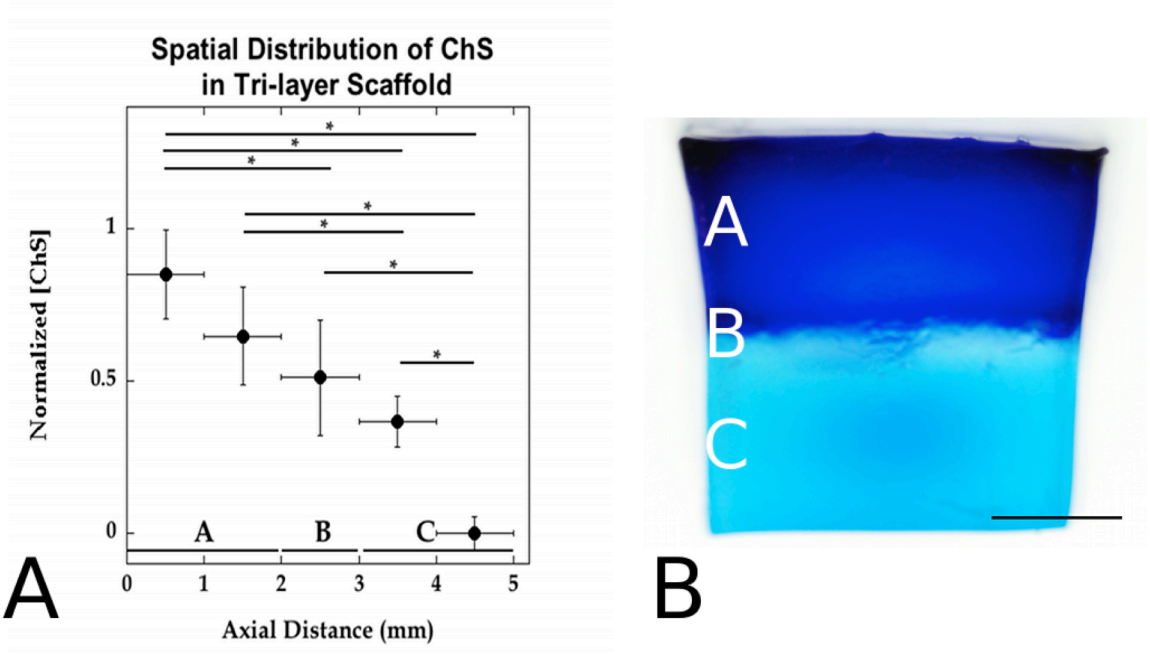

Figure 6.2: A) Normalized biochemical analysis of the axial ChS composition of a typical tri-layered hydrogel (n=3). The x-axis error bars are not error bars, but rather are used to denote the region that the pooled sections span. A-C labels correspond to chondrogenic (top) layer = A, interface (middle) layer = B, and osteogenic (bottom) layer = C. * $p < 0.05$. B) Representative image of a tri-layered scaffold grossly stained with toluidine blue for glycosaminoglycans. There is a slight blue background staining by the plain PEG (bottom). The intense dark blue staining corresponds to the presence of chondroitin sulfate (top and interface). Scale bar = 1 mm.

methacrylated chondroitin sulfate (ChSMA), with a 10% (g/g) final macromer concentration (80% PEGDM, 20% ChSMA) as the cartilage niche. The interfacial region then became a combination of RGD and chondroitin sulfate to yield the osteochondral interface. We assessed the axial spatial distribution of chemical composition by probing for the presence of ChS in serial sections by measuring its concentration through a quantitative spectroscopy based assay. The highest concentration of ChS was measured in the top ~40% of the hydrogel, and it decreased rapidly beyond the interface layer with little to no ChS detected in the bottom ~20% of the scaffold (Fig. 6.2A). Acellular hydrogels were also grossly stained with toluidine blue, which stains for negatively charged glycosaminoglycans to highlight the spatial location of chondroitin sulfate within the multi-layered scaffold. A representative image is shown in Fig. 6.2B.

Table 6.1: Unconfined compressive modulus for tri-layered hydrogels.

	Compressive Modulus (kPa)
Cartilage-like layer	48 ± 6[a]
Interfacial layer	~100[b]
Bone-like layer	345 ± 35 [a]
Tri-layered Hydrogel	90 ± 22 [c]

[a]determined experimentally from single component hydrogel, [b]estimated from neo-Hookean model, [c]determined experimentally.

The mechanical properties of the biomimetic tri-layered hydrogel were characterized by the unconfined compressive modulus (Table 6.1). The top and bottom layers were determined from hydrogels prepared from the individual components of each layer. The average modulus of the top layer was 48 kPa and the bottom layer was 345 kPa. A tri-layered hydrogel was also characterized and its modulus was 90 kPa.

Finite Element (FE) Modeling

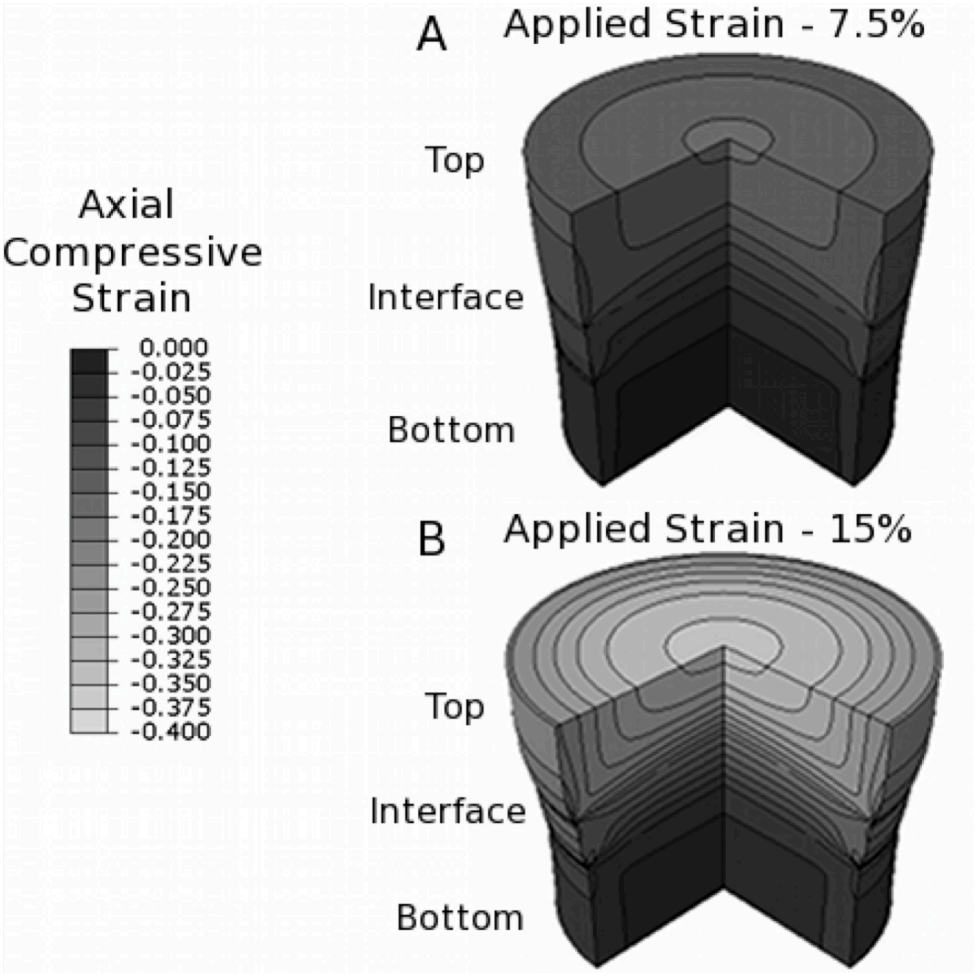

Figure 6.3: Finite elemental analysis results describing the axial true strain for a tri-layered hydrogel subjected to A) a static 7.5% gross unconfined compressive strain and B) a static 15% gross unconfined compressive strain. Negative values correspond to compressive strain.

A FE model was used to predict the local strain profile produced within the tri-layered hydrogel when subjected to an unconfined gross compressive strain. The model assumed three distinct regions each with a homogeneous modulus. The moduli for the top and bottom regions were taken from experimental measurements of the individual components of their respective layer. The modulus of the interfacial region was approximated through curve fitting the overall tri-layer hydrogel modulus data and estimated to be ~100 kPa. This finding indicates that the

mechanical properties of the real interface is likely between that of the two layers. Using this model, strain profiles were generated for two scenarios, the application of a 7.5% and a 15% unconfined gross compressive strain applied along the cylindrical axis. The strain profiles, presented in Fig. 6.3, illustrate that the local strain decreases from top to bottom, with the majority of the applied strain being transferred to the top layer and to a lesser extent the interface with the stiffer bottom layer experiencing little deformation. When comparing the 7.5 and 15% gross strains, it is evident that the smaller gross strain produces more uniform radial and axial profiles strains.

hMSC Deformation

While finite element analysis (FEA) confirmed variations in the local strain profile in acellular tri-layered gels, it remained to be determined whether this translated into observable differences in strains experienced by cells. hMSCs were encapsulated in tri-layered hydrogels and subjected to the same gross compressive strains that were applied in the FE model. Using a custom cell straining device in combination with confocal microscopy, changes in cell morphology were investigated as a measure of cell deformation. Gross static unconfined compressive strains of 0%, 7.5%, and 15% strain were applied to the tri-layered hydrogels and representative images of cells in each of the three layers are shown in Fig. 6.4A-I. Cell deformation was quantified from confocal microscopy images taken at full width half maximum diameter for each gross strain and reported as a diameter ratio (x/y), where the value of x is the cell diameter in the axis parallel to the applied strain, and the y value is the cell diameter in the axis perpendicular to the applied strain (Fig. 6.4J). The application of a gross compressive strain led to a general change in cell morphology from rounded to an ellipsoidal shape under strain in

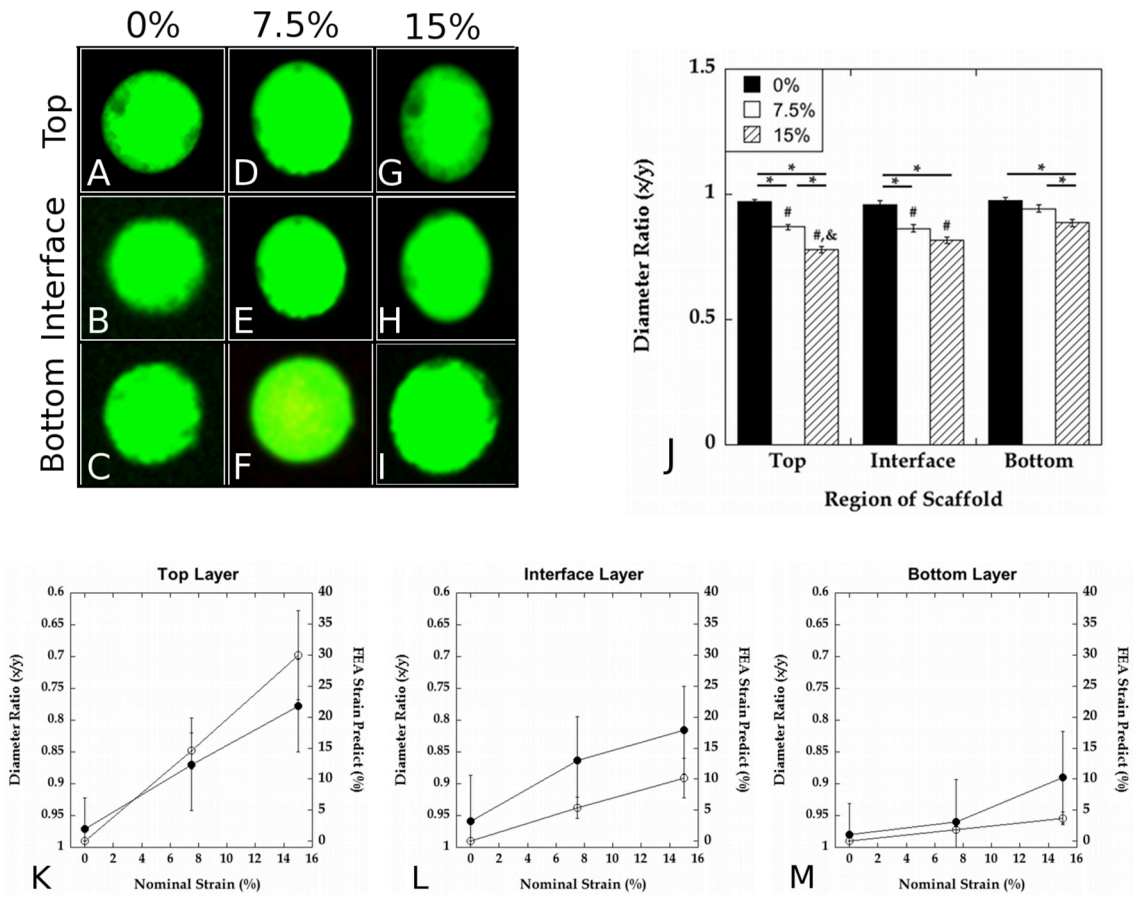

Figure 6.4: A-I) Representative confocal microscopy images of hMSCs (green) encapsulated in the top layer, interface layer, and bottom layer of a representative tri-layered hydrogel subjected to no strain (A-C), 7.5% gross static compressive strain (D-F), or 15% gross static compressive strain (G-I). Original magnification is 200x. J) hMSC deformation was quantitatively assessed by a diameter ratio in each layer (top, interface, and bottom) of the multi-layered scaffold under 0% (black), 7.5% (white), and 15% (grey) gross static compressive strains. A diameter ratio of one indicates a perfectly round cell with no deformation and a diameter ratio of less than one indicates cell deformation. * indicates $p < 0.05$, & indicates $p < 0.1$. (K-M) Line plots for the experimentally determined diameter ratio and the strain predicted by FEA for each layer in the tri-layered hydrogel as a function of the nominal gross strain.

all layers. However, the degree to which the cells deformed depended on the magnitude of the gross strain and the location of the cell, i.e. the layer within the hydrogel. Qualitative analysis from confocal microscopy images revealed that cells in the top least stiff layer of the hydrogel underwent the most dramatic morphological change under the 15% gross strain, which was confirmed by the smallest diameter ratio. In contrast, changes in cell morphology in the bottom

(stiffest) layer were not substantial under the 7.5% strain but were observable under the 15% strain with a significantly lower diameter ratio. Cells in the interfacial layer when compared to the top layer exhibited similar levels of cell deformation under 7.5% strain, but were less deformed under 15% strain. To compare with results from the FEA, diameter ratios were plotted along side the average axial strain predicted from FEA, where the average strain was determined from the central axis region of each layer. Experimental and simulation data display similar trends with increasing gross strain (Fig. 6.4K-L). It is important to note that one limitation with directly comparing the trends predicted by FEA to those in the cell straining device is that the shapes of the scaffolds are different, cylindrical versus square, respectively.

Expression of ECM Molecules by hMSCs Encapsulated in Tri-layered Hydrogels in Osteochondral Differentiation Media Under Free Swelling and Dynamic Loading Conditions

As a proof of concept, undifferentiated hMSCs were encapsulated in a tri-layered hydrogel with compositional and stiffness variations. The scaffolds were fabricated as described above with a stiff layer comprised of RGD ligands, a compliant layer comprised of ChS and an interface comprising both RGD and ChS. The cell-laden tri-layered hydrogels were cultured in osteochondral medium under either free swelling conditions for 14 days or free swelling conditions for the first week and then subjected to unconfined dynamic compressive strains applied intermittently from 0%-7.5% at a frequency of 0.3 Hz during week two. Samples were assessed by immunohistochemistry for aggrecan, and collagens I, II, and X protein expression at day 14. Representative histology images are shown in Fig. 6.5 with general qualitative observations given in Table 6.2.

After 14 days under free swelling, hMSCs in the top layer expressed aggrecan and collagens I, II and X (Fig 6.5A, G, M, S, Table 6.2). hMSCs in the interfacial layer expressed similar levels of aggrecan and collagens I and X, but less collagen II when compared to the top layer (Fig 6.5B, H, N, T, Table 6.2). hMSCs in the bottom layer expressed collagens I, II, and X but no detectable aggrecan (Fig 6.5C, I, O, U, Table 6.2). Under loading, hMSCs in the top layer had increased aggrecan expression, no effect in collagen I and X expression, but reduced collagen II expression when compared to its free swelling counterpart (Fig 6.5D, J, P, V, Table 6.2). In the interfacial layer, hMSCs expressed reduced collagen X expression, but enhanced collagen II expression with no effect in aggrecan and collagen I expression (Fig 6.5E, K, Q, W, Table 6.2). In the bottom layer, hMSCs showed reduced expressions of collagen X and II, weak aggrecan expression with loading, with no effect in collagen I expression (Fig 6.5F, L, R, X, Table 6.2).

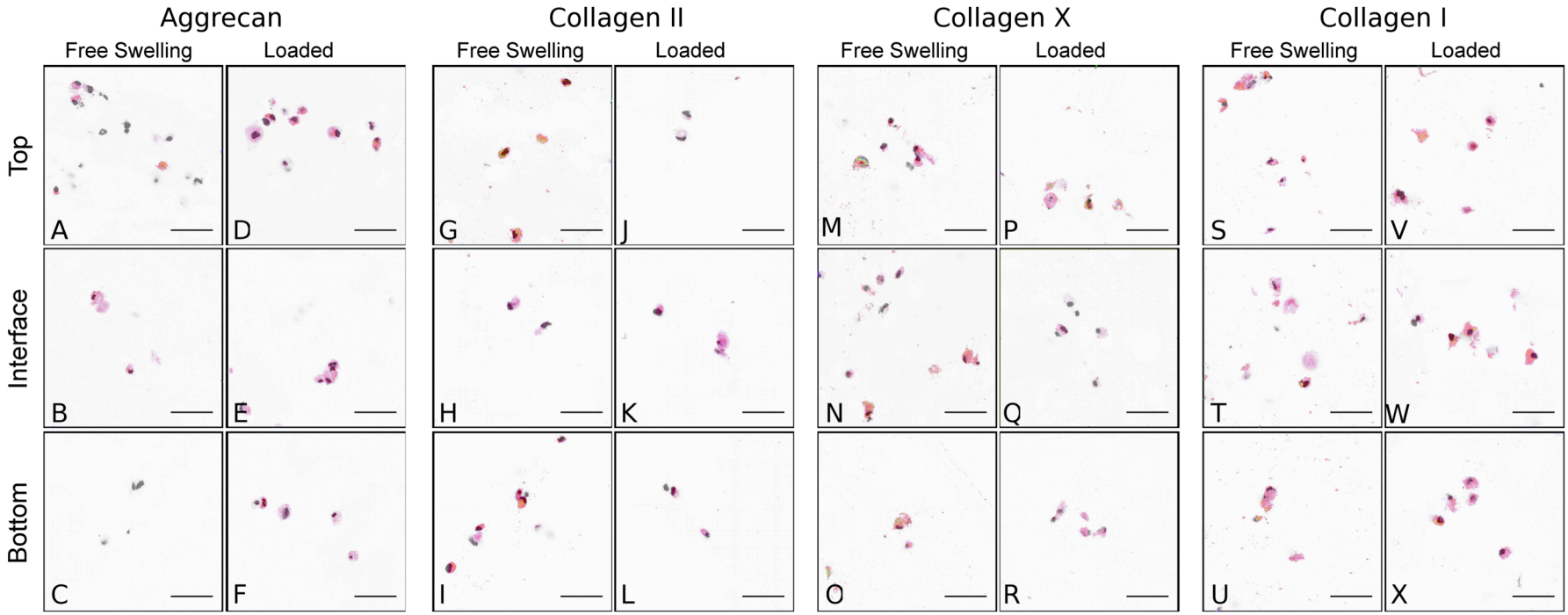

Figure 6.5: Immunohistochemical analysis of protein expression by hMSCS encapsulated in tri-layered hydrogels and cultured under free swelling or dynamic loading conditions after 14 days. Original magnification is 400x. Staining intensity is visualized with a color spectrum scale from red to violet, with red indicating low intensity and violet indicating high intensity.

Table 6.2: Denotation of qualitative observations for IHC staining in Figure 6.5 (n=2).

	Aggrecan		**Col II**		**Col X**		**Col I**	
	Free Swelling	Loaded	Free Swelling	Loaded	Free Swelling	Loaded	Free Swelling	Loaded
Top	+	++	++	+	++	++	++	++
load effect		#		-		ne		ne
Interface	+	+	+	++	++	+	++	++
load effect		ne		#		-		ne
Bottom	X	+	++	+	++	+	++	++
load effect		#		-		-		ne

X denotes no detected staining, + denotes weak staining, ++ denotes stronger staining in free swelling and loaded samples. # denotes an increase in staining with the application of load, - denotes a reduction in staining with load, and "ne" denotes no effect from load.

6.3 Discussion

The current study has developed and characterized the property-function relationships of a multi-layered hydrogel with varying biochemical and mechanical properties, with a special emphasis on the interface. As a first step towards designing scaffolds for osteochondral tissue engineering, the local biochemical and mechanical environments were designed to mimic certain aspects of the native junction of the osteochondral interface. This study focused on two key aspects: i) the differential mechanical properties of the native tissue and ii) the biochemical make-up of the extracellular matrix. By spatially controlling the mechanical properties, this study demonstrated that the application of a gross static compressive strain applied to multi-layered hydrogels leads to dramatic changes in the level of cell deformation within each layer, which correlated with local strains predicted by FE models. As a proof of concept, the impact of variations in the local biochemical and mechanical properties on hMSC differentiation was demonstrated in dynamically loaded hMSC-laden tri-layer hydrogels. Together, this study aimed to demonstrate the importance of property-function relationships for spatially controlling the local mechanotransduction cues, which will be critical to the success of many interfacial tissue engineering strategies.

To create an environment that captured two distinct tissue niches, a chondrogenic-like layer that was compliant and an osteogenic-like layer that was stiff, separated by an interfacial region, a simple sequential polymerization method was developed. The thickness of the interfacial layer was readily controlled by manipulating the polymerization time, i.e. conversion of monomer into polymer, of the bottom layer during fabrication. In addition, the type of interface formed varied from gradual, when polymerization times were short and conversion was low, to distinct interfaces when polymerization times were long and conversion was high. For

polymerization times beyond five minutes, which is sufficient to reach near complete conversion, shearing of the two layers resulted under a gross strain, which prohibited these hydrogels from use in mechanically compressive applications. Therefore, hydrogels with a bottom layer polymerization time of one minute were chosen to ensure a mechanically robust interfacial layer (>20% of total hydrogel height), given the implementation of mechanical loading.

The osteochondral interface is the transitional region between the more compliant hyaline cartilage and the stiff underlying subchondral bone in articulating joints of the body. This interface is typically thought of as the calcified cartilage layer that has mechanical properties that reside between cartilage and bone [31]. These differential mechanical properties give rise to one of the primary functions of cartilage, which is to absorb most of the load thus protecting the underlying bone. As such during physiological loading, cartilage which has a modulus of ~450-800 kPa[32] experiences large strains (e.g., 2-9% are typical [33]), but strains as high as 30% can be generated[34, 35] while the underlying bone which has a modulus of ~1-5 GPa[31, 36] experiences very little strain, less than 1% [37]. While the absolute mechanical properties were not captured in the multi-layered hydrogels in this study, the differential strain levels were captured. Under large 15% nominal gross strains applied to the hydrogel, the local strains in the cartilage-like layer were ~30%, while the bone-like layer were ~4%. Under the smaller 7.5% nominal gross strain, the local strains in the cartilage-like layer were ~15%, while the bone-like layer were ~2%. While local strains in the interfacial region are not well characterized, the Young's modulus has been estimated to be ~10-fold lower than that of the subchondral bone[31] supporting the idea that the strains will be between cartilage and bone. It is important to recognize that during healing, strains that are larger than those that exist normally in the native tissue dictate the type of tissue that is formed (e.g., in fracture healing ~5% strains have been

shown to lead to bone formation, while higher strains can preferentially lead to cartilage formation[38, 39]). Therefore, the hydrogels developed in this study when subjected to 7.5% strain are within targeted strain levels necessary for promoting cartilage and bone tissue formation.

The composition of cartilage, bone and the interface have their own unique biochemical make-up, which ultimately gives rise to their mechanical properties and hence their function. The biochemical composition provides important insoluble cues to cells, which together with mechanical cues helps maintain tissue homeostasis. The major constituents for hyaline cartilage are collagen type II and aggrecan, for bone are collagen type I among other bone specific proteins and mineralized matrix, and for the interface are collagen type X and mineralized matrix, and to a lesser extent collagen type II and GAGs [40]. In designing the biochemical composition of the multi-layer hydrogels, a simple approach was chosen where chondroitin sulfate, a GAG in articular cartilage, was selected for the cartilage-like layer, and RGD, a cell adhesion peptide, was selected for the bone-like region. Chondroitin sulfate was chosen because it is the main building block of aggrecan[41] as well as an important structural component of cartilage[42] and has been shown to support chondrogenic differentiation of MSCs [43]. RGD was chosen because it is a ubiquitous cell binding domain that is present in several bone specific proteins (e.g., osteopontin and bone sialoprotein II [44]) and has been shown to support osteogenic differentiation of MSCs in 3D hydrogels [45, 46]. The interface subsequently was comprised of both chondroitin sulfate and RGD. This combination may give rise to a unique cell phenotype where chondroitin sulfate, while small, is present in calcified cartilage[47] and the persistent presence of RGD has been shown to inhibit collagen II-expressing MSCs long-term[48] and therefore together may promote a hypertrophic cartilage phenotype.

As a proof of concept, the ability to control the differentiation fate of *undifferentiated* human adult MSCs by controlling the spatial presentation of biochemical and biomechanical cues in a multi-layered photopolymerizable hydrogel for osteochondral applications was explored. It is important to note that ideal loading regimes that guide differentiation of hMSCs down either a chondrogenic or osteogenic lineage have not yet been elucidated. Therefore, the primary goal of this work was to determine whether it was possible to differentially impact how hMSCs respond, through the type of proteins they express, to biochemical and mechanical cues in a multi-layered hydrogel during the early stages of differentiation. By in large under free swelling conditions, all collagens investigated were expressed in all three layers. Expressions of collagen II and aggrecan appear to be most prevalent in the cartilage-like layer, suggesting an environment supportive of chondrogenesis. In the bone-like layer, there was a lack of detectable aggrecan. These observations suggest the insoluble biochemical cues presented by the hydrogel itself have a modest impact on the types of proteins expressed. Under loading, notable changes in the types of proteins expressed were observed. Most notably, the expression of collagen II was reduced in the cartilage-like layer, while simultaneously being elevated in the interfacial region. This observation suggests that while the chondroitin sulfate biochemical cue promotes chondrogenic differentiation, chondrogenesis may be inhibited by the relatively high strains in the cartilage-like layer [49], but stimulated by the smaller strains in the interfacial region. While the strains are small in the bone-like region, loading did have an observable impact on the type of proteins expressed, leading to detectable aggrecan, but a down regulation in collagen II. This observation suggest that either small strains or fluid flow, which may arise as a result of the high compression in the upper regions is sufficient to impact the hMSCs encapsulated in this layer. Interestingly, loading had a general inhibitory affect on type X collagen expression, but did not

affect type I collagen expression. Taken together, our findings confirm that it is possible to impact undifferentiated hMSCs through the combined presentation of biochemical and biomechanical cues; however further fine tuning of both the biochemical and biomechanical environmental will be necessary to optimize hMSC differentiation. Recent findings from Nguyen *et al.* [50] suggest that a combination of biochemical cues may be necessary to direct stem cell differentiation by insoluble cues.

In this study, hMSCs were also presented with a cocktail of soluble factors that are a combination of chondrogenic and osteogenic factors. The primary chondrogenic factor, TGF-β3 is a relatively large molecule, and as a result its diffusion into the hydrogel can be in part controlled through the crosslinking density of the hydrogel. The crosslinked structure of the boney-like layer is relatively small, such that diffusion of TGF-β3 should be substantially reduced, while permitting diffusion of the much smaller osteogenic factors that present in the culture medium. However, dynamic loading will enhance transport properties[51] and therefore may increase that amount of TGF-β3 into the boney region, thus leading to positive expression for aggrecan under loaded conditions. Alternative strategies for a more targeted delivery of TGF-β include co-encapsulating TGF-β-loaded microparticles into the cartilage-like layer [52] or via tethered moieties [27], both of which would be easily incorporated into our current multi-layer hydrogel fabrication scheme.

FEA was employed to gain insights into the local strains that are generated in the multi-layered hydrogels as a result of a gross strain, and is an effective engineering tool that can guide the design of tissue engineering scaffolds [17, 53, 54]. Therefore, once optimal loading regimes are identified for differentiating hMSCs down chondrogenic and osteogenic lineages, the predictive models developed in this study will be used to identify *a priori* gel mechanical

properties and hence gel structures for each layer and gross strains to achieve the desired local cues.

6.4 Conclusions

This study describes the development and property-function characterization of a multi-layered hydrogel for osteochondral tissue engineering applications. Spatially controlling the local biochemical *and* mechanical properties gave rise to characteristically different levels of cell deformation under static gross strains and to characteristically different protein expressions in hMSCs under free swelling and dynamic gross strains. This study aimed to demonstrate that starting with undifferentiated hMSCs and by controlling local physical cues in a single differentiation medium cocktail, it was possible to affect hMSCs by altering the types of proteins expressed. Because this study was limited to the early stages of differentiation, an exact determination of the terminal differentiation fate of the hMSCs in each layer was not possible. This observation is further confounded by the fact that the initial chondrogenic and osteogenic differentiation pathways of hMSCs are linked [55]. Nonetheless, clear differences were observed. As the cues necessary to guide chondrogenesis and osteogenesis of hMSCs become more defined, the facile and versatile fabrication process combined with the predictive modeling tool will enable the development of fine-tuned multi-layered hydrogels for osteochondral tissue engineering strategies. This strategy can easily be adapted to engineering other interfacial tissue engineering applications, particularly those where mechanical forces are prevalent.

6.5 Experimental

Macromer Synthesis

Poly(ethylene glycol) dimethacrylate (PEGDM) macromolecular monomers were synthesized via microwave methacrylation [56]. Briefly, 4600 g mol^{-1} poly(ethylene glycol) (PEG) (Fluka, Sigma-Aldrich) was melted and reacted with methacrylic anhydride in the presence of hydroquinone (Sigma-Aldrich). The reaction mixture was dissolved in methylene chloride and purified by multiple precipitations with ethyl ether, filtered, and dried under vacuum. The degree of methacrylate substitution on each end of the PEG molecules was determined to be 93% by ^{1}HNMR (Varian VYR-500). Specifically, the area under the curve for the vinyl resonance peaks (d= 5.7 ppm, d = 6.1 ppm) was compared to the area under the curve for the methylene peaks associated with the PEG backbone (d =4.3 ppm).

YRGDS (Genscript) was reacted in a 1:1.1 molar ratio with excess acryloyl-PEG-N-hydroxysuccinimide (3400Da; Laysan Bio, Inc.) in 50 mM sodium bicarbonate buffer (pH 8.4) overnight at room temperature. The degree of attachment was determined to be 94% using the spectroscopic Fluoraldehyde™ o-Phthalaldehyde (Pierce) method of detection. The product, acryloyl-PEG-RGD was dialyzed for 24 hrs, lyophilized, and stored at 4 *ºC.*

Methacrylated chondroitin sulfate (ChSMA) was synthesized as previously described [57, 58]. Briefly, chondroitin sulfate A (Sigma), containing ~30% chondroitin-6-sulfate and ~70% chondroitin-4 sulfate was dissolved at 25% (w/v) in deionized water (dI-H_2O) and reacted in a 1:8 ratio with methacrylic anhydride. The reaction temperature was held at 4 ºC for 24 hrs and the reaction pH was maintained at pH=8. The reaction product was precipitated in chilled methanol and dialyzed in dI-H_2O for six hrs with three dI-H_2O water changes. Multiple mechacrylate substitutions are possible due to the free hydroxyl groups present in each repeat

unit of the ChS [58].The purified product was recovered via lyophilization and the degree of methacrylation was determined to be 23% via ^{1}HNMR (Varian VYR-500), indicating that, on average, there were 23 methacrylate groups present on each ChSMA molecule. Specifically, the area under the curve for the vinyl resonance peaks (d= 5.5-6.2 ppm) was compared to the area for the acetyl groups (d =1.7-2.0 ppm).

Acellular Multi-layered Scaffold Fabrication and Characterization

Two macromer solutions were used to create the multi-layered scaffolds for acellular fabrication characterization: 10% (g/g) PEGDM, top, and 30% (g/g) PEGDM, bottom. Each macromer solution was combined with 0.05% (g/g) photoinitiator Irgacure 2959 (Ciba Specialty Chemicals). To visualize the multi-layers using fluorescent microscopy, 0.1% (g/g) fluorescein-*o*-methacrylate (Sigma) was added to the 10% PEGDM macromer solution, and 0.1% (g/g) rhodamine methacrylate (Sigma) was added to the bulk 30% PEGDM macromer solution. The macromer solutions were exposed to 365 nm light with an intensity of ~5 mW cm^{-2} for a range of times, referred to as polymerization time (0-10 minutes: bottom, plus 10 minutes: top). Dually fluorescent cubic (5 mm x 5 mm x 5 mm) multi-layered scaffolds were fabricated and imaged using confocal laser scanning microscopy. Image J software was used to characterize the resultant interface thicknesses.

Additionally, multi-layered hydrogels and corresponding single component hydrogels were fabricated with biochemical cues. Two macromer solutions were prepared: 10% (g/g) comprised of 80:20 (PEGDM:ChSMA) by weight (top layer) or 30% (g/g) PEGDM with 2.8 mM RGD (bottom). Single component hydrogels were formed from each macromer solution and polymerized as describe above for 10 minutes. Multi-layered hydrogels were fabricated using 1

minute for the bottom layer plus 10 minutes for the top layer. Cylindrical hydrogels (5 mm in height x 5 mm in diameter) were fabricated. Hydrogels were allowed to free swell in PBS for 24 hrs at 37 °C. The tangent compressive modulus was determined in hydrated hydrogels under unconfined compression, using a mechanical tester (Bose LM1 Test Bench). The samples were strained at a constant strain rate of 0.3 mm sec^{-1} using nonporous platens. The resulting tangent modulus of the individual layers and the multi-layered hydrogels was determined for the linear region of the stress/strain curve (n=5). It should be noted that because PEG hydrogels exhibit largely elastic behavior, the tangent modulus is similar to the equilibrium modulus previously reported for similar hydrogel formulations [59].

Acellular Composite Biochemical Analysis

Cylindrical acellular tri-layered hydrogels were embedded in tissue mounting media and serially sectioned in the axial direction, starting at the top layer and continuing down the axis of the cylinder, using a cryosectioner (Leica). 200 mm sections were homogenized and then sequentially degraded in 1M NaOH at 60ºC for 24 hrs, then neutralized followed by enzyme treatment in 2 ml of $6.6x10^{-3}$ U ml^{-1} chondroitinase ABC (Sigma) at 37 ºC for 24 hrs. The ChS content was assessed using the DMMB dye assay [60] and 5 sections were pooled and analyzed. Fully hydrated acellular tri-layered scaffolds were also stained with a working solution of toluidine blue (stock: 1% toluidine blue in 70% ethanol, working solution: 10% stock solution in 1% NaCl, pH <2.5). Toluidine blue stains negatively charged glycosaminoglycans blue and was used to grossly visualize the spatial distribution of the ChS in the tri-layered scaffold. In addition, the soluble fraction of ChSMA, i.e. the fraction not incorporated into the hydrogel, was determined by assaying for the ChSMA (by DMMB) that diffused out of the hydrogel after the

24 hour free swelling period. It was confirmed that 80% of the ChSMA was incorporated into the hydrogel.

Finite Element Modeling

The FEA software package ABAQUS (Simulia) was used to conduct simulations. Finite element discretization was carried out using 8-node axisymmetric hybrid elements (*CAX8H*) using a relatively fine mesh of 5,000 elements. Because the model describes behavior in a relatively small stretch regime, Gaussian chain statistics are applicable [61]. From experimental results, it was assumed the relative heights of the cylindrical hydrogel layers for the top, bottom, and interface layers were 2 mm, 2 mm and 1 mm, respectively. Strain energy models were used to capture the stress-strain behavior for hyperelastic materials such as the hydrogels studied in this work. The neo-Hookean model was chosen because it provided the best fit with experimental data and required only one fitting parameter. The strain energy (U_{NH}) for the neo-Hookean material model is given by:

$$U_{NH} = \frac{\mu}{2}\left(I_1 - 3\right) \qquad (1)$$

where m is the initial rubbery shear modulus and $\bar{I}_1$, is the first strain invariant of the deviatoric, isochoric left Cauchy-Green strain tensor. The rubbery shear modulus used in the simulations for the top and bottom layer of the multi-layered scaffold were estimated from the bulk modulus and assumed to be 16 kPa and 115 kPa, respectively. The layers were assumed to be incompressible. The shear modulus for the interface was determined through curve fitting of the tri-layered experimental results and determined to be 33 kPa. The modeling results are reported as the axial logarithmic strain.

hMSC Cell Culture

Adult hMSCs (24 year old male) were purchased from Texas A&M Health Science Center College of Medicine Institute for Regenerative Medicine and expanded in basal stem cell medium (20% fetal bovine serum (FBS, Atlanta Biologicals), 1mg mL^{-1} amphotericin B, 50 U mL^{-1} penicillin, 50 mg mL^{-1} streptomycin, and 20 mg mL^{-1} gentamicin in low glucose Dulbecco's modified Eagle medium (aMEM, Invitrogen) containing 1g L^{-1} glucose). The cells were grown under standard cell culture conditions (in a regulated incubator at 37 ºC with 5% CO_2) and were plated at ~60 cells cm^{-2} till passage 2 (P2, 1:10) and allowed to grow to 80% confluency before being frozen down. Cells were thawed and plated at approximately 4500 cells cm^{-2} in T-275 tissue culture polystyrene flasks (P3). Media was changed twice weekly and cells were cultured in basal medium until Passage 5 (P5) (1:2 for P3-P4, 1:3 for P4-P5).

Cell Encapsulation

hMSCs were combined at a cell concentration of $10x10^6$ cells mL^{-1} with either a sterile 10% 80:20 PEGDM:PEGDM/ChSMA (g/g) macromer solution or a with a sterile 30% (g/g) PEGDM solution containing 2.8 mM acryloyl-PEG-RGD and 0.05% (g/g) photoinitiator Irgacure 2959 (Ciba Specialty Chemicals). The macromers and initiator were dissolved in defined osteochondral differentiation medium (OCDM). OCDM included 1ml/100 ml media ITS+ Premix (BD), 100 nM dexamethasone, 5 ng mL^{-1} TGF-b3 (R&D Systems), 50 mg ml^{-1} l-ascorbic acid 2-phosphate trisodium salt, 100 mg ml^{-1} sodium pyruvate, 20mM b-glycerophosphate, 1mg mL^{-1} amphotericin B, 50 U mL^{-1} penicillin, 50 mg mL^{-1} streptomycin, and 20 mg mL^{-1} gentamicin in high glucose Dulbecco's modified Eagle medium (DMEM, Invitrogen) containing 4.5g L^{-1} glucose. A tri-layered hydrogel was produced as described above

for the acellular scaffold fabrication. Samples were either cube (5 mm x 5 mm x 5mm) or cylindrical (5 mm diameter x 5 mm height) in shape for use in cell straining or dynamic loading experiments, respectively.

Cell Straining

hMSC deformation was assessed for each of the two layers as well as the resulting interface. Cells were pretreated with Cell Tracker™ Green CMFDA (Invitrogen) per manufacturer and encapsulated as described above. After a 24 hour free swelling period, cubic hydrogels were placed in a custom-built cell straining device similar to that described by Knight *et al.* [62]. Three samples were analyzed, and three areas within each layer (top, bottom, and interface of the multi-layered scaffold) were visualized for n=~30-45 cells/layer.

Mechanical Loading

A custom-built bioreactor system, as described elsewhere [63, 64] was utilized to apply intermittent dynamic compressive strains to hMSC-laden tri-layered hydrogels. The hydrogels were cultured under free swelling conditions for the first week and then subjected to an intermittent dynamic loading regime applied from 0 to 7.5% amplitude strain in a sinusoidal waveform at a frequency of 0.3 Hz (0.5hr on, 1.5hr off, repeated for 16 hours, 4 hours total loading, followed by 8hr off) in the second week. Hydrogels were cultured in individual wells with 2 ml per well of OCDM, which was changed daily, for the duration of the study. Free swelling controls (n=2) were removed at 7 days and loaded scaffolds (n=2) free swelling controls were removed at 14 days immediately following a complete 16-hour intermittent loading cycle. A separate set of hydrogels (n=2) was free swollen for 14 days.

Immunohistochemistry

Hydrogels were fixed overnight in 4% paraformaldehyde and transferred to a 15% sucrose solution for storage (n=2). Scaffolds were embedded in tissue freezing medium, flash frozen in isopentane and liquid nitrogen, and sectioned using a cryostat. Sections (20mm) were stained for the presence of aggrecan and collagens I, II, and X by immunohistochemistry. All samples were pretreated with Chondroitanase-ABC (500 mU mL^{-1}) (Sigma-Aldrich) for 60 minutes. Collagen I and II samples were treated with protease (from streptomyces griseus, Sigma-Aldrich, 1mg ml^{-1}) for 30 minutes and collagen X samples were treated with pepsin (1mg ml^{-1}) for 30 minutes. After permeabilization with a 0.25% Triton-X 100™solution and blocking with 10% normal goat serum, samples were treated overnight with anti-aggrecan (US Biologicals, 1:5), anti-type I collagen (Abcam, 1:400), anti-type II collagen (Abcam, 1:100), and anti-type X collagen (Developmental Studies Hybridoma Bank, 1:2) in blocking solution at 4 ºC, rinsed with PBS, and treated for 2 hr with goat anti-mouse IgG labeled with Alexa Fluor 488 (Invitrogen, 1:200) and counterstained with DAPI. Image J software was used to analyze the data. Briefly, grayscale images for the two channels (405 nm, DAPI and either 546 or 488 nm Alexa Flour goat-anti mouse, antibody label) were separated and inverted. The 16_color lookup table was applied to the antibody channel and the images were merged. Staining intensity is visualized with a color spectrum scale from red to violet, with red indicating low intensity and violet indicating high intensity.

Statistical analysis

Data are reported as the mean ± standard deviation of the mean unless stated otherwise. Statistical differences between experimental variables were assessed by statistical analysis using One Way ANOVA with a Tukey HSD Post Hoc. P values < 0.05 were considered significant.

6.6 Acknowledgements

This study was supported by a NSF CAREER Award. The authors would like to thank Christopher Baddick for his technical assistance. Human MSCs were obtained from the Texas A&M Health Science Center College of Medicine Institute for Regenerative Medicine at Scott & White through a grant from NCRR of the NIH, Grant #P40RR017447. The type X collagen monoclonal antibody developed by Thomas F. Linsenmayer was obtained from the Developmental Studies Hybridoma Bank developed under the auspices of the NICHD and maintained by The University of Iowa. Confocal microscopy was performed at the Nanomaterials Characterization Facility at the University of Colorado.

6.7 References

[1] Moffat KL, Sun WH, Pena PE, Chahine NO, Doty SB, Ateshian GA, Hung CT, Lu HH. Characterization of the structure-function relationship at the ligament-to-bone interface. Proceedings of the National Academy of Sciences of the United States of America 2008;105:7947.

[2] Martin RB, Burr DB, Sharkey NA. Skeletal Tissue Mechanics. New York: Springer, 1998.

[3] AufderHeide AC, Athanasiou KA. Mechanical stimulation toward tissue engineering of the knee meniscus. Ann Biomed Eng 2004;32:1161.

[4] Imbeni V, Kruzic JJ, Marshall GW, Marshall SJ, Ritchie RO. The dentin-enamel junction and the fracture of human teeth. Nature materials 2005;4:229.

[5] Sahoo S, Teh T, He P, Toh S, Goh J. Interface Tissue Engineering: Next Phase in Musculoskeletal Repair Annals, Academy of Medicine, Singapore 2011;40:245.

[6] Lu HH, Subramony SD, Boushell MK, Zhang XZ. Tissue Engineering Strategies for the Regeneration of Orthopedic Interfaces. Ann Biomed Eng 2010;38:2142.

[7] Kon E, Delcogliano M, Filardo G, Pressato D, Busacca M, Grigolo B, Desando G, Marcacci M. A novel nano-composite multi-layered biomaterial for treatment of osteochondral lesions: Technique note and an early stability pilot clinical trial. Injury-International Journal of the Care of the Injured 2010;41:778.

[8] Yilgor P, Sousa RA, Reis RL, Hasirci N, Hasirci V. Effect of scaffold architecture and BMP-2/BMP-7 delivery on in vitro bone regeneration. J. Mater. Sci.-Mater. Med. 2010;21:2999.

[9] Wang XQ, Wenk E, Zhang XH, Meinel L, Vunjak-Novakovic G, Kaplan DL. Growth factor gradients via microsphere delivery in biopolymer scaffolds for osteochondral tissue engineering. J Control Release 2009;134:81.

[10] Jiang J, Tang A, Ateshian GA, Guo XE, Hung CT, Lu HH. Bioactive Stratified Polymer Ceramic-Hydrogel Scaffold for Integrative Osteochondral Repair. Ann Biomed Eng 2010;38:2183.

[11] Lee J, Il Choi W, Tae G, Kim YH, Kang SS, Kim SE, Kim SH, Jung Y. Enhanced regeneration of the ligament-bone interface using a poly(L-lactide-co-epsilon-caprolactone) scaffold with local delivery of cells/BMP-2 using a heparin-based hydrogel. Acta Biomaterialia 2011;7:244.

[12] Park CH, Rios HF, Jin QM, Bland ME, Flanagan CL, Hollister SJ, Giannobile WV. Biomimetic hybrid scaffolds for engineering human tooth-ligament interfaces. Biomaterials 2010;31:5945.

[13] Hammoudi TM, Lu H, Temenoff JS. Long-Term Spatially Defined Coculture Within Three-Dimensional Photopatterned Hydrogels. Tissue Engineering Part C-Methods 2010;16:1621.

[14] Schaefer D, Martin I, Shastri P, Padera RF, Langer R, Freed LE, Vunjak-Novakovic G. In vitro generation of osteochondral composites. Biomaterials 2000;21:2599.

[15] Sherwood JK, Riley SL, Palazzolo R, Brown SC, Monkhouse DC, Coates M, Griffith LG, Landeen LK, Ratcliffe A. A three-dimensional osteochondral composite scaffold for articular cartilage repair. Biomaterials 2002;23:4739.

[16] Jiang CC, Chiang H, Liao CJ, Lin YJ, Kuo TF, Shieh CS, Huang YY, Tuan RS. Repair of porcine articular cartilage defect with a biphasic osteochondral composite. J. Orthop. Res. 2007;25:1277.

[17] Lima EG, Mauck RL, Han SH, Park S, Ng KW, Ateshian GA, Hung CT. Functional tissue engineering of chondral and osteochondral constructs. Biorheology 2004;41:577.

[18] Hung CT, Lima EG, Mauck RL, Taki E, LeRoux MA, Lu HH, Stark RG, Guo XE, Ateshian GA. Anatomically shaped osteochondral constructs for articular cartilage repair. J Biomech 2003;36:1853.

[19] Lima EG, Chao PHG, Ateshian GA, Bal BS, Cook JL, Vunjak-Novakovic G, Hung CT. The effect of devitalized trabecular bone on the formation of osteochondral tissue-engineered constructs. Biomaterials 2008;29:4292.

[20] Holland TA, Bodde EWH, Baggett LS, Tabata Y, Mikos AG, Jansen JA. Osteochondral repair in the rabbit model utilizing bilayered, degradable oligo(poly(ethylene glycol) fumarate) hydrogel scaffolds. Journal of Biomedical Materials Research Part A 2005;75A:156.

[21] Liu C, Xia Z, Czernuszka JT. Design and development of three-dimensional scaffolds for tissue engineering. Chem. Eng. Res. Des. 2007;85:1051.

[22] Harley BA, Lynn AK, Wissner-Gross Z, Bonfield W, Yannas IV, Gibson LJ. Design of a multiphase osteochondral scaffold III: Fabrication of layered scaffolds with continuous interfaces. Journal of Biomedical Materials Research Part A 2010;92A:1078.

[23] Kelly DJ, Prendergast PJ. Prediction of the optimal mechanical properties for a scaffold used in osteochondral defect repair. Tissue Eng 2006;12:2509.

[24] McMahon LA, Reid AJ, Campbell VA, Prendergast PJ. Regulatory effects of mechanical strain on the chondrogenic differentiation of MSCs in a collagen-GAG scaffold: Experimental and computational analysis. Ann Biomed Eng 2008;36:185.

[25] Marenzana M, Kelly DJ, Prendergast PJ, Brown RA. A collagen-based interface construct for the assessment of cell-dependent mechanical integration of tissue surfaces. Cell Tissue Res. 2007;327:293.

[26] Bryant SJ, Arthur JA, Anseth KS. Incorporation of tissue-specific molecules alters chondrocyte metabolism and gene expression in photocrosslinked hydrogels. Acta Biomaterialia 2005;1:243.

[27] Mann BK, Schmedlen RH, West JL. Tethered-TGF-beta increases extracellular matrix production of vascular smooth muscle cells. Biomaterials 2001;22:439.

[28] Qiu YZ, Lim JJ, Scott L, Adams RC, Bui HT, Temenoff JS. PEG-based hydrogels with tunable degradation characteristics to control delivery of marrow stromal cells for tendon overuse injuries. Acta Biomaterialia 2011;7:959.

[29] Felson DT, Zhang YQ. An update on the epidemiology of knee and hip osteoarthritis with a view to prevention. Arthritis Rheum 1998;41:1343.

[30] O'shea TM, Miao XG. Bilayered Scaffolds for Osteochondral Tissue Engineering. Tissue Eng. Part B-Rev. 2008;14:447.

[31] Mente PL, Lewis JL. Elastic modulus of calcified cartilage is an order of magnitued less than that of subchondral bone. J. Orthop. Res. 1994;12:637.

[32] Mansour JM. Biomechanics of Cartilage. In: C.A.Oate, editor. Kinesiology: The Mechanics and Pathomechanics of Human Movemen. Philadelphia: Lippincott Williams and Wilkins, 2003.

[33] Eckstein F, Tieschky M, Faber S, Englmeier KH, Reiser M. Functional analysis of articular cartilage deformation, recovery, and fluid flow following dynamic exercise in vivo. Anatomy and Embryology 1999;200:419.

[34] Burr DB, Milgrom C, Fyhrie D, Forwood M, Nyska M, Finestone A, Hoshaw S, Saiag E, Simkin A. In vivo measurement of human tibial strains during vigorous activity. Bone 1996;18:405.

[35] Rubin CT. Skeletal strain and the functional significance of bone architechture. Calcified Tissue International 1984;36:S11.

[36] Gardner-Morse MG, Tacy NJ, Beynnon BD, Roemhildt ML. In Situ Microindentation for Determining Local Subchondral Bone Compressive Modulus. J Biomech Eng-T Asme 2010;132.

[37] Ethier CR, Simmons CA. Introductory Biomechanics - From Cells to Organisms. Cambridge University Press.

[38] Claes LE, Heigele CA. Magnitudes of local stress and strain along bony surfaces predict the course and type of fracture healing. J Biomech 1999;32:255.

[39] Palomares KTS, Gleason RE, Mason ZD, Cullinane DM, Einhorn TA, Gerstenfeld LC, Morgan EF. Mechanical Stimulation Alters Tissue Differentiation and Molecular Expression during Bone Healing. J. Orthop. Res. 2009;27:1123.

[40] Wang FY, Ying Z, Duan XJ, Tan HB, Yang B, Guo L, Chen GX, Dai G, Ma Z, Yang L. Histomorphometric analysis of adult articular calcified cartilage zone. Journal of Structural Biology 2009;168:359.

[41] Clifford R. Wheeless III M. Wheeless' Textbook of Orthopaedics. In: Clifford R. Wheeless III M, editor. Articular Cartilage. Durham, NC: Data Trace Internet Publishing, LLC, 2011.

[42] Bollet AJ, Sturgill BC, Handy JR. Chondroitin sulfate concentration and protein polysaccharide composition of articular cartilage in osteoarthritis. Journal of Clinical Investigation 1963;42:853.

[43] Varghese S, Hwang NS, Canver AC, Theprungsirikul P, Lin DW, Elisseeff J. Chondroitin sulfate based niches for chondrogenic differentiation of mesenchymal stem cells. Matrix Biology 2008;27:12.

[44] Helfrich MH, Nesbitt SA, Dorey EL, Horton MA. Rat osteoclasts adhere to a wide range of RGD (ARG-GLY-ASP) peptide containing proteins, indluding the bone sialoproteins and fibronectin, via A beta-3 integrin. Journal of Bone and Mineral Research 1992;7:335.

[45] Nuttelman CR, Tripodi MC, Anseth KS. Synthetic hydrogel niches that promote hMSC viability. Matrix Biology 2005;24:208.

[46] Huebsch N, Arany PR, Mao AS, Shvartsman D, Ali OA, Bencherif SA, Rivera-Feliciano J, Mooney DJ. Harnessing traction-mediated manipulation of the cell/matrix interface to control stem-cell fate. Nature materials 2010;9:518.

[47] Bayliss MT, Osborne D, Woodhouse S, Davidson C. Sulfation of chondroitin sulfate in human articular cartilage - The effect of age, topographical position, and zone of cartilage on tissue composition. J. Biol. Chem. 1999;274:15892.

[48] Salinas CN, Anseth KS. The enhancement of chondrogenic differentiation of human mesenchymal stem cells by enzymatically regulated RGD functionalities. Biomaterials 2008;29:2370.

[49] Steinmetz NJ, Bryant SJ. The Effects of Intermittent Dynamic Loading on Chondrogenic and Osteogenic Differentiation of Human Marrow Stromal Cells Encapsulated in RGD Modified PEG Hydrogels Acta Biomaterialia 2011;7:3829.

[50] Nguyen LH, Kudva AK, Saxena NS, Roy K. Engineering articular cartilage with spatially-varying matrix composition and mechanical properties from a single stem cell population using a multi-layered hydrogel. Biomaterials 2011;32:6946.

[51] Chahine NO, Albro MB, Lima EG, Wei VI, Dubois CR, Hung CT, Ateshian GA. Effect of Dynamic Loading on the Transport of Solutes into Agarose Hydrogels. Biophysical Journal 2009;97:968.

[52] Guo X, Park H, Liu GP, Liu W, Cao YL, Tabata Y, Kasper FK, Mikos AG. In vitro generation of an osteochondral construct using injectable hydrogel composites encapsulating rabbit marrow mesenchymal stem cells. Biomaterials 2009;30:2741.

[53] Appelman TP, Mizrahi J, Seliktar D. A Finite Element Model of Cell-Matrix Interactions to Study the Differential Effect of Scaffold Composition on Chondrogenic Response to Mechanical Stimulation. J Biomech Eng-T Asme 2011;133.

[54] Park S, Hung CT, Ateshian GA. Mechanical response of bovine articular cartilage under dynamic unconfined compression loading at physiological stress levels. Osteoarthritis Cartilage 2004;12:65.

[55] Tate MLK, Falls TD, McBride SH, Atit R, Knothe UR. Mechanical modulation of osteochondroprogenitor cell fate. International Journal of Biochemistry & Cell Biology 2008;40:2720.

[56] Lin-Gibson S, Bencherif S, Cooper JA, Wetzel SJ, Antonucci JM, Vogel BM, Horkay F, Washburn NR. Synthesis and characterization of PEG dimethacrylates and their hydrogels. Biomacromolecules 2004;5:1280.

[57] Villanueva I, Gladem SK, Kessler J, Bryant SJ. Dynamic loading stimulates chondrocyte biosynthesis when encapsulated in charged hydrogels prepared from poly(ethylene glycol) and chondroitin sulfate. Matrix Biology 2010;29:51.

[58] Bryant SJ, Davis-Arehart KA, Luo N, Shoemaker RK, Arthur JA, Anseth KS. Synthesis and characterization of photopolymerized multifunctional hydrogels: Water-soluble poly(vinyl alcohol) and chondroitin sulfate macromers for chondrocyte encapsulation. Macromolecules 2004;37:6726.

[59] Roberts JJ, Earnshaw A, Ferguson VL, Bryant SJ. Comparative study of the viscoelastic mechanical behavior of agarose and poly(ethylene glycol) hydrogels. Journal of Biomedical Materials Research Part B-Applied Biomaterials 2011;99B:158.

[60] Barbosa I, Garcia S, Barbier-Chassefiere V, Caruelle JP, Martelly I, Papy-Garcia D. Improved and simple micro assay for sulfated glycosaminoglycans quantification in biological extracts and its use in skin and muscle tissue studies. Glycobiology 2003;13:647.

[61] Boyce MC, Arruda EM. Constitutive models of rubber elasticity: A review. Rubber Chem Technol 2000;73:504.

[62] Knight MM, Ghori SA, Lee DA, Bader DL. Measurement of the deformation of isolated chondrocytes in agarose subjected to cyclic compression. Medical Engineering & Physics 1998;20:684.

[63] Nicodemus GD, Bryant SJ. The role of hydrogel structure and dynamic loading on chondrocyte gene expression and matrix formation. J Biomech 2008;41:1528.

[64] Villanueva I, Hauschulz DS, Mejic D, Bryant SJ. Static and dynamic compressive strains influence nitric oxide production and chondrocyte bioactivity when encapsulated in PEG hydrogels of different crosslinking densities. Osteoarthritis Cartilage 2008;16:909.

Chapter 7

Conclusions and Future Work

The thesis work detailed in chapters three through six test the overarching hypothesis that spatially controlling biomechanical and biochemical cues within a multi-layered hydrogel leads to a layer of cartilage-like, a layer of bone-like, and an interfacial layer of osteochondral-like extracellular matrix deposition by encapsulated hMSCs. Taken together, the studies presented here further advance our understanding of how human MSCs behave in response to both biochemical and biomechanical cues which is important for the continued development of a tissue engineering scaffold capable of concomitantly and spatially guiding the differentiation of a single undifferentiated cell source down multiple lineages towards the development of a feasible osteochondral tissue engineering strategy.

When we, as scientists, grossly simplify a complicated, and not fully understood process that takes place within the body by conducting simplified and controlled *in vitro* studies, we aim to better understand the individual contributions of the complicated processes that take place *in vivo*. While it may not be possible to include every cue or combination of cues that takes place in a particular local environment within the body, research efforts can be made to include those that are certain to be present. As such, the work in this thesis aims to gain a better understanding of both biochemical and biomechanical cues as well as the combination of the two given that these cues are inextricably linked and ever present in the body. With the ultimate, long term, goal of developing a mechanically functional osteochondral tissue, it is critically important to consider both of these types of cues throughout the research process.

The first objective of this study gave insight into the impact of physiological intermittent dynamic loading on hMSCs in PEG based hydrogels. Previous work in the field had demonstrated that PEG based hydrogels were suitable scaffolds for directing both chondrogenic and osteogenic differentiation of human MSCs. In this study, the combined effect of the cues from the scaffold and the biomechanical cues imparted on the cells was examined.

The findings indicated that in an RGD modified PEG system, with relatively weak hydrogels (stiffness estimated at ~40 kPa), a relatively large compressive loading regime (15%) applied at the onset of differentiation inhibits chondrogenesis and osteogenesis of hMSCs. This inhibition was demonstrated through both qRT-PCR and through (immuno)histological investigation of chondrogenic and osteogenic ECM matrix molecule expression. These findings were consistent with similar studies in the literature while contradictory to others (all for either different scaffold types, different MSC sources, or both). The goal of this particular study was not to establish an "ideal" loading regime, as the compilation of studies in the literature suggest that this may be something that is different for each type of scaffold and more importantly for each species and age of MSC utilized, but rather to contribute to our understanding of how the biomechanical cues acting on hMSCs in PEG based scaffolds, which will be used throughout this thesis work, affect the differentiation potential and ECM molecule synthesis of these cells.

These findings lead us to employ a delayed loading regime for the remainder of the chondrogenic loading studies in this thesis with the hypothesis that a delaying the loading would potentially allow the hMSCs a chance to begin chondrogenically differentiating before applying the strain. Additionally, further studies incorporating osteogenically differentiating cells were not subjected to dynamic loading based on the inhibitory results of this study combined with the fact that bone cells in the body experience very small strains (<1%), which would be difficult to

implement in a controlled, repeatable manner. In future studies, a basic screening study of ECM molecule production by hMSCs over a range of physiological loading conditions applied during chondrogenic differentiation should be completed to establish if there is a loading condition that does not inhibit chondrogenesis in these PEG systems with hMSCs.

With the ultimate goal of designing scaffold materials suitable for use in the cartilage and bone layers of a multi-layer osteochondral scaffold, modification of the bioinert PEG based scaffolds with tissue specific biomimetic molecules was investigated. Objectives 2 and 3 have similar goals but are directed down two different differentiation pathways. Objective 2 incorporates a cartilage specific ECM moiety, chondroitin sulfate, into the PEG based hydrogels, and Objective 3 incorporates P-15, a collagen I peptide analog into the PEG based hydrogels with the goal of investigating the behavior of the hMSCS in more biomimetic systems.

The research from the second objective gave insight into how hMSCs would respond in a more native cartilage-like environment. Previous work in the field using goat MSCs suggested that this type of system would direct MSCs down a collagen II producing articular cartilage lineage. However, the ChS modified system employed in this study did support chondrogenesis, although it appeared to enhance the terminal differentiation of human MSCs towards the hypertrophic lineage. They hypertrophic lineage was evident from the early expression of the hypertrophic cartilage specific collagen X and aggrecan as well as enhanced production of collagen I, although collagen II was detected after 2 weeks. When delayed loading was applied to this system, the terminal differentiation marker (collagen X) was unaffected whereas the articular cartilage marker (collagen II) was no longer detected. Although the original aim was to enhance articular cartilage chondrogenesis with this system, the system still holds great promise for use in the multi-layer system where a layer of hMSCS going down the terminally

differentiating hypertrophic lineage are also required. It has been proposed in the literature that encapsulated MSCs that begin chondrogenically differentiating will start producing chondroitinase that can begin to degrade the ChS modified PEG hydrogel systems. Future studies in the area of this objective should include longer duration studies to investigate whether this system, if it does in fact become degradable, would then enhance the articular cartilage lineage of human MSCs. Additionally, thought should be given to the type of chondroitin sulfate used (chondroitin-4-sulfate vs. chondroitin-6-sulfate) as it has been suggested that chondroitin-4-sulfate binds free calcium ions (chondroitin-6-sulfate does not) and could serve as a nucleation site if phosphate ions are present in the media, which may not be beneficial for enhancing the articular cartilage lineage.

While collagen I is the most predominant collagen in the body, found in many tissue types, it is also the primary collagen in bone. In Objective 3, we incorporated a collagen I peptide, previously shown to bind hMSCs, into our PEG system to create a more bone-like environment. The results from the 2D cell attachment portion of this study demonstrated that P-15 promotes attachment of hMSCs, and there was evidence that it could direct hMSCs down on osteogenic lineage, in the absence of osteogenic differentiation cues, based on the expression of osteonectin, a bone specific protein known to initiate mineralization. However, when studies were conducted in 3D, the effect of the P-15 was unclear. P-15 modified PEG hydrogels did not significantly improve the viability of encapsulated hMSCs over unmodified PEG hydrogels, and there was not a measureable difference in the production of the osteogenic biomarker molecules (e.g. alkaline phosphatase and calcium) investigated. Although the P-15 system investigated in this thesis did not appear to enhance osteogenesis of hMSCs in 3D, the positive results obtained in 2D combined with the reports in the literature of enhanced osteogenesis with this peptide warrant

additional investigation into the inclusion of P-15 within the bone-like layer of the multi-layer osteochondral scaffold design. It is possible that the P-15 alone does not provide a strong enough cell binding interaction in the 3D system. Another area that would be interesting to investigate would be whether the combined effect of an RGD/P-15 modified system would enhance the osteogenic potential of hMSCs over an RGD system alone.

Additionally, while chondrogenic differentiation of MSCs in cell culture takes place in a 3D pellet culture environment, osteogenic differentiation of MSCs takes place in 2D, allowing the cells to remain attached and spread on a surface. Bearing this in mind, future studies with P-15 may benefit from creating a "local" 2D environment within the 3D PEG hydrogels in which the hMSCs can interact with the P-15 in a spread morphology, rather than the rounded morphology typically adopted in the 3D hydrogel environment. This could be accomplished by incorporating anorganic bone matrix (ABM) particles modified with P-15 into the PEG hydrogels where the ABM particles would serve as a "local" 2D environment on which the hMSCs could attach and spread as well as a surface on which to present the P-15 peptide. Given the low viability observed for osteogenically differentiating hMSCs, incorporating this "local" 2D environment may also help to enhance the cell viability. One could easily envision utilizing a biomaterial that incorporates ABM particles as the bone-like layer in the design of an osteochondral multi-layer hydrogel, as the AMB particles may also enhance the mechanical properties of the PEG hydrogels.

Objective 4 was the culminating objective for this thesis: the engineering approach to applying the basic science knowledge gained in the previous objectives. Given that the "ideal" biomaterials to use in the bone-like and cartilage-like layers were not elucidated in Objectives 2 and 3, the focus of this objective was largely on fabricating a multi-layer hydrogel capable of

imparting spatially controlled biochemical and mechanical cues with aim of property-function characterization as the focus. Finite element analysis (FEA) was used to guide the design of the spatially controlled mechanical properties within the layers. The model developed was verified with experimental results, proving that the model is a useful tool that can be used to guide the design of future scaffolds. Based on the results from the previous objectives combined with the information from the model, we demonstrated a proof of concept where we could differentially affect encapsulated hMSCs via spatially controlled biochemical and biomechanical cues. A multi-layer hydrogel was designed and fabricated that contained a stiff RGD/PEG layer as the bone-like layer and a compliant ChS/PEG layer as the cartilage-like layer. Due to the nature of the fabrication process, a third, interfacial layer was formed between the cartilage-like and bone-like layers which contained both RGD and ChS. When undifferentiated hMSCs were encapsulated in these multi-layered hydrogels and cultured under free swelling or subjected to dynamic loading in osteochondral differentiation medium, the spatial presentation of biochemical and mechanical cues gave rise to characteristically different cartilage and bone protein expressions in hMSCs in each layer. This demonstrates that the property-function relationships that arise in a multi-layered scaffold with distinctly varied biochemical and mechanical properties influence the local strains sensed by the cells and differentially affect the fate of encapsulated undifferentiated hMSCs.

The main aim of this thesis was to develop a multi-layer scaffold capable of providing spatially controlled biochemical and biomechanical cues that when combined with inextricably linked external physiological biomechanical cues would differentially impact the behavior of a single encapsulated cell source towards the goal of developing an osteochondral tissue engineering strategy. Although the culminating multi-layer scaffold designed in this study did

not lead to spatially organized deposition of ECM molecules specific to a cartilage-like, osteochondral interface-like, and bone-like layer, it was possible to differentially and spatially affect the ECM molecule expression of encapsulated hMSCs within the multi-layered scaffold. The design, fabrication, and characterization process developed in Objective 4 of this thesis provides invaluable insight on which to build the next "generation" of the multi-layer hydrogel. Once PEG based cartilage-like and bone-like biomaterials capable of independently enhancing chondrogenesis and osteogenesis, respectively, are elucidated, it will be relatively simple to apply the basic tools developed in this last objective to designing a multi-layer scaffold capable of spatially directing the production of osteochondral ECM molecules. Additionally, future osteochondral scaffold designs should take the highly irregular subchondral bone surface and the interdigitation between the calcified cartilage zone and the non-calcified cartilage zone into consideration. This work not only expands our understanding of how human MSCs behave in a variety of tissue engineering environments, but it provides an excellent foundation on which to further develop multi-functional, multi-layer scaffolds towards the development of a feasible osteochondral tissue engineering strategy.

Chapter 8

Bibliography

8.1 Chapter 1 references

[1] Bullough PG. Histology for Pathologists, 3rd Edition In: Mills SE, editor. Philladelphia, PA: Lippincott Williams & Wilkins 2007.

[2] Hunter DJ. Osteoarthritis Preface. Clinics in Geriatric Medicine 2010;26:Xi.

[3] Losina E, Walensky RP, Reichmann WM, Holt HL, Gerlovin H, Solomon DH, Jordan JM, Hunter DJ, Suter LG, Weinstein AM, Paltiel AD, Katz JN. Impact of Obesity and Knee Osteoarthritis on Morbidity and Mortality in Older Americans. Ann. Intern. Med. 2011;154:217.

[4] Kyriacos A. Athanasiou EMD, Jerry C. Hu. Articular Cartilage Tissue Engineering. Kyriacos A. Athanasiou, editor. Synthesis Lectures on Tissue Engineering. electronic: Morgan & Claypool, 2010. p.182.

[5] X. Wang JSN, X. Dong, H. Leng, M. Reyes. Fundamental Biomechanics in Bone Tissue Engineering. In: Kyriacos A. Athanasiou JKL, editor. Synthesis Lectures on Tissue Engineering: Morgan & Claypool Publishers, 2010.

[6] Aszodi A, Hunziker EB, Olsen BR, Fassler R. The role of collagen II and cartilage fibril-associated molecules in skeletal development. Osteoarthritis Cartilage 2001;9:S150.

[7] Johnstone B, Hering TM, Caplan AI, Goldberg VM, Yoo JU. In vitro chondrogenesis of bone marrow-derived mesenchymal progenitor cells. Exp. Cell Res. 1998;238:265.

[8] Burr DB. Anatomy and physiology of the mineralized tissues: roles in the pathogenesis of osteoarthritis. Osteoarthritis Cartilage 2004;12:S20.

[9] Oegema TR, Carpenter RJ, Hofmeister F, Thompson RC. The interaction of the zone of calcified cartilage and subchondral bone in osteoarthritis. Microscopy Research and Technique 1997;37:324.

[10] Kress BC. Bone alkaline phosphatase: Methods of quantitation and clinical utility. Journal of Clinical Ligand Assay 1998;21:139.

[11] Termine JD, Kleinman HK, Whitson SW, Conn KM, McGarvey ML, Martin GR. Osteonectin, a bone-specific protein linking mineral to collagen. Cell 1981;26:99.

[12] Partial Knee Resurfacing. 2011.

[13] Mirzayan R. Cartilage Injury in the Athlete. New York, NY: Thieme Medical Publishers, 2006.

[14] Mithoefer K, Williams RJ, Warren RF, Wickiewicz TL, Marx RG. High-impact athletics after knee articular cartilage repair: a prospective evaluation of the microfracture technique. The American journal of sports medicine 2006;34:1413.

[15] Simon H Palmer MMJC, MBBS, FRACS. Total Knee Arthroplasty. WebMD, Sep 21, 2010.

[16] Friess W, Uludag H, Foskett S, Biron R. Bone regeneration with recombinant human bone morphogenetic protein-2 (rhBMP-2) using absorbable collagen sponges (ACS): Influence of processing on ACS characteristics and formulation. Pharmaceutical Development and Technology 1999;4:387.

[17] Geiger M, Li RH, Friess W. Collagen sponges for bone regeneration with rhBMP-2. Advanced Drug Delivery Reviews 2003;55:1613.

[18] Paletta GA, Arnoczky SP, Warren RF. The Repair of Osteochondral Defects Using an Exogenous Fibrin Clot - an Experimental-Study in Dogs. American Journal of Sports Medicine 1992;20:725.

[19] Lenas P, Luyten FP. An Emerging Paradigm in Tissue Engineering: From Chemical Engineering to Developmental Engineering for Bioartificial Tissue Formation through a Series of Unit Operations that Simulate the In Vivo Successive Developmental Stages. Industrial & Engineering Chemistry Research 2011;50:482.

[20] Caplan AI. Mesenchymal stem cells. J. Orthop. Res. 1991;9:641.

[21] Pittenger MF, Mackay AM, Beck SC, Jaiswal RK, Douglas R, Mosca JD, Moorman MA, Simonetti DW, Craig S, Marshak DR. Multilineage potential of adult human mesenchymal stem cells. Science 1999;284:143.

[22] Yoo JU, Barthel TS, Nishimura K, Solchaga L, Caplan AI, Goldberg VM, Johnstone B. The chondrogenic potential of human bone-marrow-derived mesenchymal progenitor cells. J Bone Joint Surg Am 1998;80A:1745.

[23] Richardson SM, Hoyland JA, Mobasheri R, Csaki C, Shakibaei M, Mobasheri A. Mesenchymal Stem Cells in Regenerative Medicine: Opportunities and Challenges for Articular Cartilage and Intervertebral Disc Tissue Engineering. J. Cell. Physiol. 2010;222:23.

[24] Bruder SP, Fink DJ, Caplan AI. Mesenchymal stem cells in bone development, bone repair, and skeletal regeneration therapy. Journal of Cellular Biochemistry 1994;56:283.

[25] Otto WR, Rao J. Tomorrow's skeleton staff: mesenchymal stem cells and the repair of bone and cartilage. Cell Proliferation 2004;37:97.

[26] Gimble JM, Guilak F, Nuttall ME, Sathishkumar S, Vidal M, Bunnell BA. In vitro differentiation potential of mesenchymal stem cells. Transfusion Medicine and Hemotherapy 2008;35:228.

[27] Bruder SP, Jaiswal N, Ricalton NS, Mosca JD, Kraus KH, Kadiyala S. Mesenchymal stem cells in osteobiology and applied bone regeneration. Clinical Orthopaedics and Related Research 1998:S247.

[28] Huang CYC, Hagar KL, Frost LE, Sun YB, Cheung HS. Effects of cyclic compressive loading on chondrogenesis of rabbit bone-marrow derived mesenchymal stem cells. Stem Cells 2004;22:313.

[29] Campbell JJ, Lee DA, Bader DL. Dynamic compressive strain influences chondrogenic gene expression in human mesenchymal stem cells. Biorheology 2006;43:455.

[30] Terraciano V, Hwang N, Moroni L, Park HB, Zhang Z, Mizrahi J, Seliktar D, Elisseeff J. Differential response of adult and embryonic mesenchymal progenitor cells to mechanical compression in hydrogels. Stem Cells 2007;25:2730.

[31] Bosnakovski D, Mizuno M, Kim G, Ishiguro T, Okumura M, Iwanaga T, Kadosawa T, Fujinaga T. Chondrogenic differentiation of bovine bone marrow mesenchymal stem cells in pellet cultural system. Experimental Hematology 2004;32:502.

[32] Kisiday JD, Frisbie DD, McIlwraith CW, Grodzinsky AJ. Dynamic Compression Stimulates Proteoglycan Synthesis by Mesenchymal Stem Cells in the Absence of Chondrogenic Cytokines. Tissue Engineering Part A 2009;15:2817.

[33] Oliveira JM, Rodrigues MT, Silva SS, Malafaya PB, Gomes ME, Viegas CA, Dias IR, Azevedo JT, Mano JF, Reis RL. Novel hydroxyapatite/chitosan bilayered scaffold for osteochondral tissue-engineering applications: Scaffold design and its performance when seeded with goat bone marrow stromal cells. Biomaterials 2006;27:6123.

[34] Venugopal J, Prabhakaran MP, Zhang YZ, Low S, Choon AT, Ramakrishna S. Biomimetic hydroxyapatite-containing composite nanofibrous substrates for bone tissue engineering. Philos. Trans. R. Soc. A-Math. Phys. Eng. Sci. 2010;368:2065.

[35] Yoshikawa H, Tamai N, Murase T, Myoui A. Interconnected porous hydroxyapatite ceramics for bone tissue engineering. J. R. Soc. Interface 2009;6:S341.

[36] Mauck RL, Soltz MA, Wang CCB, Wong DD, Chao PHG, Valhmu WB, Hung CT, Ateshian GA. Functional tissue engineering of articular cartilage through dynamic loading of chondrocyte-seeded agarose gels. J Biomech Eng-T Asme 2000;122:252.

[37] Connelly JT, Garcia AJ, Levenston ME. Inhibition of in vitro chondrogenesis in RGD-modified three-dimensional alginate gels. Biomaterials 2007;28:1071.

[38] Bryant SJ, Anseth KS. Controlling the spatial distribution of ECM components in degradable PEG hydrogels for tissue engineering cartilage. Journal of Biomedical Materials Research Part A 2003;64A:70.
[39] Bouhadir KH, Hausman DS, Mooney DJ. Synthesis of cross-linked poly(aldehyde guluronate) hydrogels. Polymer 1999;40:3575.

[40] Martens P, Anseth KS. Characterization of hydrogels formed from acrylate modified poly(vinyl alcohol) macromers. Polymer 2000;41:7715.

[41] Drury JL, Mooney DJ. Hydrogels for tissue engineering: scaffold design variables and applications. Biomaterials 2003;24:4337.

[42] Liu SQ, Tay R, Khan M, Ee PLR, Hedrick JL, Yang YY. Synthetic hydrogels for controlled stem cell differentiation. Soft Matter 2010;6:67.

[43] Bryant SJ, Anseth KS, Lee DA, Bader DL. Crosslinking density influences the morphology of chondrocytes photoencapsulated in PEG hydrogels during the application of compressive strain. J. Orthop. Res. 2004;22:1143.

[44] Bryant SJ, Anseth, K. S. . Photopolymerization of Hydogel Scaffolds.69.

[45] Bryant SJ, Anseth KS. Hydrogel properties influence ECM production by chondrocytes photoencapsulated in poly(ethylene glycol) hydrogels. Journal of Biomedical Materials Research 2002;59:63.

[46] Anseth KS, Metters AT, Bryant SJ, Martens PJ, Elisseeff JH, Bowman CN. In situ forming degradable networks and their application in tissue engineering and drug delivery. J Control Release 2002;78:199.

[47] Hern DL, Hubbell JA. Incorporation of adhesion peptides into nonadhesive hydrogels useful for tissue resurfacing. Journal of Biomedical Materials Research 1998;39:266.

[48] Zhu JM. Bioactive modification of poly(ethylene glycol) hydrogels for tissue engineering. Biomaterials 2010;31:4639.

[49] Ho STB, Cool SM, Hui JH, Hutmacher DW. The influence of fibrin based hydrogels on the chondrogenic differentiation of human bone marrow stromal cells. Biomaterials 2010;31:38.

[50] Zhou XZ, Leung VY, Dong QR, Cheung KM, Chan D, Lu WW. Mesenchymal stem cell-based repair of articular cartilage with polyglycolic acid-hydroxyapatite biphasic scaffold. International Journal of Artificial Organs 2008;31:480.

[51] Wang W, Li B, Yang JZ, Xin L, Li YL, Yin HP, Qi YY, Jiang YZ, Ouyang HW, Gao CY. The restoration of full-thickness cartilage defects with BMSCs and TGF-beta 1 loaded PLGA/fibrin gel constructs. Biomaterials 2010;31:8964.

[52] Tampieri A, Sandri M, Landi E, Pressato D, Francioli S, Quarto R, Martin I. Design of graded biomimetic osteochondral composite scaffolds. Biomaterials 2008;29:3539.

[53] Noth U, Rackwitz L, Heymer A, Weber M, Baumann B, Steinert A, Schutze N, Jakob F, Eulert J. Chondrogenic differentiation of human mesenchymal stem cells in collagen type I hydrogels. Journal of Biomedical Materials Research Part A 2007;83A:626.

[54] Bhatnagar RS, Qian JJ, Wedrychowska A, Sadeghi M, Wu YM, Smith N. Design of biomimetic habitats for tissue engineering with P-15, a synthetic peptide analogue of collagen. Tissue Eng 1999;5:53.

[55] Bikle DD, Halloran BP. The response of bone to unloading. Journal of Bone and Mineral Metabolism 1999;17:233.

[56] Skerry TM. The response of bone to mechanical loading and disuse: Fundamental principles and influences on osteoblast/osteocyte homeostasis. Archives of Biochemistry and Biophysics 2008;473:117.

[57] Mullender M, El Haj AJ, Yang Y, van Duin MA, Burger EH, Klein-Nulend J. Mechanotransduction of bone cells in vitro: mechanobiology of bone tissue. Medical & Biological Engineering & Computing 2004;42:14.

[58] Sandell LJ, Aigner T. Articular cartilage and changes in arthritis - An introduction: Cell biology of osteoarthritis. Arthritis Research 2001;3:107.

[59] Temenoff JS, Park H, Jabbari E, Conway DE, Sheffield TL, Ambrose CG, Mikos AG. Thermally cross-linked oligo(poly(ethylene glycol) fumarate) hydrogels support osteogenic differentiation of encapsulated marrow stromal cells in vitro. Biomacromolecules 2004;5:5.

[60] Nuttelman CR, Tripodi MC, Anseth KS. In vitro osteogenic differentiation of human mesenchymal stem cells photoencapsulated in PEG hydrogels. Journal of Biomedical Materials Research Part A 2004;68A:773.

[61] Mauck RL, Yuan X, Tuan RS. Chondrogenic differentiation and functional maturation of bovine mesenchymal stem cells in long-term agarose culture. Osteoarthritis Cartilage 2006;14:179.

[62] Engler AJ, Sen S, Sweeney HL, Discher DE. Matrix elasticity directs stem cell lineage specification. Cell 2006;126:677.

[63] Thorpe SD, Buckley CT, Vinardell T, O'Brien FJ, Campbell VA, Kelly DJ. Dynamic compression can inhibit chondrogenesis of mesenchymal stem cells. Biochemical and Biophysical Research Communications 2008;377:458.

[64] Qi MC, Hu J, Zou SJ, Chen HQ, Zhou HX, Han LC. Mechanical strain induces osteogenic differentiation: Cbfa1 and Ets-1 expression in stretched rat mesenchymal stem cells. International Journal of Oral and Maxillofacial Surgery 2008;37:453.

[65] Zhao HB, Lu TD, Ma J, Ma H, Zhang XZ. Mechanotransduction in differentiation of osteogenic from mesenchymal stem cells. Progress In Biochemistry And Biophysics 2007;34:718.

[66] Sumanasinghe RD, Bernacki SH, Loboa EG. Osteogenic differentiation of human mesenchymal stem cells in collagen matrices: Effect of uniaxial cyclic tensile strain on bone morphogenetic protein (BMP-2) mRNA expression. Tissue Eng 2006;12:3459.

[67] Byrne EM, Farrell E, McMahon LA, Haugh MG, O'Brien FJ, Campbell VA, Prendergast PJ, O'Connell BC. Gene expression by marrow stromal cells in a porous collagen-glycosaminoglycan scaffold is affected by pore size and mechanical stimulation. J. Mater. Sci.-Mater. Med. 2008;19:3455.

[68] Yanagisawa M, Suzuki N, Mitsui N, Koyama Y, Otsuka K, Shimizu N. Compressive force stimulates the expression of osteogenesis-related transcription factors in ROS 17/2.8 cells. Archives Of Oral Biology 2008;53:214.

[69] Rath B, Nam J, Knobloch TJ, Lannutti JJ, Agarwal S. Compressive forces induce osteogenic gene expression in calvarial osteoblasts. J Biomech 2008;41:1095.

[70] Kelly DJ, Prendergast PJ. Mechano-regulation of stem cell differentiation and tissue regeneration in osteochondral defects. J Biomech 2005;38:1413.

[71] McMahon LA, Reid AJ, Campbell VA, Prendergast PJ. Regulatory effects of mechanical strain on the chondrogenic differentiation of MSCs in a collagen-GAG scaffold: Experimental and computational analysis. Ann Biomed Eng 2008;36:185.

[72] Schaefer D, Martin I, Shastri P, Padera RF, Langer R, Freed LE, Vunjak-Novakovic G. In vitro generation of osteochondral composites. Biomaterials 2000;21:2599.

[73] Sherwood JK, Riley SL, Palazzolo R, Brown SC, Monkhouse DC, Coates M, Griffith LG, Landeen LK, Ratcliffe A. A three-dimensional osteochondral composite scaffold for articular cartilage repair. Biomaterials 2002;23:4739.

[74] Jiang CC, Chiang H, Liao CJ, Lin YJ, Kuo TF, Shieh CS, Huang YY, Tuan RS. Repair of porcine articular cartilage defect with a biphasic osteochondral composite. J. Orthop. Res. 2007;25:1277.

[75] Lima EG, Mauck RL, Han SH, Park S, Ng KW, Ateshian GA, Hung CT. Functional tissue engineering of chondral and osteochondral constructs. Biorheology 2004;41:577.

[76] Hung CT, Lima EG, Mauck RL, Taki E, LeRoux MA, Lu HH, Stark RG, Guo XE, Ateshian GA. Anatomically shaped osteochondral constructs for articular cartilage repair. J Biomech 2003;36:1853.

[77] Lima EG, Chao PHG, Ateshian GA, Bal BS, Cook JL, Vunjak-Novakovic G, Hung CT. The effect of devitalized trabecular bone on the formation of osteochondral tissue-engineered constructs. Biomaterials 2008;29:4292.

[78] Holland TA, Bodde EWH, Baggett LS, Tabata Y, Mikos AG, Jansen JA. Osteochondral repair in the rabbit model utilizing bilayered, degradable oligo(poly(ethylene glycol) fumarate) hydrogel scaffolds. Journal of Biomedical Materials Research Part A 2005;75A:156.

[79] Liu C, Xia Z, Czernuszka JT. Design and development of three-dimensional scaffolds for tissue engineering. Chem. Eng. Res. Des. 2007;85:1051.

[80] Varghese S, Hwang NS, Canver AC, Theprungsirikul P, Lin DW, Elisseeff J. Chondroitin sulfate based niches for chondrogenic differentiation of mesenchymal stem cells. Matrix Biology 2008;27:12.

[81] Hole BB, Schwarz JA, Gilbert JL, Atkinson BL. A study of biologically active peptide sequences (P-15) on the surface of an ABM scaffold (PepGen P-15 (TM)) using AFM and FTIR. Journal of Biomedical Materials Research Part A 2005;74A:712.

[82] Nguyen H, Qian JJ, Bhatnagar RS, Li S. Enhanced cell attachment and osteoblastic activity by P-15 peptide-coated matrix in hydrogels. Biochemical and Biophysical Research Communications 2003;311:179.

[83] Lindley EM, Guerra FA, Krauser JT, Matos SM, Burger EL, Patel VV. Small peptide (P-15) bone substitute efficacy in a rabbit cancellous bone model. Journal of Biomedical Materials Research Part B-Applied Biomaterials 2010;94B:463.

8.2 Chapter 3 references

[1] Ehrlich PJ, Lanyon LE. Mechanical strain and bone cell function: A review. Osteoporosis International 2002;13:688.

[2] Grodzinsky AJ, Levenston ME, Jin M, Frank EH. Cartilage tissue remodeling in response to mechanical forces. Annual Review of Biomedical Engineering 2000;2:691.

[3] Mauck RL, Nicoll SB, Seyhan SL, Ateshian GA, Hung CT. Synergistic action of growth factors and dynamic loading for articular cartilage tissue engineering. Tissue Engineering 2003;9:597.

[4] Skerry TM. The response of bone to mechanical loading and disuse: Fundamental principles and influences on osteoblast/osteocyte homeostasis. Archives of Biochemistry and Biophysics 2008;473:117.
s
[5] Sarraf CE, Otto WR, Eastwood M. In vitro mesenchymal stem cell differentiation after mechanical stimulation. Cell Proliferat 2011;44:99.

[6] Bikle DD, Halloran BP. The response of bone to unloading. Journal of Bone and Mineral Metabolism 1999;17:233.

[7] Mullender M, El Haj AJ, Yang Y, van Duin MA, Burger EH, Klein-Nulend J. Mechanotransduction of bone cells in vitro: mechanobiology of bone tissue. Medical & Biological Engineering & Computing 2004;42:14.

[8] Sandell LJ, Aigner T. Articular cartilage and changes in arthritis - An introduction: Cell biology of osteoarthritis. Arthritis Research 2001;3:107.

[9] Damsky CH. Extracellular matrix-integrin interactions in osteoblast function and tissue remodeling. Bone 1999;25:95.

[10] Mauck RL, Seyhan SL, Ateshian GA, Hung CT. Influence of seeding density and dynamic deformational loading on the developing structure/function relationships of chondrocyte-seeded agarose hydrogels. Ann Biomed Eng 2002;30:1046.

[11] Davisson T, Kunig S, Chen A, Sah R, Ratcliffe A. Static and dynamic compression modulate matrix metabolism in tissue engineered cartilage. J. Orthop. Res. 2002;20:842.

[12] Lima EG, Bian L, Ng KW, Mauck RL, Byers BA, Tuan RS, Ateshian GA, Hung CT. The beneficial effect of delayed compressive loading on tissue-engineered cartilage constructs cultured with TGF-beta 3. Osteoarthr Cartilage 2007;15:1025.

[13] Sikavitsas VI, Temenoff JS, Mikos AG. Biomaterials and bone mechanotransduction. Biomaterials 2001;22:2581.

[14] Yanagisawa M, Suzuki N, Mitsui N, Koyama Y, Otsuka K, Shimizu N. Compressive force stimulates the expression of osteogenesis-related transcription factors in ROS 17/2.8 cells. Archives Of Oral Biology 2008;53:214.

[15] Rath B, Nam J, Knobloch TJ, Lannutti JJ, Agarwal S. Compressive forces induce osteogenic gene expression in calvarial osteoblasts. J Biomech 2008;41:1095.

[16] Pittenger MF, Mackay AM, Beck SC, Jaiswal RK, Douglas R, Mosca JD, Moorman MA, Simonetti DW, Craig S, Marshak DR. Multilineage potential of adult human mesenchymal stem cells. Science 1999;284:143.

[17] Meinel L, Karageorgiou V, Fajardo R, Snyder B, Shinde-Patil V, Zichner L, Kaplan D, Langer R, Vunjak-Novakovic G. Bone tissue engineering using human mesenchymal stem cells: Effects of scaffold material and medium flow. Ann Biomed Eng 2004;32:112.

[18] Martino MM, Mochizuki M, Rothenfluh DA, Rempel SA, Hubbell JA, Barker TH. Controlling integrin specificity and stem cell differentiation in 2D and 3D environments through regulation of fibronectin domain stability. Biomaterials 2009;30:1089.

[19] Temenoff JS, Park H, Jabbari E, Conway DE, Sheffield TL, Ambrose CG, Mikos AG. Thermally cross-linked oligo(poly(ethylene glycol) fumarate) hydrogels support osteogenic differentiation of encapsulated marrow stromal cells in vitro. Biomacromolecules 2004;5:5.

[20] Salinas CN, Cole BB, Kasko AM, Anseth KS. Chondrogenic differentiation potential of human mesenchymal stem cells photoencapsulated within poly(ethylene glycol)-arginine-glycine-aspartic acid-serine thiol-methacrylate mixed-mode networks. Tissue Engineering 2007;13:1025.

[21] Mauck RL, Yuan X, Tuan RS. Chondrogenic differentiation and functional maturation of bovine mesenchymal stem cells in long-term agarose culture. Osteoarthr Cartilage 2006;14:179.

[22] Kelly DJ, Jacobs CR. The Role of Mechanical Signals in Regulating Chondrogenesis and Osteogenesis of Mesenchymal Stem Cells. Birth Defects Research Part C-Embryo Today-Reviews 2010;90:75.

[23] Huang CYC, Hagar KL, Frost LE, Sun YB, Cheung HS. Effects of cyclic compressive loading on chondrogenesis of rabbit bone-marrow derived mesenchymal stem cells. Stem Cells 2004;22:313.

[24] Campbell JJ, Lee DA, Bader DL. Dynamic compressive strain influences chondrogenic gene expression in human mesenchymal stem cells. Biorheology 2006;43:455.

[25] Kisiday JD, Frisbie DD, McIlwraith CW, Grodzinsky AJ. Dynamic Compression Stimulates Proteoglycan Synthesis by Mesenchymal Stem Cells in the Absence of Chondrogenic Cytokines. Tissue Eng Pt A 2009;15:2817.

[26] Terraciano V, Hwang N, Moroni L, Park HB, Zhang Z, Mizrahi J, Seliktar D, Elisseeff J. Differential response of adult and embryonic mesenchymal progenitor cells to mechanical compression in hydrogels. Stem Cells 2007;25:2730.

[27] Thorpe SD, Buckley CT, Vinardell T, O'Brien FJ, Campbell VA, Kelly DJ. Dynamic compression can inhibit chondrogenesis of mesenchymal stem cells. Biochemical and Biophysical Research Communications 2008;377:458.

[28] Qi MC, Hu J, Zou SJ, Chen HQ, Zhou HX, Han LC. Mechanical strain induces osteogenic differentiation: Cbfa1 and Ets-1 expression in stretched rat mesenchymal stem cells. International Journal of Oral and Maxillofacial Surgery 2008;37:453.

[29] Zhao HB, Lu TD, Ma J, Ma H, Zhang XZ. Mechanotransduction in differentiation of osteogenic from mesenchymal stem cells. Progress In Biochemistry And Biophysics 2007;34:718.

[30] Sumanasinghe RD, Bernacki SH, Loboa EG. Osteogenic differentiation of human mesenchymal stem cells in collagen matrices: Effect of uniaxial cyclic tensile strain on bone morphogenetic protein (BMP-2) mRNA expression. Tissue Engineering 2006;12:3459.

[31] Byrne EM, Farrell E, McMahon LA, Haugh MG, O'Brien FJ, Campbell VA, Prendergast PJ, O'Connell BC. Gene expression by marrow stromal cells in a porous collagen-glycosaminoglycan scaffold is affected by pore size and mechanical stimulation. Journal of Materials Science-Materials in Medicine 2008;19:3455.

[32] Bryant SJ, Anseth KS. Hydrogel properties influence ECM production by chondrocytes photoencapsulated in poly(ethylene glycol) hydrogels. Journal of Biomedical Materials Research 2002;59:63.

[33] Hern DL, Hubbell JA. Incorporation of adhesion peptides into nonadhesive hydrogels useful for tissue resurfacing. Journal of Biomedical Materials Research 1998;39:266.

[34] Nuttelman CR, Tripodi MC, Anseth KS. In vitro osteogenic differentiation of human mesenchymal stem cells photoencapsulated in PEG hydrogels. J Biomed Mater Res A 2004;68A:773.

[35] Benoit DSW, Anseth KS. Heparin functionalized PEG gels that modulate protein adsorption for hMSC adhesion and differentiation. Acta Biomater 2005;1:461.

[36] Buxton AN, Zhu J, Marchant R, West JL, Yoo JU, Johnstone B. Design and characterization of poly(ethylene glycol) photopolymerizable semi-interpenetrating networks for chondrogenesis of human mesenchymal stem cells. Tissue Engineering 2007;13:2549.

[37] Nicodemus GD, Bryant SJ. Mechanical loading regimes affect the anabolic and catabolic activities by chondrocytes encapsulated in PEG hydrogels. Osteoarthr Cartilage 2010;18:126.

[38] Bryant SJ, Durand KL, Anseth KS. Manipulations in hydrogel chemistry control photoencapsulated chondrocyte behavior and their extracellular matrix production. J Biomed Mater Res A 2003;67A:1430.

[39] Nuttelman CR, Tripodi MC, Anseth KS. Synthetic hydrogel niches that promote hMSC viability. Matrix Biology 2005;24:208.

[40] Bryant SJ, Chowdhury TT, Lee DA, Bader DL, Anseth KS. Crosslinking density influences chondrocyte metabolism in dynamically loaded photocrosslinked poly(ethylene glycol) hydrogels. Ann Biomed Eng 2004;32:407.

[41] Ruoslahti E, Pierschbacher MD. New Perspectives in Cell-Adhesion - Rgd and Integrins. Science 1987;238:491.

[42] Ruoslahti E, Reed JC. ANCHORAGE DEPENDENCE, INTEGRINS, AND APOPTOSIS. Cell 1994;77:477.

[43] Babalola OM, Bonassar LJ. Parametric Finite Element Analysis of Physical Stimuli Resulting From Mechanical Stimulation of Tissue Engineered Cartilage. Journal of Biomechanical Engineering-Transactions of the Asme 2009;131.

[44] Nicodemus GD, Bryant SJ. The role of hydrogel structure and dynamic loading on chondrocyte gene expression and matrix formation. J Biomech 2008;41:1528.

[45] Villanueva I, Hauschulz DS, Mejic D, Bryant SJ. Static and dynamic compressive strains influence nitric oxide production and chondrocyte bioactivity when encapsulated in PEG hydrogels of different crosslinking densities. Osteoarthr Cartilage 2008;16:909.

[46] Pfaffl MW. A new mathematical model for relative quantification in real-time RT-PCR. Nucleic Acids Research 2001;29.

[47] Palma PFR, Baggio GL, Spada C, da Silva R, Ferreira S, Treitinger A. Evaluation of annexin V and calcein-AM as markers of mononuclear cell apoptosis during human immunodeficiency virus infection. Braz. J. Infect. Dis. 2008;12:108.

[48] Salinas CN, Anseth KS. The influence of the RGD peptide motif and its contextual presentation in PEG gels on human mesenchymal stem cell viability. J Tissue Eng Regen Med 2008;2:296.

[49] Coleman RM, Case ND, Guldberg RE. Hydrogel effects on bone marrow stromal cell response to chondrogenic growth factors. Biomaterials 2007;28:2077.

[50] Fedorovich NE, Oudshoorn MH, van Geemen D, Hennink WE, Alblas J, Dhert WJA. The effect of photopolymerization on stem cells embedded in hydrogels. Biomaterials 2009;30:344.

[51] McBeath R, Pirone DM, Nelson CM, Bhadriraju K, Chen CS. Cell shape, cytoskeletal tension, and RhoA regulate stem cell lineage commitment. Dev. Cell 2004;6:483.

[52] Villanueva I, Weigel CA, Bryant SJ. Cell-matrix interactions and dynamic mechanical loading influence chondrocyte gene expression and bioactivity in PEG-RGD hydrogels. Acta Biomater 2009;5:2832.

[53] Gao L, McBeath R, Chen CS. Stem Cell Shape Regulates a Chondrogenic Versus Myogenic Fate Through Rac1 and N-Cadherin. Stem Cells 2010;28:564.

[54] Huebsch N, Arany PR, Mao AS, Shvartsman D, Ali OA, Bencherif SA, Rivera-Feliciano J, Mooney DJ. Harnessing traction-mediated manipulation of the cell/matrix interface to control stem-cell fate. Nature Materials 2010;9:518.

[55] Temenoff JS, Park H, Jabbari E, Sheffield TL, LeBaron RG, Ambrose CG, Mikos AG. In vitro osteogenic differentiation of marrow stromal cells encapsulated in biodegradable hydrogels. J Biomed Mater Res A 2004;70A:235.

[56] Hsiong SX, Boontheekul T, Huebsch N, Mooney DJ. Cyclic Arginine-Glycine-Aspartate Peptides Enhance Three-Dimensional Stem Cell Osteogenic Differentiation. Tissue Eng Pt A 2009;15:263.

[57] Yang F, Williams CG, Wang DA, Lee H, Manson PN, Elisseeff J. The effect of incorporating RGD adhesive peptide in polyethylene glycol diacrylate hydrogel on osteogenesis of bone marrow stromal cells. Biomaterials 2005;26:5991.

[58] Cushing MC, Anseth KS. Hydrogel cell cultures. Science 2007;316:1133.

[59] Sharma B, Williams CG, Khan M, Manson P, Elisseeff JH. In vivo chondrogenesis of mesenchymal stem cells in a photopolymerized hydrogel. Plastic and Reconstructive Surgery 2007;119:112.

[60] Nuttelman CR, Benoit DSW, Tripodi MC, Anseth KS. The effect of ethylene glycol methacrylate phosphate in PEG hydrogels on mineralization and viability of encapsulated hMSCs. Biomaterials 2006;27:1377.

[61] Salinas CN, Anseth KS. The enhancement of chondrogenic differentiation of human mesenchymal stem cells by enzymatically regulated RGD functionalities. Biomaterials 2008;29:2370.

[62] Lefebvre V, Huang WD, Harley VR, Goodfellow PN, deCrombrugghe B. SOX9 is a potent activator of the chondrocyte-specific enhancer of the pro alpha 1(II) collagen gene. Mol. Cell. Biol. 1997;17:2336.

[63] Mwale F, Stachura D, Roughley P, Antoniou J. Limitations of using aggrecan and type X collagen as markers of chondrogenesis in mesenchymal stem cell differentiation. J. Orthop. Res. 2006;24:1791.

[64] Djouad F, Tuan RS. Fundamentals of Tissue Engineering and Regenerative Medicine, 2009.

[65] Thorpe SD, Buckley CT, Vinardell T, O'Brien FJ, Campbell VA, Kelly DJ. The Response of Bone Marrow-Derived Mesenchymal Stem Cells to Dynamic Compression Following TGF-beta 3 Induced Chondrogenic Differentiation. Ann Biomed Eng 2010;38:2896.

[66] Angele P, Schumann D, Angele M, Kinner B, Englert C, Hente R, Fuchtmeier B, Nerlich M, Neumann C, Kujat R. Cyclic, mechanical compression enhances chondrogenesis of mesenchymal progenitor cells in tissue engineering scaffolds. Biorheology 2004;41:335.

[67] Pelaez D, Huang CYC, Cheung HS. Cyclic Compression Maintains Viability and Induces Chondrogenesis of Human Mesenchymal Stem Cells in Fibrin Gel Scaffolds. Stem Cells Dev 2009;18:93.

[68] Crolet JM, Stroe MC, Racila M. Decreasing of mechanotransduction process with age. Comput Method Biomec 2010;13:43.

[69] Wu MZ, Fannin J, Rice KM, Wang B, Blough ER. Effect of aging on cellular mechanotransduction. Ageing Res Rev 2011;10:1.

[70] Le Maitre CL, Frain J, Millward-Sadler J, Fotheringham AP, Freemont AJ, Hoyland JA. Altered integrin mechanotransduction in human nucleus pulposus cells derived from degenerated discs. Arthritis Rheum 2009;60:460.

[71] Connelly JT, Garcia AJ, Levenston ME. Interactions between integrin ligand density and cytoskeletal integrity regulate BMSC chondrogenesis. Journal of Cellular Physiology 2008;217:145.

[72] Connelly JT, Garcia AJ, Levenston ME. Inhibition of in vitro chondrogenesis in RGD-modified three-dimensional alginate gels. Biomaterials 2007;28:1071.

[73] Kasten A, Muller P, Bulnheim U, Groll J, Bruellhoff K, Beck U, Steinhoff G, Moller M, Rychly J. Mechanical Integrin Stress and Magnetic Forces Induce Biological Responses in Mesenchymal Stem Cells Which Depend on Environmental Factors. Journal of Cellular Biochemistry 2010;111:1586.

[74] Chun C, Lim HJ, Hong KY, Park KH, Song SC. The use of injectable, thermosensitive poly(organophosphazene)-RGD conjugates for the enhancement of mesenchymal stem cell osteogenic differentiation. Biomaterials 2009;30:6295.

[75] Hosseinkhani H, Hosseinkhani M, Tian F, Kobayashi H, Tabata Y. Osteogenic differentiation of mesenchymal stem cells in self-assembled peptide-amphiphile nanofibers. Biomaterials 2006;27:4079.

[76] Guilak F, Alexopoulos LG, Upton ML, Youn I, Choi JB, Cao L, Setton LA, Haider MA. The pericellular matrix as a transducer of biomechanical and biochemical signals in articular cartilage. Ann Ny Acad Sci 2006;1068:498.

8.3 Chapter 4 references

[1] Mirzayan R. Cartilage Injury in the Athlete. New York, NY: Thieme Medical Publishers; 2006.

[2] Clifford R. Wheeless III M. Wheeless' Textbook of Orthopaedics. In: Clifford R. Wheeless III M, editor. Articular Cartilage. Durham, NC: Data Trace Internet Publishing, LLC; 2011.

[3] Nordin M, Frankel VH. Basic biomechanics of the musculoskeletal system. In: Butler J, editor. Baltimore, MD: Lippincott Williams & Wilkins; 2001.

[4] Kotlarz H, Gunnarsson CL, Fang H, Rizzo JA. Insurer and Out-of-Pocket Costs of Osteoarthritis in the US Evidence From National Survey Data. Arthritis Rheum 2009;60:3546-53.

[5] Caplan AI. Mesenchyman stem cells. J Orthop Res 1991;9:641-50.

[6] Bosnakovski D, Mizuno M, Kim G, Ishiguro T, Okumura M, Iwanaga T, et al. Chondrogenic differentiation of bovine bone marrow mesenchymal stem cells in pellet cultural system. Experimental Hematology 2004;32:502-9.

[7] Gao L, McBeath R, Chen CS. Stem Cell Shape Regulates a Chondrogenic Versus Myogenic Fate Through Rac1 and N-Cadherin. Stem Cells 2010;28:564-72.

[8] Bryant SJ, Anseth KS. Hydrogel properties influence ECM production by chondrocytes photoencapsulated in poly(ethylene glycol) hydrogels. Journal of Biomedical Materials Research 2002;59:63-72.

[9] Bryant SJ, Arthur JA, Anseth KS. Incorporation of tissue-specific molecules alters chondrocyte metabolism and gene expression in photocrosslinked hydrogels. Acta Biomaterialia 2005;1:243-52.

[10] Li Q, Wang DA, Elisseeff JH. Heterogeneous-phase reaction of glycidyl methacrylate and chondroitin sulfate: Mechanism of ring-opening-transesterification competition. Macromolecules 2003;36:2556-62.

[11] Dziewiatkowski DD. Isolation of chondroitin sulfate-S-35 from articular cartilage of rats. J Biol Chem 1951;189:187-90.

[12] Bassleer C, Rovati L, Franchimont P. Stimulation of proteoglycan production by glucosamine sulfate in chondrocytes isolated from human osteoarthritic articular cartilage in vitro. Osteoarthritis Cartilage 1998;6:427-34.

[13] Pipitone VR. Chondroprotecition with chondroitin sulfate. Drugs under Experimental and Clinical Research 1991;17:3-7.

[14] Ronca F, Palmieri L, Panicucci P, Ronca G. Anti-inflammatory activity of chondroitin sulfate. Osteoarthritis Cartilage 1998;6:14-21.

[15] Varghese S, Hwang NS, Canver AC, Theprungsirikul P, Lin DW, Elisseeff J. Chondroitin sulfate based niches for chondrogenic differentiation of mesenchymal stem cells. Matrix Biology 2008;27:12-21.

[16] Villanueva I, Gladem SK, Kessler J, Bryant SJ. Dynamic loading stimulates chondrocyte biosynthesis when encapsulated in charged hydrogels prepared from poly(ethylene glycol) and chondroitin sulfate. Matrix Biology 2010;29:51-62.

[17] Johnstone B, Hering TM, Caplan AI, Goldberg VM, Yoo JU. In vitro chondrogenesis of bone marrow-derived mesenchymal progenitor cells. Exp Cell Res 1998;238:265-72.

[18] Lin-Gibson S, Bencherif S, Cooper JA, Wetzel SJ, Antonucci JM, Vogel BM, et al. Synthesis and characterization of PEG dimethacrylates and their hydrogels. Biomacromolecules 2004;5:1280-7.

[19] Bryant SJ, Davis-Arehart KA, Luo N, Shoemaker RK, Arthur JA, Anseth KS. Synthesis and characterization of photopolymerized multifunctional hydrogels: Water-soluble poly(vinyl alcohol) and chondroitin sulfate macromers for chondrocyte encapsulation. Macromolecules 2004;37:6726-33.

[20] Barbosa I, Garcia S, Barbier-Chassefiere V, Caruelle JP, Martelly I, Papy-Garcia D. Improved and simple micro assay for sulfated glycosaminoglycans quantification in biological extracts and its use in skin and muscle tissue studies. Glycobiology 2003;13:647-53.

[21] Metters AT, Anseth KS, Bowman CN. Fundamental studies of a novel, biodegradable PEG-b-PLA hydrogel. Polymer 2000;41:3993-4004.

[22] Nicodemus GD, Bryant SJ. The role of hydrogel structure and dynamic loading on chondrocyte gene expression and matrix formation. J Biomech 2008;41:1528-36.

[23] Villanueva I, Hauschulz DS, Mejic D, Bryant SJ. Static and dynamic compressive strains influence nitric oxide production and chondrocyte bioactivity when encapsulated in PEG hydrogels of different crosslinking densities. Osteoarthritis Cartilage 2008;16:909-18.

[24] Nicodemus GD, Bryant SJ. Mechanical loading regimes affect the anabolic and catabolic activities by chondrocytes encapsulated in PEG hydrogels. Osteoarthritis Cartilage 2010;18:126-37.

[25] Steinmetz NJ, Bryant SJ. The Effects of Intermittent Dynamic Loading on Chondrogenic and Osteogenic Differentiation of Human Marrow Stromal Cells Encapsulated in RGD Modified PEG Hydrogels Acta Biomaterialia 2011;7:3829-40.

[26] Thorpe SD, Buckley CT, Vinardell T, O'Brien FJ, Campbell VA, Kelly DJ. Dynamic compression can inhibit chondrogenesis of mesenchymal stem cells. Biochemical and Biophysical Research Communications 2008;377:458-62.

[27] Pfaffl MW. A new mathematical model for relative quantification in real-time RT-PCR. Nucleic Acids Research 2001;29:-.

[28] Knight MM, Ghori SA, Lee DA, Bader DL. Measurement of the deformation of isolated chondrocytes in agarose subjected to cyclic compression. Medical Engineering & Physics 1998;20:684-8.

[29] Chen SS, Falcovitz YH, Schneiderman R, Maroudas A, Sah RL. Depth-dependent compressive properties of normal aged human femoral head articular cartilage: relationship to fixed charge density. Osteoarthritis Cartilage 2001;9:561-9.

[30] Dickhut A, Pelttari K, Janicki P, Wagner W, Eckstein V, Egermann M, et al. Calcification or Dedifferentiation: Requirement to Lock Mesenchymal Stem Cells in a Desired Differentiation Stage. J Cell Physiol 2009;219:219-26.

[31] Dickhut A, Pelttari K, Janicki P, Wagner W, Eckstein V, Egermann M, et al. Low ALP Activity and Reduced In Vivo Calcification after In Vitro Chondrogenesis of Human Synovium Derived Mesenchymal Stem Cells. Tissue Engineering Part A 2009;15:704-.

[32] Pelttari K, Winter A, Steck E, Goetzke K, Hennig T, Ochs BG, et al. Premature induction of hypertrophy during in vitro chondrogenesis of human mesenchymal stem cells correlates with calcification and vascular invasion after ectopic transplantation in SCID mice. Arthritis Rheum 2006;54:3254-66.

[33] Dickhut A, Gottwald E, Steck E, Heisel C, Richter W. Chondrogenesis of mesenchymal stem cells in gel-like biomaterials in vitro and in vivo. Frontiers in Bioscience 2008;13:4517-28.

[34] Barry F, Boynton RE, Liu BS, Murphy JM. Chondrogenic differentiation of mesenchymal stem cells from bone marrow: Differentiation-dependent gene expression of matrix components. Exp Cell Res 2001;268:189-200.

[35] Bahrami S, Plate U, Dreier R, DuChesne A, Willital GH, Bruckner P. Endochondral ossification of costal cartilage is arrested after chondrocytes have reached hypertrophic stage of late differentiation. Matrix Biology 2001;19:707-15.

[36] Weber LM, Lopez CG, Anseth KS. Effects of PEG hydrogel crosslinking density on protein diffusion and encapsulated islet survival and function. Journal of Biomedical Materials Research Part A 2009;90A:720-9.

[37] Williams CG, Kim TK, Taboas A, Malik A, Manson P, Elisseeff J. In vitro chondrogenesis of bone marrow-derived mesenchymal stem cells in a photopolymerizing hydrogel. Tissue Eng 2003;9:679-88.

[38] Eyre DR, Wu JJ. Collagen of fibrocartilage - A distinctive molecular phenotype in bovine meniscus. Febs Letters 1983;158:265-70.

[39] Lozito TP, Kolf CM, Tuan RS. Regulatory Networks in Stem Cells. In: Rajasekhar VK, Vemuri MC, editors. Regulatory Networks in Stem Cells. New York City: Humana Press; 2009. p. 185-210.

[40] Mow VC, Wang CC, Hung CT. The extracellular matrix, interstitial fluid and ions as a mechanical signal transducer in articular cartilage. Osteoarthritis Cartilage 1999;7:41-58.

[41] Li YM, Schilling T, Benisch P, Zeck S, Meissner-Weigl J, Schneider D, et al. Effects of high glucose on mesenchymal stem cell proliferation and differentiation. Biochemical and Biophysical Research Communications 2007;363:209-15.

[42] Wuertz K, Godburn K, Neidlinger-Wilke C, Urban J, Iatridis JC. Behavior of mesenchymal stem cells in the chemical microenvironment of the intervertebral disc. Spine 2008;33:1843-9.

[43] Jurgens WJFM, Lu Z, Zandieh-Doulabi B, Kuik DJ, Ritt MJPF, Helder MN. Hyperosmolarity and hypoxia induce chondrogenesis of adipose-derived stem cells in a collagen type 2 hydrogel. J Tissue Eng Regen M 2011.

[44] Hung CT. Transient Receptor Potential Vanilloid 4 Channel as an Important Modulator of Chondrocyte Mechanotransduction of Osmotic Loading. Arthritis Rheum 2010;62:2850-1.

[45] Chen WC, Yao CL, Chu IM, Wei YH. Compare the effects of chondrogenesis by culture of human mesenchymal stem cells with various type of the chondroitin sulfate C. Journal of Bioscience and Bioengineering 2011;111:226-31.

[46] Nguyen LH, Kudva AK, Guckert NL, Linse KD, Roy K. Unique biomaterial compositions direct bone marrow stem cells into specific chondrocytic phenotypes corresponding to the various zones of articular cartilage. Biomaterials 2011;32:1327-38.

[47] Park JS, Yang HJ, Woo DG, Yang HN, Na K, Park KH. Chondrogenic differentiation of mesenchymal stem cells embedded in a scaffold by long-term release of TGF-beta 3 complexed with chondroitin sulfate. Journal of Biomedical Materials Research Part A 2010;92A:806-16.

[48] Thorpe SD, Buckley CT, Vinardell T, O'Brien FJ, Campbell VA, Kelly DJ. The Response of Bone Marrow-Derived Mesenchymal Stem Cells to Dynamic Compression Following TGF-beta 3 Induced Chondrogenic Differentiation. Ann Biomed Eng 2010;38:2896-909.

[49] Lu HH, Subramony SD, Boushell MK, Zhang XZ. Tissue Engineering Strategies for the Regeneration of Orthopedic Interfaces. Ann Biomed Eng 2010;38:2142-54.

8.4 Chapter 5 references

[1] Lu HH, Subramony SD, Boushell MK, Zhang XZ. Tissue Engineering Strategies for the Regeneration of Orthopedic Interfaces. Ann Biomed Eng 2010;38:2142-54.

[2] Benoit DSW, Nuttelman CR, Collins SD, Anseth KS. Synthesis and characterization of a fluvastatin-releasing hydrogel delivery system to modulate hMSC differentiation and function for bone regeneration. Biomaterials 2006;27:6102-10.

[3] Nuttelman CR, Tripodi MC, Anseth KS. Dexamethasone-functionalized gels induce osteogenic differentiation of encapsulated hMSCs. Journal of Biomedical Materials Research Part A 2006;76A:183-95.

[4] Nuttelman CR, Tripodi MC, Anseth KS. In vitro osteogenic differentiation of human mesenchymal stem cells photoencapsulated in PEG hydrogels. Journal of Biomedical Materials Research Part A 2004;68A:773-82.

[5] Burdick JA, Mason MN, Hinman AD, Thorne K, Anseth KS. Delivery of osteoinductive growth factors from degradable PEG hydrogels influences osteoblast differentiation and mineralization. J Control Release 2002;83:53-63.

[6] Burdick JA, Anseth KS. Photoencapsulation of osteoblasts in injectable RGD-modified PEG hydrogels for bone tissue engineering. Biomaterials 2002;23:4315-23.

[7] Pratt AB, Weber FE, Schmoekel HG, Muller R, Hubbell JA. Synthetic extracellular matrices for in situ tissue engineering. Biotechnology and Bioengineering 2004;86:27-36.

[8] Gurav N, Lutolf MP, Raeber GP, Hubbell JA, Di Silvio L. Differentiation of human bone marrow stem cells within RGD functionalised, proteolytically sensitive PEG gels. Tissue Eng 2007;13:1675-.

[9] Ehrbar M, Lutolf MP, Rizzi SC, Hubbell JA, Weber FE. Artificial extracellular matrices for bone tissue engineering. Bone 2008;42:S72-S.

[10] Bryant SJ, Arthur JA, Anseth KS. Incorporation of tissue-specific molecules alters chondrocyte metabolism and gene expression in photocrosslinked hydrogels. Acta Biomaterialia 2005;1:243-52.

[11] Nuttelman CR, Rice MA, Rydholm AE, Salinas CN, Shah DN, Anseth KS. Macromolecular monomers for the synthesis of hydrogel niches and their application in cell encapsulation and tissue engineering. Progress in Polymer Science 2008;33:167-79.

[12] Nuttelman CR, Tripodi MC, Anseth KS. Synthetic hydrogel niches that promote hMSC viability. Matrix Biology 2005;24:208-18.

[13] Gentili C, Cancedda R. Cartilage and Bone Extracellular Matrix. Current Pharmaceutical Design 2009;15:1334-48.

[14] Gelse K, Poschl E, Aigner T. Collagens - structure, function, and biosynthesis. Advanced Drug Delivery Reviews 2003;55:1531-46.

[15] Heng BC, Cao T, Stanton LW, Robson P, Olsen B. Strategies for directing the differentiation of stem cells into the osteogenic lineage in vitro. Journal of Bone and Mineral Research 2004;19:1379-94.

[16] Lozito TP, Kolf CM, Tuan RS. Regulatory Networks in Stem Cells. In: Rajasekhar VK, Vemuri MC, editors. Regulatory Networks in Stem Cells. New York City: Humana Press; 2009. p. 185-210.

[17] Salinas CN, Cole BB, Kasko AM, Anseth KS. Chondrogenic differentiation potential of human mesenchymal stem cells photoencapsulated within poly(ethylene glycol)-arginine-glycine-aspartic acid-serine thiol-methacrylate mixed-mode networks. Tissue Eng 2007;13:1025-34.

[18] Yang F, Williams CG, Wang DA, Lee H, Manson PN, Elisseeff J. The effect of incorporating RGD adhesive peptide in polyethylene glycol diacrylate hydrogel on osteogenesis of bone marrow stromal cells. Biomaterials 2005;26:5991-8.

[19] Hern DL, Hubbell JA. Incorporation of adhesion peptides into nonadhesive hydrogels useful for tissue resurfacing. Journal of Biomedical Materials Research 1998;39:266-76.

[20] Yang XBB, Bhatnagar RS, Li S, Oreffo ROC. Biomimetic collagen scaffolds for human bone cell growth and differentiation. Tissue Eng 2004;10:1148-59.

[21] Qian JJ, Bhatnagar RS. Enhanced cell attachment to anorganic bone mineral in the presence of a synthetic peptide related to collagen. Journal of Biomedical Materials Research 1996;31:545-54.

[22] Nguyen H, Qian JJ, Bhatnagar RS, Li S. Enhanced cell attachment and osteoblastic activity by P-15 peptide-coated matrix in hydrogels. Biochemical and Biophysical Research Communications 2003;311:179-86.

[23] Lin-Gibson S, Bencherif S, Cooper JA, Wetzel SJ, Antonucci JM, Vogel BM, et al. Synthesis and characterization of PEG dimethacrylates and their hydrogels. Biomacromolecules 2004;5:1280-7.

[24] van den Dolder J, Bancroft GN, Sikavitsas VI, Spauwen PHM, Jansen JA, Mikos AG. Flow perfusion culture of marrow stromal osteoblasts in titanium fiber mesh. Journal of Biomedical Materials Research Part A 2003;64A:235-41.

[25] Steinmetz NJ, Bryant SJ. The Effects of Intermittent Dynamic Loading on Chondrogenic and Osteogenic Differentiation of Human Marrow Stromal Cells Encapsulated in RGD Modified PEG Hydrogels Acta Biomaterialia 2011;7:3829-40.

[26] Salinas CN, Anseth KS. The influence of the RGD peptide motif and its contextual presentation in PEG gels on human mesenchymal stem cell viability. J Tissue Eng Regen Med 2008;2:296-304.

[27] Termine JD, Kleinman HK, Whitson SW, Conn KM, McGarvey ML, Martin GR. Osteonectin, a bone-specific protein linking mineral to collagen. Cell 1981;26:99-105.

[28] Knight CG, Morton LF, Onley DJ, Peachey AR, Messent AJ, Smethurst PA, et al. Identification in collagen type I of an integrin alpha(2)beta(1)-binding site containing an essential GER sequence. J Biol Chem 1998;273:33287-94.

[29] Morton LF, Peachey AR, Knight CG, Farndale RW, Barnes MJ. The platelet reactivity of synthetic peptides based on collagen III fragment alpha 1(III)CB4 - Evidence for an integrin alpha(2)beta(1) recognition site involving residues 522-528 of the alpha 1(III) collagen chain. J Biol Chem 1997;272:11044-8.

[30] Weber LM, Lopez CG, Anseth KS. Effects of PEG hydrogel crosslinking density on protein diffusion and encapsulated islet survival and function. Journal of Biomedical Materials Research Part A 2009;90A:720-9.

[31] Sikavitsas VI, Temenoff JS, Mikos AG. Biomaterials and bone mechanotransduction. Biomaterials 2001;22:2581-93.

[32] Di Lullo GA, Sweeney SM, Korkko J, Ala-Kokko L, San Antonio JD. Mapping the ligand-binding sites and disease-associated mutations on the most abundant protein in the human, type I collagen. J Biol Chem 2002;277:4223-31.

[33] Pelttari K, Winter A, Steck E, Goetzke K, Hennig T, Ochs BG, et al. Premature induction of hypertrophy during in vitro chondrogenesis of human mesenchymal stem cells correlates with calcification and vascular invasion after ectopic transplantation in SCID mice. Arthritis Rheum 2006;54:3254-66.

[34] Suaid FA, Macedo GO, Novaes AB, Borges GJ, Souza SLS, Taba M, et al. The Bone Formation Capabilities of the Anorganic Bone Matrix-Synthetic Cell-Binding Peptide 15 Grafts in an Animal Periodontal Model: A Histologic and Histomorphometric Study in Dogs. Journal of Periodontology 2010;81:594-603.

[35] Bhatnagar RS, Qian JJ, Wedrychowska A, Sadeghi M, Wu YM, Smith N. Design of biomimetic habitats for tissue engineering with P-15, a synthetic peptide analogue of collagen. Tissue Eng 1999;5:53-65.

[36] Lindley EM, Guerra FA, Krauser JT, Matos SM, Burger EL, Patel VV. Small peptide (P-15) bone substitute efficacy in a rabbit cancellous bone model. Journal of Biomedical Materials Research Part B-Applied Biomaterials 2010;94B:463-8.

[37] Lutz R, Srour S, Nonhoff J, Weisel T, Damien CJ, Schlegel Ka. Biofunctionalization of titanium implants with a biomimetic active peptide (P-15) promotes early osseointegration. Clinical oral implants research 2010;21:726-34.

[38] Garkhal K, Mittal A, Verma S, Kumar N. P-15 functionalized porous microspheres as biomimetic habitats for bone tissue engineering applications. Polymers for Advanced Technologies 2011;22:190-8.

[39] Jaiswal N, Haynesworth SE, Caplan AI, Bruder SP. Osteogenic differentiation of purified, culture-expanded human mesenchymal stem cells in vitro. Journal of Cellular Biochemistry 1997;64:295-312.

[40] Johnstone B, Hering TM, Caplan AI, Goldberg VM, Yoo JU. In vitro chondrogenesis of bone marrow-derived mesenchymal progenitor cells. Exp Cell Res 1998;238:265-72.

8.5 Chapter 6 references

[1] Moffat KL, Sun WH, Pena PE, Chahine NO, Doty SB, Ateshian GA, Hung CT, Lu HH. Characterization of the structure-function relationship at the ligament-to-bone interface. Proceedings of the National Academy of Sciences of the United States of America 2008;105:7947.

[2] Martin RB, Burr DB, Sharkey NA. Skeletal Tissue Mechanics. New York: Springer, 1998.

[3] AufderHeide AC, Athanasiou KA. Mechanical stimulation toward tissue engineering of the knee meniscus. Ann Biomed Eng 2004;32:1161.

[4] Imbeni V, Kruzic JJ, Marshall GW, Marshall SJ, Ritchie RO. The dentin-enamel junction and the fracture of human teeth. Nature materials 2005;4:229.

[5] Sahoo S, Teh T, He P, Toh S, Goh J. Interface Tissue Engineering: Next Phase in Musculoskeletal Repair Annals, Academy of Medicine, Singapore 2011;40:245.

[6] Lu HH, Subramony SD, Boushell MK, Zhang XZ. Tissue Engineering Strategies for the Regeneration of Orthopedic Interfaces. Ann Biomed Eng 2010;38:2142.

[7] Kon E, Delcogliano M, Filardo G, Pressato D, Busacca M, Grigolo B, Desando G, Marcacci M. A novel nano-composite multi-layered biomaterial for treatment of osteochondral

lesions: Technique note and an early stability pilot clinical trial. Injury-International Journal of the Care of the Injured 2010;41:778.

[8] Yilgor P, Sousa RA, Reis RL, Hasirci N, Hasirci V. Effect of scaffold architecture and BMP-2/BMP-7 delivery on in vitro bone regeneration. J. Mater. Sci.-Mater. Med. 2010;21:2999.

[9] Wang XQ, Wenk E, Zhang XH, Meinel L, Vunjak-Novakovic G, Kaplan DL. Growth factor gradients via microsphere delivery in biopolymer scaffolds for osteochondral tissue engineering. J Control Release 2009;134:81.

[10] Jiang J, Tang A, Ateshian GA, Guo XE, Hung CT, Lu HH. Bioactive Stratified Polymer Ceramic-Hydrogel Scaffold for Integrative Osteochondral Repair. Ann Biomed Eng 2010;38:2183.

[11] Lee J, Il Choi W, Tae G, Kim YH, Kang SS, Kim SE, Kim SH, Jung Y. Enhanced regeneration of the ligament-bone interface using a poly(L-lactide-co-epsilon-caprolactone) scaffold with local delivery of cells/BMP-2 using a heparin-based hydrogel. Acta Biomaterialia 2011;7:244.

[12] Park CH, Rios HF, Jin QM, Bland ME, Flanagan CL, Hollister SJ, Giannobile WV. Biomimetic hybrid scaffolds for engineering human tooth-ligament interfaces. Biomaterials 2010;31:5945.

[13] Hammoudi TM, Lu H, Temenoff JS. Long-Term Spatially Defined Coculture Within Three-Dimensional Photopatterned Hydrogels. Tissue Engineering Part C-Methods 2010;16:1621.

[14] Schaefer D, Martin I, Shastri P, Padera RF, Langer R, Freed LE, Vunjak-Novakovic G. In vitro generation of osteochondral composites. Biomaterials 2000;21:2599.

[15] Sherwood JK, Riley SL, Palazzolo R, Brown SC, Monkhouse DC, Coates M, Griffith LG, Landeen LK, Ratcliffe A. A three-dimensional osteochondral composite scaffold for articular cartilage repair. Biomaterials 2002;23:4739.

[16] Jiang CC, Chiang H, Liao CJ, Lin YJ, Kuo TF, Shieh CS, Huang YY, Tuan RS. Repair of porcine articular cartilage defect with a biphasic osteochondral composite. J. Orthop. Res. 2007;25:1277.

[17] Lima EG, Mauck RL, Han SH, Park S, Ng KW, Ateshian GA, Hung CT. Functional tissue engineering of chondral and osteochondral constructs. Biorheology 2004;41:577.

[18] Hung CT, Lima EG, Mauck RL, Taki E, LeRoux MA, Lu HH, Stark RG, Guo XE, Ateshian GA. Anatomically shaped osteochondral constructs for articular cartilage repair. J Biomech 2003;36:1853.

[19] Lima EG, Chao PHG, Ateshian GA, Bal BS, Cook JL, Vunjak-Novakovic G, Hung CT. The effect of devitalized trabecular bone on the formation of osteochondral tissue-engineered constructs. Biomaterials 2008;29:4292.

[20] Holland TA, Bodde EWH, Baggett LS, Tabata Y, Mikos AG, Jansen JA. Osteochondral repair in the rabbit model utilizing bilayered, degradable oligo(poly(ethylene glycol) fumarate) hydrogel scaffolds. Journal of Biomedical Materials Research Part A 2005;75A:156.

[21] Liu C, Xia Z, Czernuszka JT. Design and development of three-dimensional scaffolds for tissue engineering. Chem. Eng. Res. Des. 2007;85:1051.

[22] Harley BA, Lynn AK, Wissner-Gross Z, Bonfield W, Yannas IV, Gibson LJ. Design of a multiphase osteochondral scaffold III: Fabrication of layered scaffolds with continuous interfaces. Journal of Biomedical Materials Research Part A 2010;92A:1078.

[23] Kelly DJ, Prendergast PJ. Prediction of the optimal mechanical properties for a scaffold used in osteochondral defect repair. Tissue Eng 2006;12:2509.

[24] McMahon LA, Reid AJ, Campbell VA, Prendergast PJ. Regulatory effects of mechanical strain on the chondrogenic differentiation of MSCs in a collagen-GAG scaffold: Experimental and computational analysis. Ann Biomed Eng 2008;36:185.

[25] Marenzana M, Kelly DJ, Prendergast PJ, Brown RA. A collagen-based interface construct for the assessment of cell-dependent mechanical integration of tissue surfaces. Cell Tissue Res. 2007;327:293.

[26] Bryant SJ, Arthur JA, Anseth KS. Incorporation of tissue-specific molecules alters chondrocyte metabolism and gene expression in photocrosslinked hydrogels. Acta Biomaterialia 2005;1:243.

[27] Mann BK, Schmedlen RH, West JL. Tethered-TGF-beta increases extracellular matrix production of vascular smooth muscle cells. Biomaterials 2001;22:439.

[28] Qiu YZ, Lim JJ, Scott L, Adams RC, Bui HT, Temenoff JS. PEG-based hydrogels with tunable degradation characteristics to control delivery of marrow stromal cells for tendon overuse injuries. Acta Biomaterialia 2011;7:959.

[29] Felson DT, Zhang YQ. An update on the epidemiology of knee and hip osteoarthritis with a view to prevention. Arthritis Rheum 1998;41:1343.

[30] O'shea TM, Miao XG. Bilayered Scaffolds for Osteochondral Tissue Engineering. Tissue Eng. Part B-Rev. 2008;14:447.

[31] Mente PL, Lewis JL. Elastic modulus of calcified cartilage is an order of magnitued less than that of subchondral bone. J. Orthop. Res. 1994;12:637.

[32] Mansour JM. Biomechanics of Cartilage. In: C.A.Oate, editor. Kinesiology: The Mechanics and Pathomechanics of Human Movemen. Philadelphia: Lippincott Williams and Wilkins, 2003.

[33] Eckstein F, Tieschky M, Faber S, Englmeier KH, Reiser M. Functional analysis of articular cartilage deformation, recovery, and fluid flow following dynamic exercise in vivo. Anatomy and Embryology 1999;200:419.

[34] Burr DB, Milgrom C, Fyhrie D, Forwood M, Nyska M, Finestone A, Hoshaw S, Saiag E, Simkin A. In vivo measurement of human tibial strains during vigorous activity. Bone 1996;18:405.

[35] Rubin CT. Skeletal strain and the functional significance of bone architechture. Calcified Tissue International 1984;36:S11.

[36] Gardner-Morse MG, Tacy NJ, Beynnon BD, Roemhildt ML. In Situ Microindentation for Determining Local Subchondral Bone Compressive Modulus. J Biomech Eng-T Asme 2010;132.

[37] Ethier CR, Simmons CA. Introductory Biomechanics - From Cells to Organisms. Cambridge University Press.

[38] Claes LE, Heigele CA. Magnitudes of local stress and strain along bony surfaces predict the course and type of fracture healing. J Biomech 1999;32:255.

[39] Palomares KTS, Gleason RE, Mason ZD, Cullinane DM, Einhorn TA, Gerstenfeld LC, Morgan EF. Mechanical Stimulation Alters Tissue Differentiation and Molecular Expression during Bone Healing. J. Orthop. Res. 2009;27:1123.

[40] Wang FY, Ying Z, Duan XJ, Tan HB, Yang B, Guo L, Chen GX, Dai G, Ma Z, Yang L. Histomorphometric analysis of adult articular calcified cartilage zone. Journal of Structural Biology 2009;168:359.

[41] Clifford R. Wheeless III M. Wheeless' Textbook of Orthopaedics. In: Clifford R. Wheeless III M, editor. Articular Cartilage. Durham, NC: Data Trace Internet Publishing, LLC, 2011.

[42] Bollet AJ, Sturgill BC, Handy JR. Chondroitin sulfate concentration and protein polysaccharide composition of articular cartilage in osteoarthritis. Journal of Clinical Investigation 1963;42:853.

[43] Varghese S, Hwang NS, Canver AC, Theprungsirikul P, Lin DW, Elisseeff J. Chondroitin sulfate based niches for chondrogenic differentiation of mesenchymal stem cells. Matrix Biology 2008;27:12.

[44] Helfrich MH, Nesbitt SA, Dorey EL, Horton MA. Rat osteoclasts adhere to a wide range of RGD (ARG-GLY-ASP) peptide containing proteins, indluding the bone sialoproteins and fibronectin, via A beta-3 integrin. Journal of Bone and Mineral Research 1992;7:335.

[45] Nuttelman CR, Tripodi MC, Anseth KS. Synthetic hydrogel niches that promote hMSC viability. Matrix Biology 2005;24:208.

[46] Huebsch N, Arany PR, Mao AS, Shvartsman D, Ali OA, Bencherif SA, Rivera-Feliciano J, Mooney DJ. Harnessing traction-mediated manipulation of the cell/matrix interface to control stem-cell fate. Nature materials 2010;9:518.

[47] Bayliss MT, Osborne D, Woodhouse S, Davidson C. Sulfation of chondroitin sulfate in human articular cartilage - The effect of age, topographical position, and zone of cartilage on tissue composition. J. Biol. Chem. 1999;274:15892.

[48] Salinas CN, Anseth KS. The enhancement of chondrogenic differentiation of human mesenchymal stem cells by enzymatically regulated RGD functionalities. Biomaterials 2008;29:2370.

[49] Steinmetz NJ, Bryant SJ. The Effects of Intermittent Dynamic Loading on Chondrogenic and Osteogenic Differentiation of Human Marrow Stromal Cells Encapsulated in RGD Modified PEG Hydrogels Acta Biomaterialia 2011;*7*:3829.

[50] Nguyen LH, Kudva AK, Saxena NS, Roy K. Engineering articular cartilage with spatially-varying matrix composition and mechanical properties from a single stem cell population using a multi-layered hydrogel. Biomaterials 2011;32:6946.

[51] Chahine NO, Albro MB, Lima EG, Wei VI, Dubois CR, Hung CT, Ateshian GA. Effect of Dynamic Loading on the Transport of Solutes into Agarose Hydrogels. Biophysical Journal 2009;97:968.

[52] Guo X, Park H, Liu GP, Liu W, Cao YL, Tabata Y, Kasper FK, Mikos AG. In vitro generation of an osteochondral construct using injectable hydrogel composites encapsulating rabbit marrow mesenchymal stem cells. Biomaterials 2009;30:2741.

[53] Appelman TP, Mizrahi J, Seliktar D. A Finite Element Model of Cell-Matrix Interactions to Study the Differential Effect of Scaffold Composition on Chondrogenic Response to Mechanical Stimulation. J Biomech Eng-T Asme 2011;133.

[54] Park S, Hung CT, Ateshian GA. Mechanical response of bovine articular cartilage under dynamic unconfined compression loading at physiological stress levels. Osteoarthritis Cartilage 2004;12:65.

[55] Tate MLK, Falls TD, McBride SH, Atit R, Knothe UR. Mechanical modulation of osteochondroprogenitor cell fate. International Journal of Biochemistry & Cell Biology 2008;40:2720.

[56] Lin-Gibson S, Bencherif S, Cooper JA, Wetzel SJ, Antonucci JM, Vogel BM, Horkay F, Washburn NR. Synthesis and characterization of PEG dimethacrylates and their hydrogels. Biomacromolecules 2004;5:1280.

[57] Villanueva I, Gladem SK, Kessler J, Bryant SJ. Dynamic loading stimulates chondrocyte biosynthesis when encapsulated in charged hydrogels prepared from poly(ethylene glycol) and chondroitin sulfate. Matrix Biology 2010;29:51.

[58] Bryant SJ, Davis-Arehart KA, Luo N, Shoemaker RK, Arthur JA, Anseth KS. Synthesis and characterization of photopolymerized multifunctional hydrogels: Water-soluble poly(vinyl alcohol) and chondroitin sulfate macromers for chondrocyte encapsulation. Macromolecules 2004;37:6726.

[59] Roberts JJ, Earnshaw A, Ferguson VL, Bryant SJ. Comparative study of the viscoelastic mechanical behavior of agarose and poly(ethylene glycol) hydrogels. Journal of Biomedical Materials Research Part B-Applied Biomaterials 2011;99B:158.

[60] Barbosa I, Garcia S, Barbier-Chassefiere V, Caruelle JP, Martelly I, Papy-Garcia D. Improved and simple micro assay for sulfated glycosaminoglycans quantification in biological extracts and its use in skin and muscle tissue studies. Glycobiology 2003;13:647.

[61] Boyce MC, Arruda EM. Constitutive models of rubber elasticity: A review. Rubber Chem Technol 2000;73:504.

[62] Knight MM, Ghori SA, Lee DA, Bader DL. Measurement of the deformation of isolated chondrocytes in agarose subjected to cyclic compression. Medical Engineering & Physics 1998;20:684.

[63] Nicodemus GD, Bryant SJ. The role of hydrogel structure and dynamic loading on chondrocyte gene expression and matrix formation. J Biomech 2008;41:1528.

[64] Villanueva I, Hauschulz DS, Mejic D, Bryant SJ. Static and dynamic compressive strains influence nitric oxide production and chondrocyte bioactivity when encapsulated in PEG hydrogels of different crosslinking densities. Osteoarthritis Cartilage 2008;16:909.